

**NASA
Technical
Paper
2427**

May 1985

Flight Investigation of
Stall, Spin, and Recovery
Characteristics of a
Low-Wing, Single-Engine,
T-Tail Light Airplane

H. Paul Stough III,
Daniel J. DiCarlo,
and James M. Patton, Jr.



**NASA
Technical
Paper
2427**

1985

**Flight Investigation of
Stall, Spin, and Recovery
Characteristics of a
Low-Wing, Single-Engine,
T-Tail Light Airplane**

H. Paul Stough III,
Daniel J. DiCarlo,
and James M. Patton, Jr.

*Langley Research Center
Hampton, Virginia*



National Aeronautics
and Space Administration

**Scientific and Technical
Information Branch**

Contents

List of Figures	v
Summary	1
Introduction	1
Symbols and Abbreviations	1
Description of Airplane	2
Instrumentation	3
Evaluation Procedure	3
Results and Discussion	3
Stall Characteristics	3
Idle-power stalls	4
Power-on stalls	4
Full-flaps stalls	4
Spin Characteristics	4
Recovery Characteristics	5
Control Force Change During Spin Recovery	6
One-Turn Spins	7
Summary of Results	7
References	8
Tables	9
Figures	17

List of Figures

		Page
Figure 1	System of body axes. Arrows indicate positive direction of quantities.	17
Figure 2	Test airplane.	18
Figure 3	Three-view drawing of test airplane. Dimensions are in feet.	19
Figure 4	Sections through wing illustrating progressive increase in leading-edge droop starting at wing planform taper break.	20
Figure 5	Airplane design center-of-gravity envelope showing loading at test altitude.	20
Figure 6	True angle of attack as a function of measured angle of attack at wing-tip boom location.	21
Figure 7	Slow deceleration to idle-power, 1g, wings-level stall with flaps and gear retracted.	22
Figure 8	Idle-power, 1g, wings-level stall with maximum stabilator deflection, flaps and gear retracted.	26
Figure 9	Idle-power stall from 60° banked left turn with flaps and gear retracted.	30
Figure 10	Idle-power stall from right slip with flaps and gear retracted.	34
Figure 11	Slow deceleration to maximum-power, 1g, wings-level stall with flaps and gear retracted.	38
Figure 12	Maximum-power stall from right slip with flaps and gear retracted.	42
Figure 13	Maximum-power stall with flaps extended 40° and gear retracted.	46
Figure 14	One- and six-turn right spins at idle power with ailerons neutral, flaps and gear retracted. Normal recovery controls.	50
Figure 15	One- and ten-turn left spins at idle power, ailerons with the spin, flaps and gear retracted. Normal recovery controls.	54
Figure 16	One- and six-turn right spins at idle power, ailerons against the spin, flaps and gear retracted. Normal recovery controls.	58
Figure 17	Comparison of spiral and spin entered from idle-power, 1g stalls, flaps and gear retracted.	62
Figure 18	Left spin at idle power, ailerons neutral, flaps extended 40°, gear retracted. Normal recovery controls were unable to stop the spin until flaps were retracted.	66
Figure 19	Right spin at maximum power, ailerons neutral, flaps and gear retracted. Initial application of normal recovery controls failed to stop spin.	70
Figure 20	Right spin at idle power, ailerons neutral, flaps and gear retracted. Airplane stabilized in a steeper spin following release of controls.	74
Figure 21	Very steep spin bordering on spiral at idle power, ailerons with the spin, flaps and gear retracted.	78
Figure 22	Recovery time as a function of number of turns required to recover from steady spins at idle power, flaps and gear retracted. Twenty-seven spins that did not stop when initial recovery controls were applied are not included.	83
Figure 23	Examples of failure of rudder reversal alone to stop one- and six-turn spins at idle power, ailerons against the spin, flaps and gear retracted.	84

Figure 24	Left spin at idle power, ailerons neutral, flaps and gear retracted. Longitudinal wheel force changes during spin recovery are shown.	88
Figure 25	NACA 0012 wing section characteristics. (From ref. 18.)	92

Summary

Flight tests were performed to investigate the stall, spin, and recovery characteristics of a four-place, low-wing, single-engine, T-tail, general aviation research airplane. Stalls, incipient spins, and fully developed spins were performed at an aft center-of-gravity position for combinations of flap deflection, landing gear position, and power. Most stalls resulted in roll-offs. With prospin controls, the airplane spun at 43° angle of attack with large oscillations in both roll rate and pitch rate. Aileron position did not affect the angle of attack of the spin, but did strongly affect the magnitude of the oscillations. Deflecting the ailerons with the spin increased the oscillations; deflecting the ailerons against the spin reduced the oscillations. Spin characteristics were essentially unaffected by power level, flap deflection, and/or landing gear position. Antispin rudder followed by forward wheel with ailerons neutral produced the fastest and most consistent recoveries, but the initial application of recovery controls did not always stop a spin.

Introduction

In response to the need for improving the stall/spin characteristics of general aviation airplanes, the National Aeronautics and Space Administration (NASA) is conducting a comprehensive program to develop new stall/spin technology for this class of airplane (ref. 1). The program incorporates spin tunnel model tests, static- and rotary-balance wind tunnel tests, analytic studies, and airplane flight tests for a number of configurations representative of typical general aviation airplanes weighing under 4000 lb.

Airplane flight test results provide a reference base for correlation of theoretical predictions and model experimental results. Four single-engine airplanes have been tested in the NASA stall/spin program: (1) a low-wing airplane with four interchangeable tails (ref. 2), (2) a low-wing airplane with wing-tip rockets for control augmentation (ref. 3), (3) a high-wing airplane (ref. 4), and (4) a low-wing airplane with a T-tail (ref. 5).

This report presents results of spin tests of the low-wing T-tail airplane. Stall, incipient spin, developed spin, and recovery characteristics are presented, along with the effects of power, flaps, landing gear, and control inputs on these characteristics. Results from related model tests are presented in references 6 to 10.

Symbols and Abbreviations

Measurements are referred to the set of body axes with the origin at the airplane center of gravity, as shown in figure 1. Measurements were made and

quantities are presented in U.S. Customary Units. Symbols in parentheses refer to labels on computer-generated figures.

a_N	(NORM ACC)	normal acceleration at center of gravity (positive in negative Z_b direction), g units
	(ALTITUDE)	pressure altitude, ft
b		wing span, ft
BL		butt line, in.
\bar{c}		mean aerodynamic chord, ft
c		chord, ft
c.g.		center-of-gravity location, percent \bar{c}
FS		fuselage station, in.
g		acceleration due to gravity, 32.2 ft/sec ²
I_x, I_y, I_z		moment of inertia about X_b , Y_b , and Z_b body axis, respectively, slug-ft ²
	(LAT ACC)	lateral acceleration at center of gravity (positive in positive Y_b direction), g units
	(LAT FORCE)	lateral wheel force (positive for forces tending to rotate wheel clockwise), lb
	(LONG ACC)	longitudinal acceleration at center of gravity (positive in positive X_b direction), g units
	(LONG FORCE)	longitudinal wheel force (positive for forces tending to pull wheel aft), lb
m		mass of airplane, slugs
	(MPR)	engine manifold pressure, in. Hg
p	(ROLL RATE)	roll rate (positive for rolling right wing down), deg/sec
	(PROP SPEED)	propeller and engine speed, rpm

q	(PITCH RATE)	pitch rate (positive for pitching nose up), deg/sec	δ_a	(AILERON)	average aileron deflection (positive for right aileron trailing edge down), deg (see fig. 1), $\delta_a = \frac{1}{2}$ (right aileron deflection + left aileron deflection)
r	(YAW RATE)	yaw rate (positive for yawing nose right), deg/sec	δ_e	(STABILATOR)	stabilator deflection (positive for trailing edge down), deg (see fig. 1)
R		spin radius, ft; $R = \frac{g}{\Omega^2 \tan \alpha}$	δ_r	(RUDDER)	rudder deflection (positive for trailing edge left), deg (see fig. 1)
Re		Reynolds number	ϕ		bank angle (positive for right wing down), deg
R/S		rate of sink, ft/sec	μ		airplane relative density $\frac{m}{\rho S b}$
	(RES ACC)	resultant linear acceleration, (LONG ACC ² + LAT ACC ² + NORM ACC ²) ^{1/2} , g units	ρ		air density, slugs/ft ³
	(RUD FORCE)	rudder pedal force (positive for forces tending to push right pedal forward), lb	Ω	(TURN RATE)	total angular velocity of airplane, $(p^2 + q^2 + r^2)^{1/2}$, with sign of r , deg/sec
S		wing area, ft ²	Description of Airplane		
T		period of spin, sec; $T = \frac{360}{\Omega}$			
	(THRUST)	propeller thrust determined using engine performance chart and assumed propeller efficiency of 0.85, lb	The test airplane was a four-place, single-engine, low-wing, retractable-gear, T-tail design. This airplane was a one-of-a-kind research airplane, but it was considered representative of this class of aircraft. A photograph and three-view drawing of the airplane are presented as figures 2 and 3, respectively; physical characteristics are presented in table 1.		
V	(SPEED)	true airspeed, ft/sec (see fig. 1)			
WL		waterline, in.	The wing incorporated a modified NACA 65 ₂ -415 airfoil section. The leading edge of the tapered portion of the wing was drooped and transitioned smoothly from no droop at the start of the taper to maximum droop at the wing tip, as shown in figure 4. The wing had slotted trailing-edge flaps and plain ailerons. The horizontal tail was mounted on the vertical tail at the top of the rudder and consisted of a stabilator with a geared antiservo tab to provide longitudinal trim. An adjustable spring in the rudder control cables served to trim out rudder forces. Aileron trim was not adjustable in flight. The airplane was equipped with a spin recovery parachute system (ref. 11), a quick-release door on the right side, and a pyrotechnic egress panel in the absence of a door on the left side (ref. 12).		
WS		wing station, in.			
X_b, Y_b, Z_b		body axes through airplane c.g. (see fig. 1)	Tests were conducted at aft center-of-gravity positions of 27.2 to 27.9 percent \bar{c} (9.4 to 8.7 percent static margin) at a weight of about 2420 lb. Figure 5 shows the test loading relative to the design c.g. envelope. The inertia yawing-moment parameter, calculated from measured moments of inertia, was -74×10^{-4}		
α	(ALPHA CG)	true angle of attack at airplane center of gravity, deg (see fig. 1)			
α_m		measured angle of attack at instrumentation boom, deg			
α_T		true angle of attack at instrumentation boom, deg			
β	(BETA CG)	angle of sideslip at airplane center of gravity, deg (see fig. 1)			

Instrumentation

The airplane was instrumented to measure and record flow angles and true airspeed ahead of each wing tip, linear accelerations along the body axes, angular rates about the body axes, control surface positions, control wheel and rudder pedal forces, engine power parameters, altitude, and spin recovery parachute load. The onboard data system was supplemented by ground-based telephoto video and movie cameras and by cockpit- and wing-tip-mounted cameras. Pilot comments were recorded on the ground-based videotape. All data were time correlated and provided a continuous time history from spin entry through recovery. The data were telemetered to a ground station and were monitored in real time along with a video display of the spinning airplane. For debriefing purposes, the videotape and telemetry records were reviewed shortly after each flight.

Linear accelerations and flow measurements were corrected to indicate conditions at the airplane center of gravity using the techniques reported in reference 13. Angle-of-attack measurements were corrected for upwash by applying the techniques reported in reference 14 to measurements of longitudinal acceleration in level flight and roll and yaw rates in steady spins. The resultant flow correction is presented in figure 6. Because true angles of attack from both wing tips were averaged, corrections to angle of attack due to sidewash at the wing tips have a tendency to cancel out. Likewise, because measurements from both wing tips were averaged, corrections to sideslip due to upwash at the wing tips have a tendency to cancel out (ref. 15).

Evaluation Procedure

The results of the investigation were based on pilot comments, time history records of airplane motions and controls, and films and videotapes of the tests. All maneuvers were flown by the same pilot to minimize differences in maneuvers caused by variations in pilot technique.

Initial tests evaluated airplane stall and departure characteristics. Maneuvers included 1g and accelerated (banked) stalls with various combinations of engine power, bank angle, and sideslip as shown in table 2.

Spin tests were performed at the NASA Wallops Flight Facility. Test altitudes ranged from 12 000 to 6000 ft. Most spins were entered at an altitude of about 10 000 ft, which corresponds to a Reynolds number at the stall of about 3×10^6 . Spin entry conditions included combinations of acceleration, roll, pitch, yaw, and power. Prospin controls were ap-

plied at or just before the stall. The control positions at entry were wheel back with prospin rudder and ailerons either neutral, with the spin (right wheel for a right spin), or against the spin (left wheel for a right spin). The spin was allowed to develop for 1, 3, 6, and in some instances 10 or more turns. Recovery control inputs investigated included:

1. Full antispin rudder followed by full forward wheel with ailerons neutralized (normal controls)
2. Simultaneous antispin rudder and elevator inputs with ailerons neutralized
3. Full antispin rudder with the wheel back (rudder only)
4. Full forward wheel with prospin rudder maintained (elevator only)
5. Rudder, elevator, and ailerons neutralized (neutral controls)
6. Controls released

The effects of power level, flap position, and landing gear position were investigated individually and in combination.

Results and Discussion

Stall Characteristics

Airplane stall characteristics are presented in table 2 and are illustrated via time histories in figures 7 through 13. Qualitatively, the pilot described the airplane stall characteristics as "good" and felt that these characteristics were more docile than those of most current airplanes of this class. Aerodynamic stall warning in the form of buffet did not cover a sufficiently wide airspeed band to meet FAR Part 23 requirements (ref. 16), but a stall warning horn could be used to compensate for this. Approach to the stall was indicated by light buffet about 4 mph above the stall speed, and buffet became heavy before the stall was reached. Full flap deflection (40°) reduced the stall speed without appreciably changing the stall angle of attack and also reduced the buffeting compared to that experienced during flaps-up stalls. Although a roll-off tendency was present after stall for some configurations and power settings, this tendency was mild when zero sideslip was maintained at the stall, and the airplane stalling characteristics met the requirements of FAR Part 23. Stall characteristics deteriorated, with sometimes uncontrollable roll-off and incipient spin entry, when sideslip was present at the stall, as would most likely be the case in an inadvertent stall situation. The pilot felt that the maximum rate of the roll-off in this case was fairly low compared to that of other current airplanes. The airplane stalled at about 20° angle of attack. For the loading tested, slow deceleration (1 mph/sec) to a

1g, wings-level stall at idle power with gear and flaps retracted produced a stall at an indicated airspeed of 71 mph and a trailing-edge-up stabilator deflection of 2°. Rapidly pulling the wheel further aft and holding it to maintain the full trailing-edge-up stabilator deflection of 10° generated a transient angle of attack of up to 34°.

Both flaps-up and flaps-down stalls tended to produce rolling departures. Pulling the wheel full aft reduced this roll-off tendency. Pulling the wheel full aft with full flaps and full power generated a transient angle of attack of up to 40° and the airplane trimmed at about 28° angle of attack.

The trim changes caused by changes in flap and power settings were the opposite of those normally expected for this type of airplane. Deflecting the flaps produced a small nose-up trim change; adding power produced a nose-down trim change.

Idle-power stalls. Slow deceleration to a 1g, wings-level stall with near-zero sideslip (fig. 7) resulted in a Dutch-roll-type motion with the airplane flying in and out of the stall. Additional trailing-edge-up stabilator deflection beyond that required to stall the airplane generally resulted in a roll-off to the left. This roll-off was often initially uncontrollable even with full rudder and aileron inputs against the roll (fig. 8).

Stalls from coordinated 30° and 60° banked turns produced little roll-off tendency (fig. 9).

Full rudder deflection with opposite aileron input could produce 12° of steady sideslip and transients of up to 28°. When stalled with sideslip (fig. 10), the airplane rolled away from the slip; that is, right sideslip produced a left roll. The roll-off was attributed to the down aileron on the raised wing increasing the lift coefficient on that tip and causing it to stall first.

Power-on stalls. When stalled with maximum power and near-zero sideslip, the airplane usually rolled to the right (fig. 11). Stalls from 30° and 60° banked left and right turns resulted in roll-offs to the right.

When stalled with sideslip, the airplane rolled away from the slip (fig. 12). These rolls often could not be controlled with rudder and aileron until the airplane was unstalled by reducing the up-stabilator deflection.

Full-flaps stalls. With flaps deflected 40°, the airplane tended to roll to the right at the stall for both idle- and maximum-power cases. For maximum-power cases, the rolling tendency could be countered by large rudder and aileron inputs (fig. 13).

Spin Characteristics

A total of 209 spins were attempted during 19 evaluation flights. Of these, 173 resulted in spins, 34 resulted in spirals, and 2 failed to produce a spin or spiral. Of the spins, 63 were one-turn spins, 43 were three-turn spins, 54 were six-turn spins, and 13 were other assorted spins. Spin characteristics are summarized in table 3 and are illustrated in figures 14 to 21.

Table 3(a) summarizes the basic spin characteristics as a function of aileron deflection. With ailerons neutralized, the airplane spun at 43° angle of attack, rotating once about every 2.7 sec while descending at 120 ft/sec. These spin characteristics are illustrated in the six-turn spin of figure 14. This spin was oscillatory, particularly in roll and pitch. Roll rate and pitch rate varied over a period of 4 to 4½ sec and were not in phase.

Deflecting the ailerons with the spin (rolling in the direction of the spin) at the stall or early in the departure tended to make the airplane spiral instead of spin. Deflecting the ailerons with the spin as prospin rudder and stabilator were applied increased the rolling motion of the departure and made distinguishing between spiral and spin tendencies even more difficult at the one-turn point. For multiturn spins, delaying deflection of the ailerons with the spin promoted spin entry, as shown in the 10-turn spin of figure 15. Deflecting the ailerons against the spin (rolling against the direction of the spin) at the stall tended to stop spin entry, but deflecting ailerons at the quarter-turn point did not stop the spin. The six-turn spin of figure 16 illustrates the large change in sideslip angle and the delay in spin development caused by the abrupt input of ailerons against the spin.

Deflecting ailerons either with or against the spin did not change the angle of attack of the spin. Ailerons with the spin (fig. 15) more than doubled the magnitude of the oscillations in roll rate (± 60 deg/sec) and pitch rate (± 37 deg/sec) from those with ailerons neutral, reduced the period of the oscillations to about 3.5 sec, and caused the oscillations to be nearer in phase, with roll rate leading pitch rate slightly. Ailerons against the spin (fig. 16) reduced the magnitude of the roll and pitch rate oscillations and resulted in relatively smooth spins. The effects of aileron deflection on the oscillatory spin were consistent with those indicated by reference 17. Both ailerons neutral and ailerons with the spin resulted in a slipping rotation (positive sideslip in a right spin), whereas ailerons against the spin resulted in a skidding rotation (negative sideslip in a right spin).

In general, the first turn was characterized primarily by a rolling motion superimposed on a pitching motion. Determining whether the airplane was entering a spin or a spiral was difficult at the one-turn point, but the tendency was usually distinguishable during the second turn, as seen in figure 17. The spin sometimes stabilized by the end of the second turn, but the oscillations usually took longer to establish a repeatable form. Deflecting the ailerons tended to increase the number of turns required for the spin to reach steady state. With the ailerons neutral, the spin usually steadied out after about $2\frac{1}{2}$ turns, but occasionally required up to 4 turns to steady out. When the ailerons were deflected either with or against the spin, the airplane usually took four or five turns to reach a steady-state spin.

The airplane spin mode was essentially unchanged by any combination of extended landing gear, fully deflected flaps (fig. 18), or full power (fig. 19). Maximum power at typical spin entry altitude was about 65 percent of the rated sea level maximum power.

Following the application of recovery controls or the release of prospin controls, the airplane occasionally entered another spin mode at about 34° angle of attack with increased sideslip. Characteristics of this spin are presented in table 3(b) and illustrated in figures 18 to 20. In this mode, the upgoing wing tip was calculated to be operating within about $\pm 5^\circ$ of its stall angle of attack, and the remainder of the wing was above the stall angle of attack.

In one instance, an idle-power, ailerons-with-the-spin entry resulted in a very steep spin-like motion at 24° angle of attack with 9° sideslip. Characteristics of this spin are presented in table 3(c) and illustrated in figure 21. The steady-state motion of this spin was characterized by angular rates twice as large as those of the spiral presented in figure 17. In this spin, at 24° angle of attack with ailerons neutral, the outer 20 percent of the upgoing wing was calculated to be unstalled. Downward aileron deflection at that tip would be expected to promote further separation and cause even less than 20 percent of the wing to remain unstalled. The motion of the spin was very smooth (fig. 21) compared to that of the higher angle of attack ailerons-with spin (fig. 15), which was marked by large variations in roll and pitch rate. As would be expected from such a steep spin-like motion bordering on a spiral, the velocity and rate of descent were very high (215 ft/sec and 200 ft/sec, respectively).

Recovery Characteristics

Airplane spin recovery characteristics were investigated for six different antispin control inputs:

1. Full antispin rudder followed by full trailing-edge-down stabilator with ailerons neutralized (normal recovery controls)
2. Simultaneous application of full antispin rudder and full trailing-edge-down stabilator with ailerons neutralized (simultaneous recovery controls)
3. Full antispin rudder alone (rudder only)
4. Neutralized rudder, stabilator, and ailerons (neutral recovery controls)
5. Full trailing-edge-down stabilator (stabilator only)
6. Controls released

Recovery controls were evaluated on their ability to stop spins at idle power with flaps and landing gear retracted for ailerons neutral, ailerons with the spin, and ailerons against the spin. Recovery control inputs were applied in left and right spins at the one-, three-, and six-turn points. The spin was considered to have stopped when the yaw rate was reduced to zero. The control input that produced the fastest and most consistent recoveries was used in an investigation of the effects of flap deflection, landing gear position, and power level on recovery from spins with ailerons neutral, with the spin, and against the spin. Because of the oscillatory nature of the spins, eight prolonged spins (9 to 13 turns) were performed to check for variation in the effectiveness of normal recovery controls when applied at various times after the steady spin was reached.

The number of turns required for recovery from idle-power spins in the clean configuration (gear and flaps retracted) are presented in table 4. No recovery control input was identified which would always stop the spin. Figure 22 shows the time required to terminate a spin as a function of the number of turns required to stop a steady, idle-power spin in the clean configuration. This relationship, approximately 2.7 sec per recovery turn, was not affected by aileron position. Data are plotted for only those recoveries that followed initial antispin control input. Twenty-seven of the developed spins did not stop following initial application of recovery controls.

Neither neutralizing the controls, releasing the controls, nor deflecting only the stabilator against the spin stopped a steady spin, regardless of aileron position. When the controls were released, the rudder floated to near neutral, the stabilator to 7.5° trailing edge up (prospin), and the ailerons to about half of full deflection with the spin, as shown in figure 20. Rudder reversal alone did not always stop developed

spins and did not stop any spin, including a one-turn spin, when ailerons were maintained against the spin, as shown in figure 23. Otherwise, rudder alone produced consistently slower recoveries than did normal recovery controls, as can be seen from figure 22. Rudder alone proved best at stopping a spin when ailerons were deflected with the spin. The change in direction of sideslip and the increase in magnitude of sideslip oscillations when ailerons were with the spin instead of against the spin may have contributed to the rudder's ability to stop these spins.

As indicated in table 4, more incidences of prolonged recoveries (more than two turns) were experienced with simultaneous recovery controls than with normal recovery controls. Otherwise, the turns and time required for recovery were similar. The combination of antispin rudder deflection to slow the yaw rate and trailing-edge-down stabilator deflection to reduce angle of attack was the most effective in stopping the spin. Phasing and timing of control inputs are also factors. Overall, results indicated that the rudder should be moved against the spin prior to moving the stabilator. The effect of rudder alone in stopping ailerons-with spins suggested that lengthening the time between antispin rudder input and stabilator input might improve recovery from such spins. In general, normal recovery controls provided the fastest and most consistent recovery from steady spins at idle power in the clean configuration.

The time required to stop a spin appeared to vary directly with the number of turns required for recovery. (Approximately 2.7 seconds were required for each recovery turn (fig. 22).) Thus either time or number of turns appeared to be a fair gauge of recovery capability.

Once the airplane reached a steady-state spin, the number of turns beyond this point did not significantly affect the ability of normal recovery controls to stop the spin. The airplane appeared to recover from a spin more readily if the nose was pitching down rather than up when recovery was initiated.

Recovery from a one-turn spin was generally quicker than from a three-turn spin and was much more forgiving of the type of recovery control input employed. Through the first turn, reduction of stabilator and rudder inputs appeared to be sufficient to break the spin. Recovery initiated at the one-turn point was faster from left spins than from right spins. Recovery initiated after the spin was fully developed was essentially the same for left spins and right spins.

The number of turns required for recovery are presented in table 5 for various combinations of flap deflection, landing gear position, and power level for normal recovery controls. None of the combinations tested significantly affected recovery characteristics

when normal recovery controls were used. All 1-turn spins recovered within $1\frac{1}{4}$ turns after recovery control input. In general, allowing the spin to progress to three turns and beyond increased the number of turns required to stop the spin. Instances of the failure of recovery controls to break the spin were encountered with maximum power in the clean configuration (fig. 19) and with idle power in the gear-up, flaps-down configuration (fig. 18). In the first case, recovery was effected by returning the controls to their prospin positions and reapplying recovery controls. In the latter case, recovery was achieved by retracting the flaps and reapplying recovery controls. For the combinations of gear, flaps, and power tested, the application of normal recovery controls always stopped the less-oscillatory ailerons-against spin.

Control Force Change During Spin Recovery

When initiating recovery from a developed spin, the pilot was unable to achieve a full trailing-edge-down stabilator deflection. Even a push force of 100 lb on the control wheel would not move the stabilator beyond 5° trailing edge down until after the spin was broken, at which time increased stabilator deflection could be achieved with reduced wheel force, as illustrated by figure 24.

The stabilator incorporates an NACA 0012 airfoil section with a 20-percent-chord tab. The stabilator is hinged at approximately 27 percent chord. The tab is geared to the stabilator to produce a moment about the stabilator hinge that opposes movement of the stabilator. In this manner, the tab contributes to the control wheel force.

As shown in figure 25 (from ref. 18), the NACA 0012 wing section has zero pitching moment about its quarter-chord for angles of attack up to its stall angle of attack (about 15°). Because the stabilator is hinged at 27 percent chord, any deflection of the surface from 0° angle of attack tends to produce a moment that further increases this deflection. The geared tab counters this moment.

Once the stabilator is stalled, a large pitching moment is produced about the quarter-chord. This pitching moment tends to reduce the stabilator angle of attack. Thus, at some angle of attack above the stall angle of attack of the stabilator, the moment about the 27-percent-chord hinge line will change sign, and this change will tend to reduce the deflection of the surface.

The effect of such a tail stall is shown in figure 24. At the instant that spin recovery controls were applied, the airplane was spinning at 41° angle of attack. Forward wheel input (push force) deflected the stabilator and caused a further increase in stabilator angle of attack. Initially, a push force of about 100 lb

caused a stabilator movement of only 15°, from 10° trailing edge up to 5° trailing edge down. As angle of attack decreased, the stabilator hinge moment also decreased, and as the airplane angle of attack fell below 15°, additional deflection of the stabilator to the full range of 10° trailing edge down was allowed. This added deflection was accompanied by reduced wheel force as the stabilator unstalled and its hinge moment changed. Only the tab then countered the pilot's input on the control wheel.

The airplane effectively loses full control authority for spin recovery at high angles of attack because the pilot is unable to overcome the large stabilator hinge moment until after the spin is broken and the tail angle of attack is reduced. For recovery, rudder reversal prior to stabilator reversal is important to reduce the yaw rate and hence the nose-up centrifugal pitching moment, which in turn reduces the angle of attack and increases the effectiveness of the stabilator input.

One-Turn Spins

In the United States, certification of general aviation aircraft in the normal and utility categories requires demonstration of recovery from a one-turn spin or a 3-sec spin, whichever takes longer, within one turn following the application of recovery controls (ref. 16). This requirement is intended to address airplane characteristics only in an abused stall condition; that is, when the airplane is stalled with controls in a prospin direction and corrective control inputs are delayed. Compliance with this standard does not clear an airplane for intentional spins.

With this standard in mind, one-turn spins were studied to address the airplane's performance under abused stall/incipient spin conditions. Within the first turn following the application of prospin controls, the airplane motion was characterized primarily by a rolling motion superimposed on a pitching motion. Determining whether the airplane was entering a spiral or a spin was difficult. (See fig. 17.) With the application of normal recovery controls, the airplane failed only once to recover within the one-turn guideline. The failure occurred after an idle-power spin in the clean configuration with ailerons deflected against the spin.

The first turn following the application of any combination of prospin controls required from 4.4 to 9.3 sec and averaged 6.2 sec. Altitude loss varied from 0 to 300 ft and averaged 140 ft. In general, a one-turn right spin took less time than the same spin to the left; however, less time did not necessarily correspond to less altitude loss. One-turn spins in the clean configuration resulted in less altitude loss (120 ft) than the average prior to recovery control

input, whereas with flaps and gear extended, more altitude (160 ft) than the average was lost. The addition of power consistently reduced the altitude loss during a one-turn spin; the effect was greatest for right spins, which typically had an altitude loss of less than 80 ft.

Altitude loss during recovery from a one-turn spin using normal recovery controls ranged from 200 to 600 ft and averaged 400 ft. Recovery took from 1.1 to 4.0 sec and averaged 2.5 sec.

Following recovery from the spin, the airplane entered a dive. The altitude lost in the dive was dependent upon how abruptly the pilot pulled the airplane out of the dive. An abrupt pullout (limited by the airplane maximum positive load factor of 3.8) resulted in less loss of altitude than a more gentle pullout (limited by the airplane never-exceed speed of 314 ft/sec). In a sample of 165 recovery dives performed within these limitations following recovery from one-turn spins, altitude loss ranged from 300 to 1200 ft and averaged 620 ft. The duration of the dive ranged from 1.9 to 6.5 sec and averaged 4.1 sec.

Taken as a whole, from stall through incipient spin, recovery, and pullout to level flight, a one-turn spin could require 500 to 2100 ft of altitude and last from 7.4 to 19.8 sec. An average one-turn spin could be expected to result in a total altitude loss of 1160 ft and could last 12.8 sec. Therefore, a stall followed by departure into an incipient spin at a typical airport traffic pattern altitude of 800 to 1000 ft above ground level would require prompt action by the pilot to recover before ground impact.

Summary of Results

Flight tests were conducted to investigate the stall, spin, and recovery characteristics of a low-wing, single-engine, T-tail, general aviation research airplane. Tests were conducted at a gross weight of 2420 lb (88 percent of maximum gross weight) with aft center-of-gravity positions (0.272 to 0.279c). Results indicated the following:

1. Most stalls resulted in roll-offs. Full rudder and aileron inputs were unable to stop some roll-offs unless aft wheel was relaxed.
2. Following the application of prospin controls, it was difficult, even with instrumentation, to determine whether the airplane was entering a spin or a spiral until about two turns of rotation had been completed.
3. The average one-turn spin took 12.8 sec and resulted in an altitude loss of 1160 ft from entry through recovery to level flight.
4. At idle power with ailerons neutral and flaps and landing gear retracted, the airplane spun at 43°

angle of attack, rotating once every 2.7 sec with large oscillations in roll rate and pitch rate while descending at 120 ft/sec.

5. The angle of attack of the spin was not affected by deflected ailerons, extended landing gear, fully deflected flaps, or power level.

6. Ailerons deflected with the spin increased the oscillations in roll rate and pitch rate during the spin; ailerons deflected against the spin decreased these oscillations.

7. Normal recovery controls (antispin rudder followed by forward wheel with ailerons centered) provided the fastest and most consistent recovery, but the initial application of these recovery controls did not always stop a spin.

8. A 100-lb push force on the control wheel was insufficient to deflect the stabilator more than 50 percent of its down travel during initiation of recovery from a developed spin.

NASA Langley Research Center
Hampton, VA 23665
January 31, 1985

References

1. Chambers, Joseph R.: Overview of Stall/Spin Technology. AIAA-80-1580, Aug. 1980.
2. Stough, H. Paul, III; and Patton, J. M., Jr.: The Effects of Configuration Changes on Spin and Recovery Characteristics of a Low-Wing General Aviation Research Airplane. AIAA Paper 79-1786, Aug. 1979.
3. O'Bryan, Thomas C.; Edwards, Thomas E.; and Glover, Kenneth E.: Some Results From the Use of a Control Augmentation System To Study the Developed Spin of a Light Plane. AIAA Paper 79-1790, Aug. 1979.
4. Stewart, Eric C.; Suit, William T.; Moul, Thomas M.; and Brown, Philip W.: *Spin Tests of a Single-Engine, High-Wing Light Airplane*. NASA TP-1927, 1982.
5. Stough, H. Paul; DiCarlo, Daniel J.; and Stewart, Eric C.: Wing Modification for Increased Spin Resistance. SAE Paper No. 830720, Apr. 1983.
6. Barnhart, Billy: *Rotary Balance Data for a Typical Single-Engine General Aviation Design for an Angle-of-Attack Range of 8° to 90°*. II—Influence of Horizontal Tail Location for Model D. NASA CR-3247, 1982.
7. White, E. Richard: *Wind-Tunnel Investigation of Effects of Wing-Leading-Edge Modifications on the High Angle-of-Attack Characteristics of a T-Tail Low-Wing General Aviation Aircraft*. NASA CR-3636, 1982.
8. Ralston, John N.: *Rotary Balance Data for a Typical Single-Engine General Aviation Design for an Angle-of-Attack Range of 8° to 90°*. I—Influence of Airplane Components for Model D. NASA CR-3246, 1983.
9. Ralston, John N.; and Barnhart, Billy P.: *Rotary Balance Data for a Typical Single-Engine General Aviation Design for an Angle-of-Attack Range of 20° to 90°*. III—Influence of Control Deflection on Predicted Model D Spin Modes. NASA CR-3248, 1984.
10. Ralston, John: Influence of Airplane Components on Rotational Aerodynamic Data for a Typical Single-Engine Airplane. AIAA-83-2135, Aug. 1983.
11. Bradshaw, Charles F.: A Spin-Recovery Parachute System for Light General-Aviation Airplanes. *14th Aerospace Mechanisms Symposium*, NASA CP-2127, 1980, pp. 195-209.
12. Bement, Laurence J.: *Emergency In-Flight Egress Opening for General Aviation Aircraft*. NASA TM-80235, 1980.
13. Sliwa, Steven M.: Some Flight Data Extraction Techniques Used on a General Aviation Spin Research Aircraft. AIAA Paper 79-1802, Aug. 1979.
14. Moul, Thomas M.; and Taylor, Lawrence W., Jr.: Determination of an Angle of Attack Sensor Correction for a General Aviation Airplane at Large Angles of Attack as Determined From Wind Tunnel and Flight Tests. AIAA-80-1845, Aug. 1980.
15. Moul, Thomas Martin: Determination of Corrections to Flow Direction Measurements Obtained With a Wing-Tip Mounted Sensor. M.S. Thesis, George Washington Univ., Aug. 1983.
16. *Airworthiness Standards: Normal, Utility, and Acrobatic Category Airplanes*. Federal Aviation Regulations, vol. III, pt. 23, FAA, June 1974.
17. Kerr, T. H.: *Part I—General Principles of Spinning. Flight Test Manual, Volume II—Stability and Control*, Courtland D. Perkins, ed., Pergamon Press, 1963, pp. 8:1-8:14.
18. Loftin, Laurence K., Jr.; and Cohen, Kenneth S.: *Aerodynamic Characteristics of a Number of Modified NACA Four-Digit-Series Airfoil Sections*. NACA TN-1591, 1948.

TABLE 1. AIRPLANE PHYSICAL CHARACTERISTICS

Overall dimensions:

Span, ft	35.43
Length, ft	27.80
Height, ft	8.26

Powerplant:

Type	Reciprocating, four cylinder, horizontally opposed
Rated power at sea level, hp	200
Rated continuous speed, rpm	2700

Propeller:

Type	Two blades, constant speed
Diameter, in.	76
Pitch (variable), deg	14 to 31

Wing:

Area, ft ²	173.7
Root chord, in.	74.0
Chord of constant section, in.	63.0
Tip chord, in.	42.2
Mean aerodynamic chord, in.	62.16
Aspect ratio	7.24
Dihedral, deg	7.0
Incidence at root, deg	2.0
Incidence at tip, deg	-1.0
Airfoil section	NACA 65 ₂ -415 modified

Flap:

Chord, in.	12.26
Span, in.	85.50
Area (each), ft ²	7.3
Hinge line, percent flap chord	20.0
Deflection, deg	40 down

Aileron:

Mean chord, in.	10.01
Span, in.	100.05
Area (each), ft ²	6.95
Deflection, deg	30 up, 16 down

Stabilator:

Area (including tab), ft ²	25.0
Chord (constant), in.	30.0
Aspect ratio	4.0
Dihedral, deg	0
Hinge line, percent stabilator chord	26.97
Deflection, deg	10 up, 10 down
Airfoil section	NACA 0012

Tab:

Chord (constant), in.	6.0
Span, in.	106.2
Area, ft ²	4.4
Tab hinge line to stabilator hinge line, in.	15.91

TABLE 1. Concluded

Vertical tail:

Area (including rudder), ft ²	17.6
Root chord, in.	54.52
Tip chord, in.	28.62
Mean aerodynamic chord, in.	42.91
Span, in.	60.84
Aspect ratio	1.47
Leading edge sweep back, deg	33.91

Rudder:

Area, ft ²	5.8
Average chord aft of hinge line, in.	11.85
Span (parallel to hinge line), in.	61.6
Deflection, deg	28 left, 28 right

Test weight at altitude, lb 2420

Relative density, μ , at 9000 ft altitude 6.7

Representative center-of-gravity position:

FS, in.	95.85 (27.82 percent \bar{c})
BL, in.	-0.56
WL, in.	38.15

Moments of inertia about body axes (based on above center-of-gravity position):

I_x , slug-ft ²	1789
I_y , slug-ft ²	2486
I_z , slug-ft ²	3796

Inertia yawing-moment parameter, $\frac{I_x - I_y}{mb^2}$ -74×10^{-4}

TABLE 2. AIRPLANE STALL CHARACTERISTICS

Power	ϕ , deg	β , deg	Description of maneuver	Result
Idle	0	0	Wheel back to stall, then controls fixed	Stable; little roll-off
	→	0	Wheel full back, then controls fixed	Roll-off to the left
		0	Wheel back to stall, then use ailerons	Very stable maneuver
		10	Right sideslip	Roll-off to the left
	→	-20	Left sideslip	Very stable; roll-off countered by aileron
		-3	Left turn	Little roll-off tendency
	→	0	Right turn	Little roll-off tendency
		-2	Wheel back to stall, then controls fixed	Roll-off to the right
		-2	Wheel full back, then controls fixed	Roll-off to the right
		-2	Wheel back to stall, then use ailerons	Roll-off easily controlled with little aileron
Maximum	→	-3	Wheel full back, then use rudder	Roll-off oscillations could not be controlled by rudder
		14	Right sideslip	Roll-off to the left uncontrollable
		-12	Left sideslip	Roll-off to the right uncontrollable
	→	0	Left turn	Roll-off to the right
		9	Skidding left turn	Roll-off to the left initially uncontrollable
	→	0	Right turn	Rapid roll-off to the right
		30	Skidding right turn	Roll-off to the right
	→	-60	Left turn	Roll-off to the right
		60	Right turn	Slight roll-off to the left, then to the right

TABLE 3. AIRPLANE SPIN CHARACTERISTICS

(a) Data presented for right spin with full prospin control deflections
for any combination of flaps, landing gear, and power tested

Quantity	Spin characteristics for—		
	Ailerons with spin	Ailerons neutral	Ailerons against spin
α , deg	43 ± 7	43 ± 4	43 ± 4
β , deg	4 ± 14	4 ± 5	-7 ± 5
p , deg/sec	81 ± 60	92 ± 25	91 ± 14
q , deg/sec	28 ± 37	19 ± 16	4 ± 6
r , deg/sec	88 ± 7	93 ± 5	86 ± 4
Ω , deg/sec	147 ± 44	135 ± 20	141 ± 12
T , sec	$2.45^{+1.05}_{-0.57}$	$2.67^{+0.46}_{-0.35}$	$2.55^{+0.20}_{-0.24}$
V , ft/sec	130	127	132
R/S , ft/sec	125	120	115
a_N , g units	1.4 ± 0.3	1.4 ± 0.2	1.4 ± 0.2
R , ft	5.2	6.2	5.7

TABLE 3. Continued

(b) Data presented for spin following attempted recovery from right spin. Time histories presented in figures 18, 19, and 20.

Quantity	Spin characteristics for—	
	Normal recovery controls	Controls released
δ_a , deg	-4	-12 ± 2
δ_e , deg	6	-7.5 ± 2.5
δ_r , deg	27	1 ± 4
α , deg	34 ± 2	31 ± 3
β , deg	11 ± 5	17 ± 7
p , deg/sec	130 ± 20	125 ± 46
q , deg/sec	39 ± 15	49 ± 21
r , deg/sec	93 ± 2	75 ± 5
Ω , deg/sec	165 ± 17	157 ± 37
T , sec	$2.18^{+0.25}_{-0.20}$	$2.29^{+0.71}_{-0.43}$
V , ft/sec	135 ± 5	150
R/S , ft/sec	120	125
a_N , g units	1.7	1.8
R , ft	5.8	7.1

TABLE 3. Concluded

(c) Data presented for left spin. Full prospin control deflections, idle power, ailerons with the spin, flaps and landing gear retracted. Time history presented in figure 21.

Quantity	Spin characteristics for ailerons with the spin
α , deg	24 ± 1
β , deg	-9 ± 1
p , deg/sec	-125 ± 7
q , deg/sec	45 ± 1
r , deg/sec	-50 ± 2
Ω , deg/sec	-137 ± 9
T , sec	$2.63^{+0.18}_{-0.15}$
V , ft/sec	215
R/S , ft/sec	200
a_N , g units	3.0
R , ft	12.6

TABLE 4. NUMBER OF TURNS REQUIRED FOR RECOVERY FROM IDLE-POWER SPINS WITH VARIOUS RECOVERY CONTROL INPUTS

[Landing gear retracted, flaps retracted]

Recovery control	Aileron position	Number and direction of turns with prospin controls										
		1			3			6			10	
		Left	Right	Left	Right	Left	Right	Left	Right	Left	Right	
		Number of turns required for recovery										
Normal	Neutral	1/2	5/8, 7/8	2	1 3/4	1 7/8, > 2	1 5/8, 2	1 7/8	2	1 7/8	2	
	With spin	1/4	1/4	1 1/8	1 5/8	(a)	1 3/8	7/8		7/8	b, c ∞	
	Against spin	7/8	1 1/4	1 1/4	1 1/2	1 1/2	1 1/2	d 1		d 1	1 1/4	
Simultaneous	Neutral	1/2	3/4	1 3/8	6 3/8	1 3/8, 1 1/2, ∞	1 3/8					
	With spin	1/4	1/2	1 1/4, 4 7/8	1 1/2	> 4 3/8	∞					
	Against spin	1	3/4	1 1/2	3/4	1 1/8	1 1/8					
Rudder only	Neutral	1/2	1 1/2	3 7/8	3	3 3/8	2 3/4, ∞					
	With spin	3/8	3/4		2	2	2, e 1 3/8					
	Against spin	∞	∞	∞	∞	∞	∞					
Neutral	Neutral	1/2	3/4	∞	∞	∞	∞					
	With spin	1/4	3/8	2 1/8, f ∞	3	∞	∞					
	Against spin	1	3/4	∞	∞	∞	∞					
Stabilator	Neutral						∞					
	With spin						∞					
	Against spin						∞					
Release	Neutral	3/4	1 1/4	4 1/2	∞	∞	∞					
	With spin						∞					
	Against spin						∞					

^aA blank space indicates that the condition was not tested.

^bAn infinity symbol indicates that the airplane stabilized in a spin with recovery controls applied.

^cRecovery controls applied after 13 turns.

^dRecovery controls applied after 9 3/8 turns.

^eRecovery controls applied after 7 turns.

^fRecovery controls applied after 4 turns.

TABLE 5. NUMBER OF TURNS REQUIRED FOR SPIN RECOVERY USING NORMAL RECOVERY CONTROLS

Number and direction of turns with prospin controls																	
Configuration				1								3		6		10	
Power	Landing gear	Flaps	Aileron position	Left	Right	Left	Right	Left	Right	Left	Right	Left	Right	Left	Right		
				Number of turns required for recovery													
Idle	Up	Up	Neutral	1/2	5/8, 7/8	2	1 3/4	1 7/8, >2	1 5/8, 2	1 7/8	2						
			With spin	1/4	1/4	1 1/8	1 5/8	(a)	1 3/8	7/8	b, c ∞						
			Against spin	7/8	1 1/4	1 1/4	1 1/2	1 1/2	1 1/2	d 1	1 1/4						
		Down 40°	Neutral	1/4	1/4	2 5/8	∞	2 1/2, ∞	2 1/4								
			With spin	1/4	1/8												
			Against spin	7/8	5/8			3 3/8	2 1/8								
	Down	Up	Neutral	3/4	3/4	>3	1 3/4	2	1 3/4								
			With spin	1/8	1/2												
			Against spin	7/8	5/8												
		Down 40°	Neutral				2 1/2		2 1/4								
			With spin														
			Against spin	e 7/8	5/8	2 3/8	1 3/4	2 1/4	1 3/4, 1 3/4								
Max	Up	Up	Neutral	3/4	3/4	1 3/8	1 1/4	1 3/8	∞			f 1 3/4					
			With spin	1/4	1/4		3/4	3/4	1 1/4								
			Against spin	1/2	1/4	3/4	1	3/4	1 1/4								
		Down 40°	Neutral	1/4, 1/4	1/2, g 1 1/4		2 1/4		1 1/2								
			With spin														
			Against spin														
	Down	Up	Neutral	3/4	1/8												
			With spin	1/8	1/8												
			Against spin	3/4	1/2												
		Down 40°	Neutral	1/4	1/2												
			With spin		1/8												
			Against spin	3/4													

^a A blank space indicates that the condition was not tested.^b An infinity symbol indicates that the airplane stabilized in a spin with recovery controls applied.^c Recovery controls applied after 13 turns.^d Recovery controls applied after 9 3/8 turns.^e Recovery controls applied after 1 1/2 turns.^f Recovery controls applied after 9 turns.^g Recovery control input not crisp.

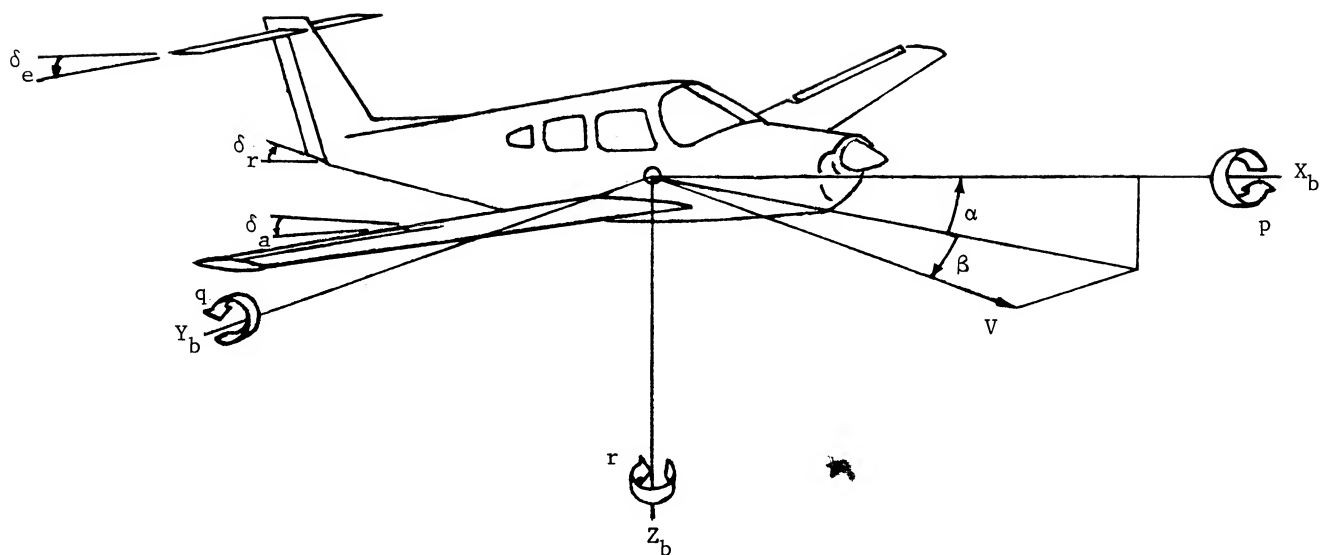
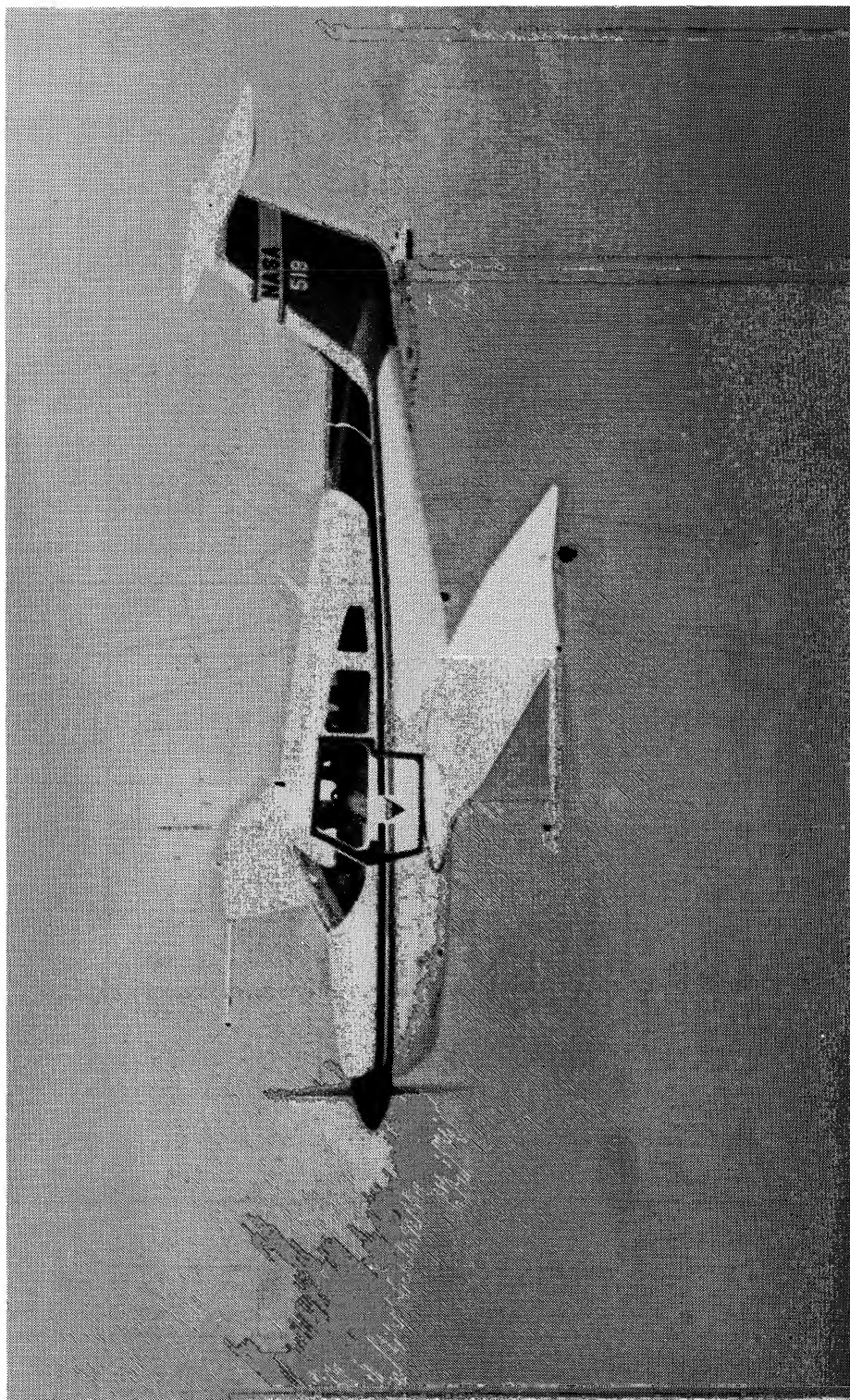


Figure 1. System of body axes. Arrows indicate positive direction of quantities.



L-81-6709

Figure 2. Test airplane.

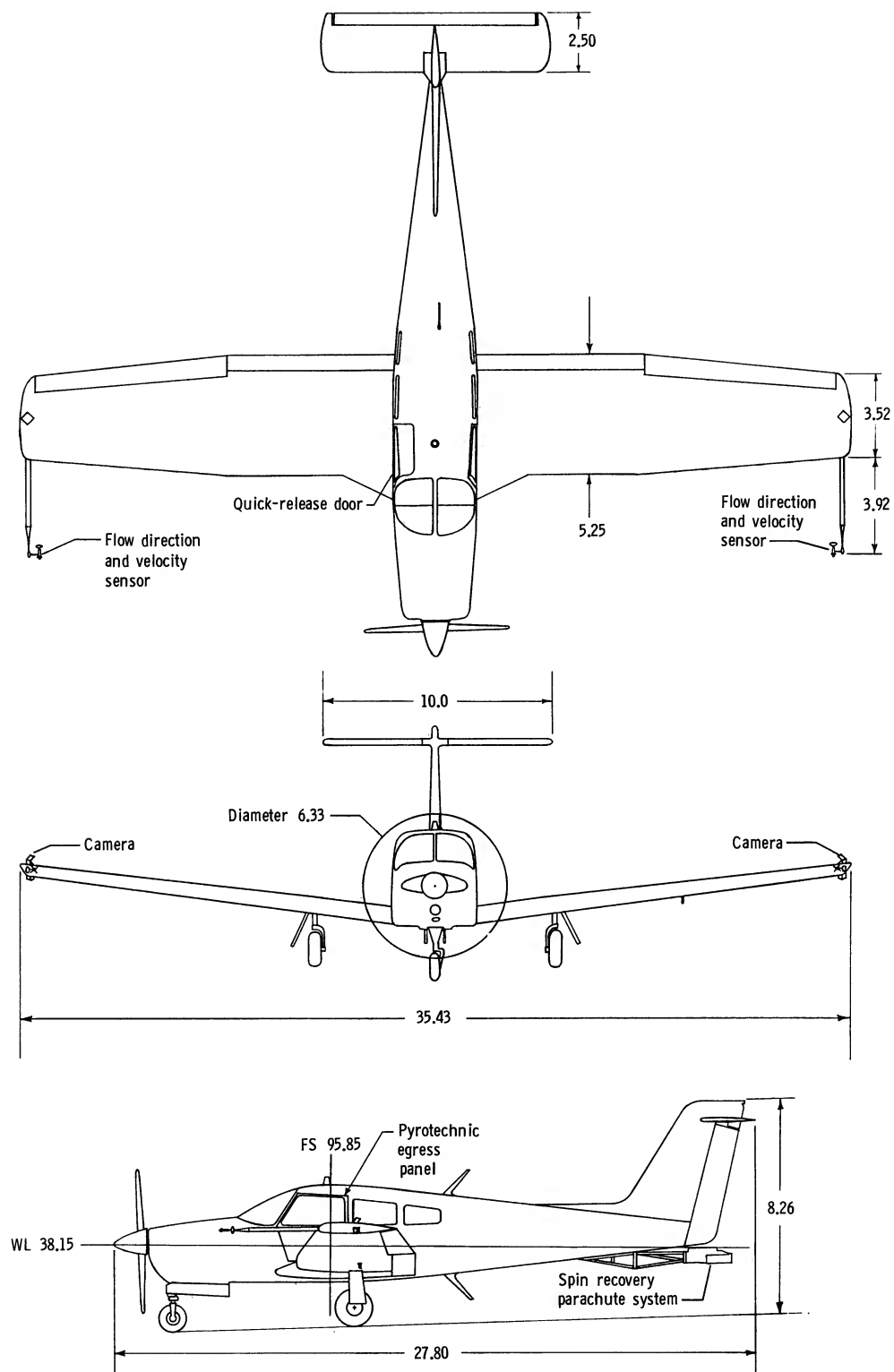


Figure 3. Three-view drawing of test airplane. Dimensions are in feet.

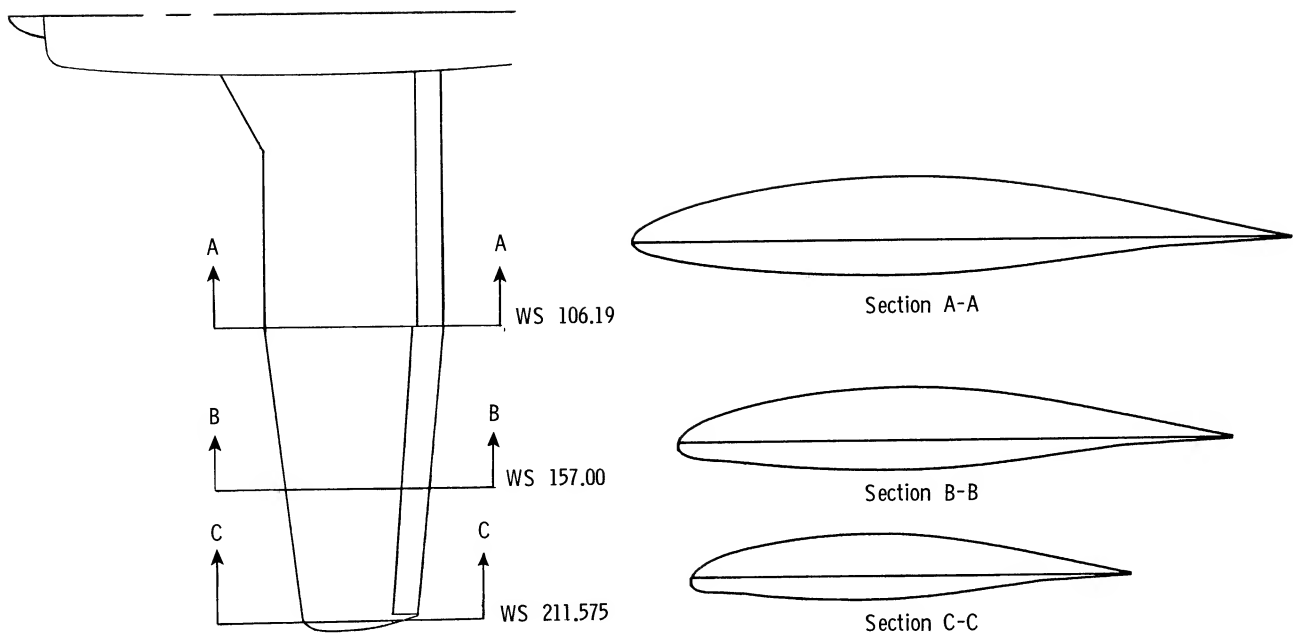


Figure 4. Sections through wing illustrating progressive increase in leading-edge droop starting at wing planform taper break.

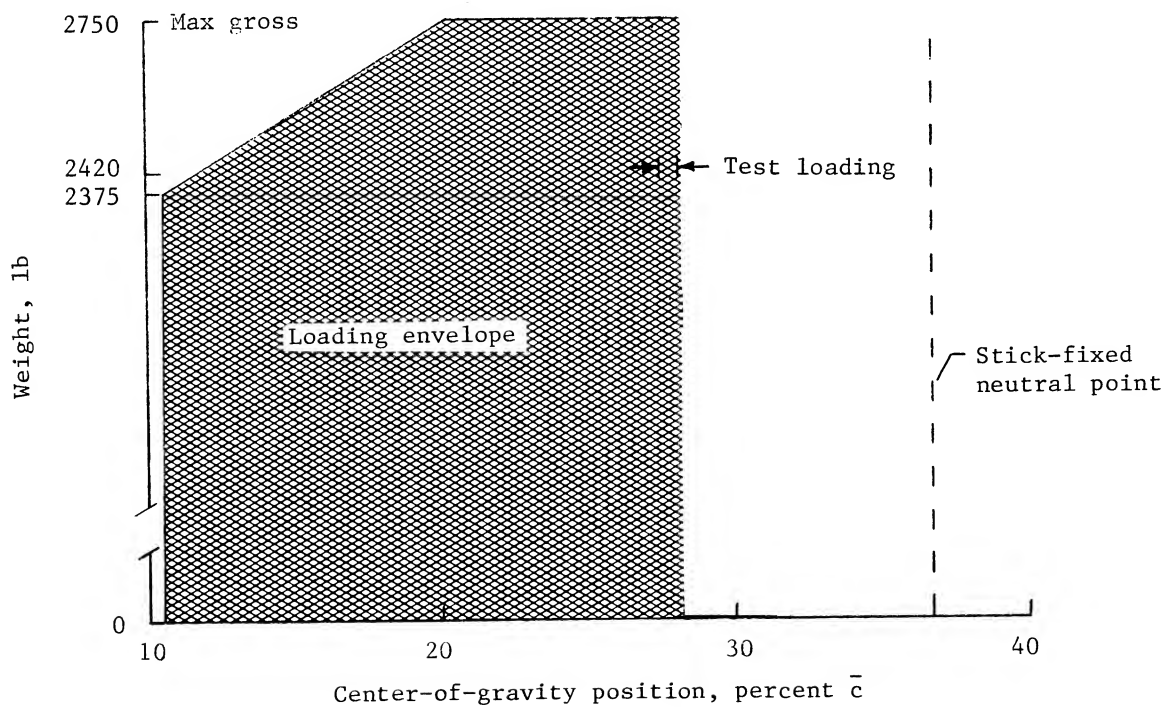


Figure 5. Airplane design center-of-gravity envelope showing loading at test altitude.

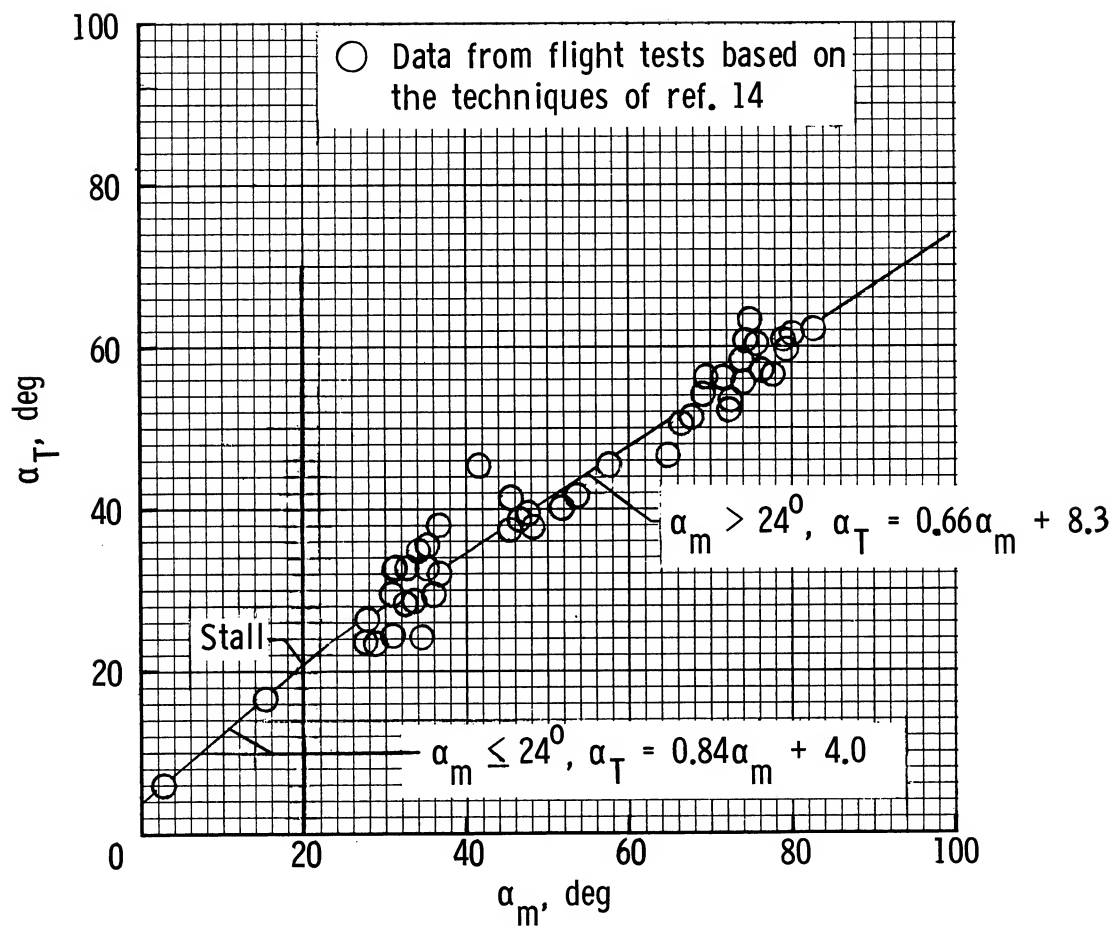


Figure 6. True angle of attack as a function of measured angle of attack at wing-tip boom location.

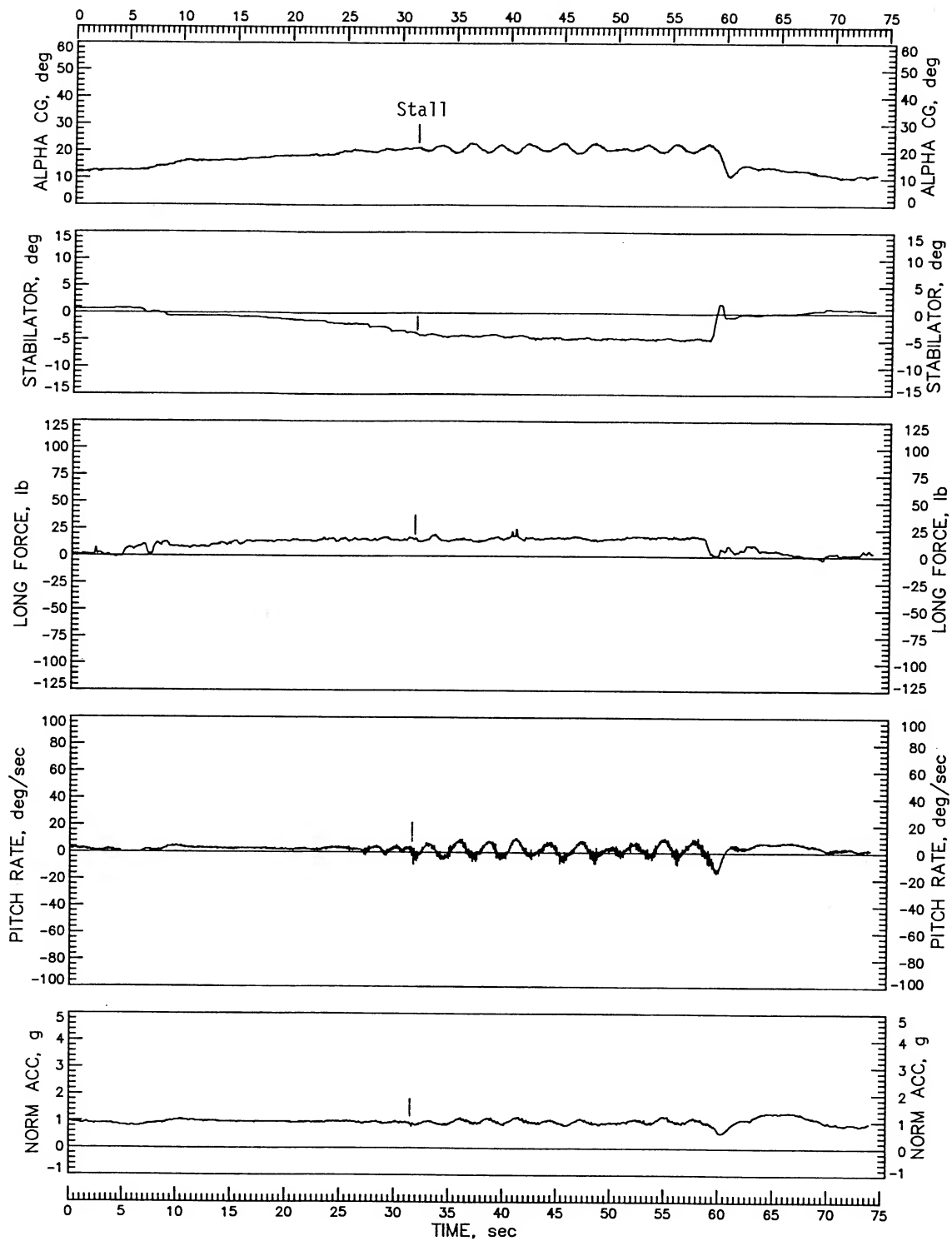


Figure 7. Slow deceleration to idle-power, 1g, wings-level stall with flaps and gear retracted.

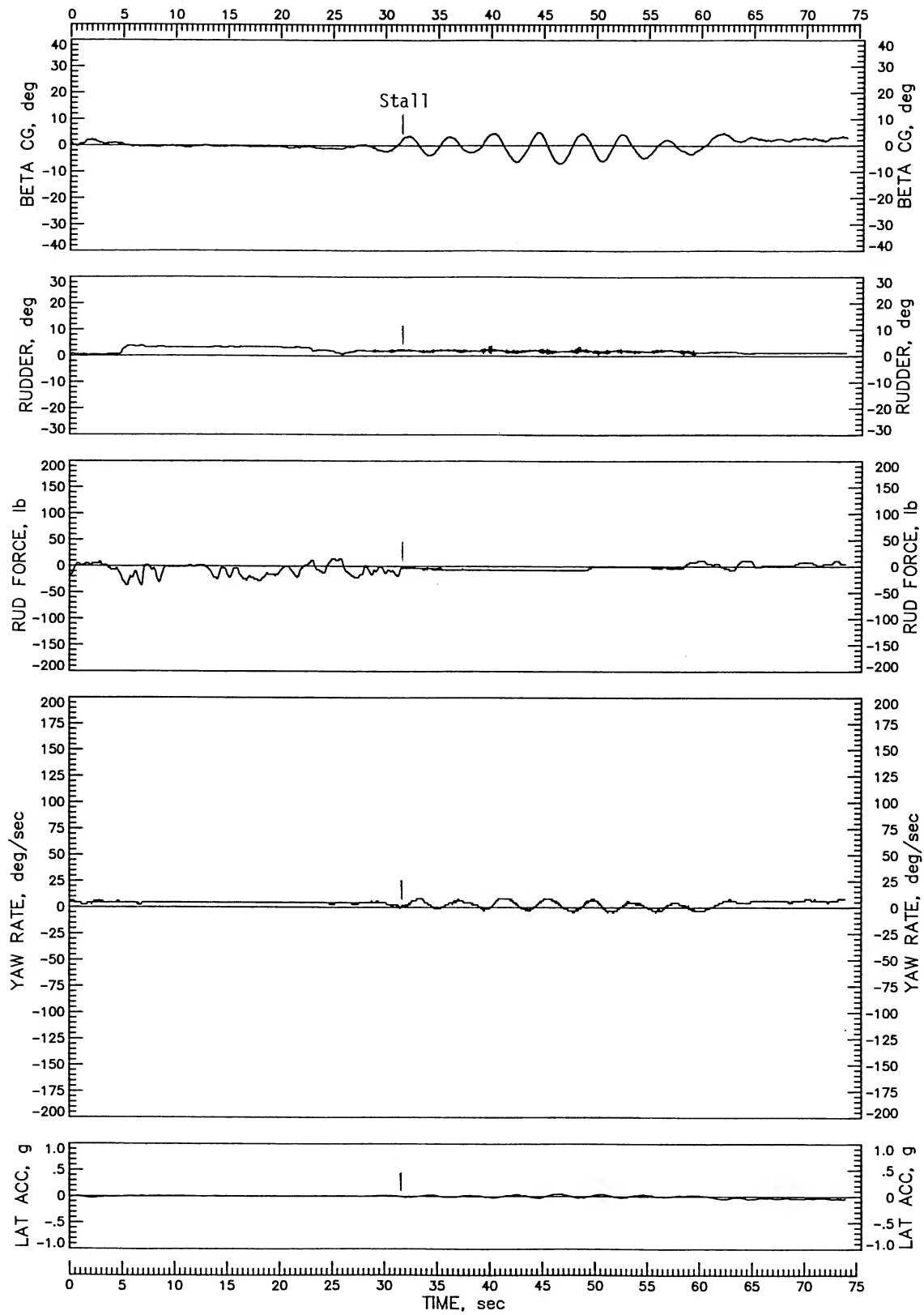


Figure 7. Continued.

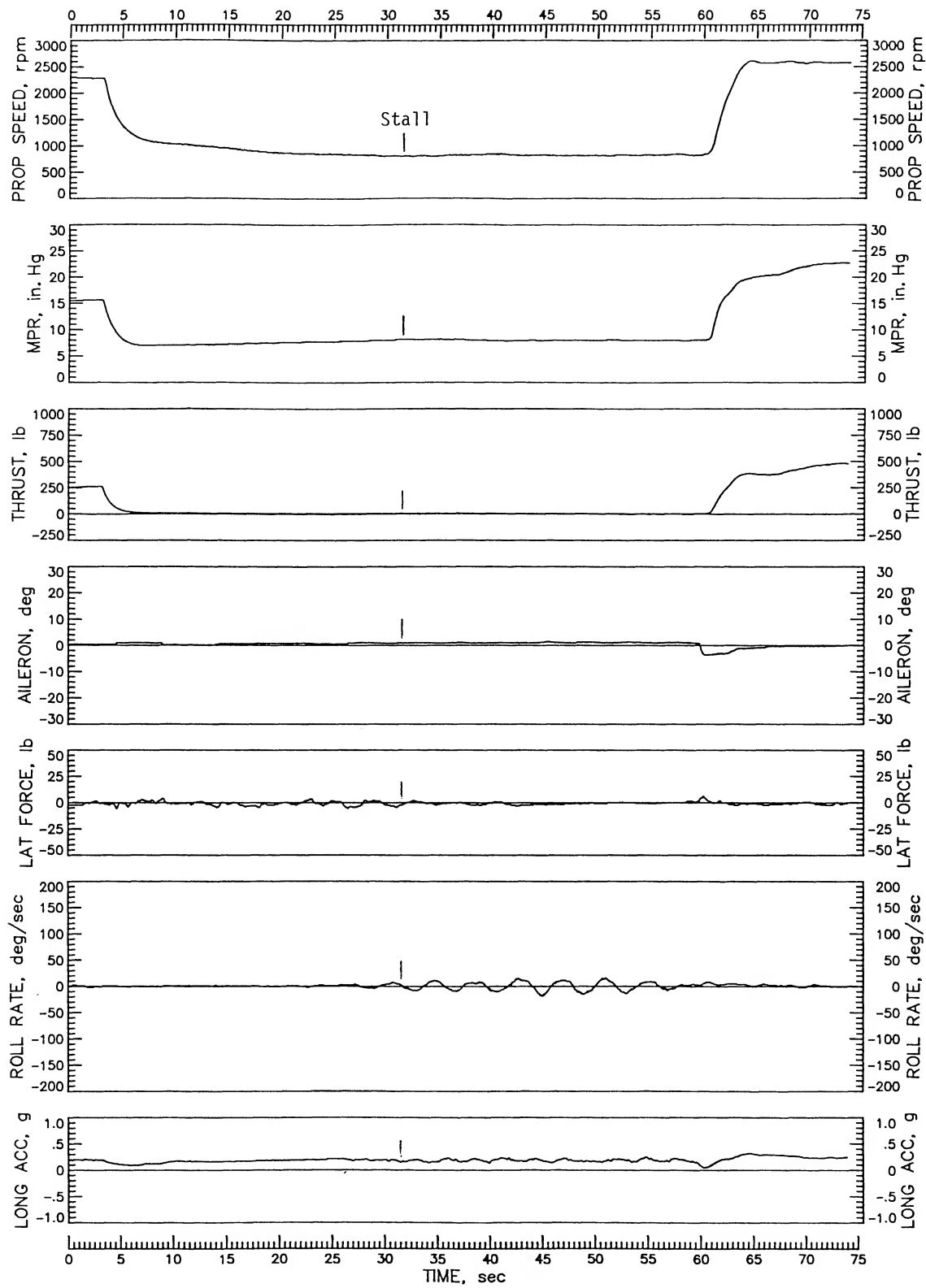


Figure 7. Continued.

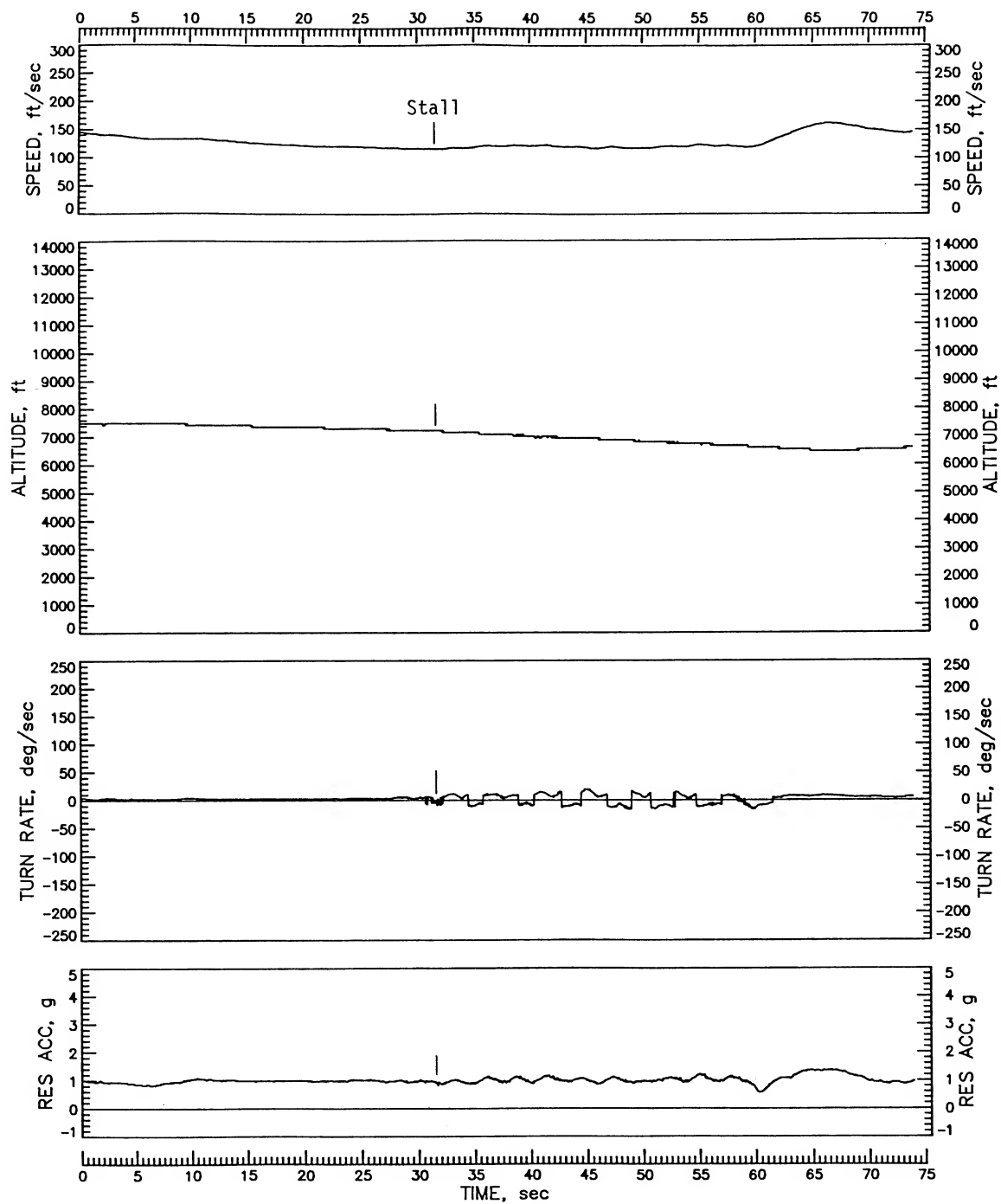


Figure 7. Concluded.

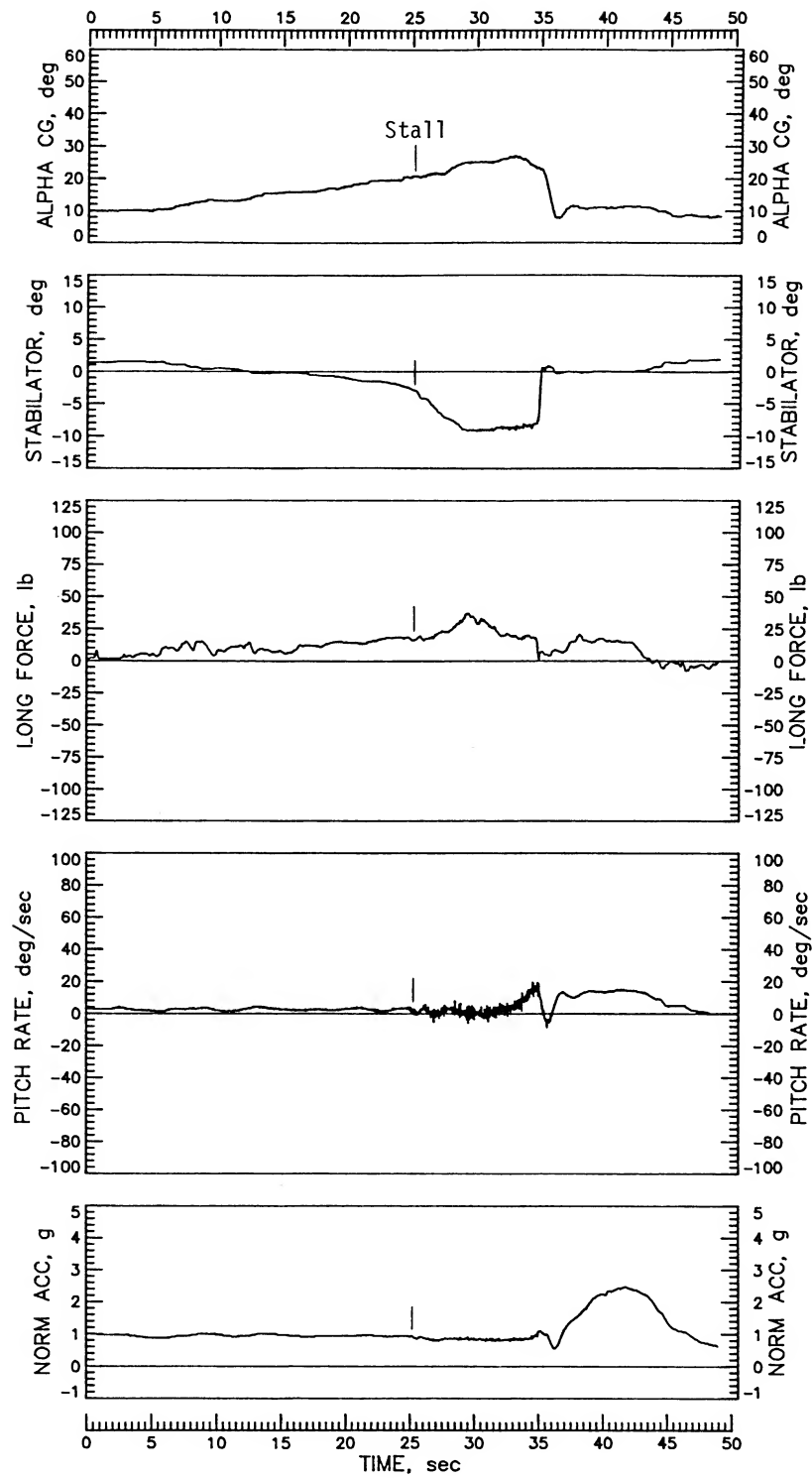


Figure 8. Idle-power, 1g, wings-level stall with maximum stabilator deflection, flaps and gear retracted.

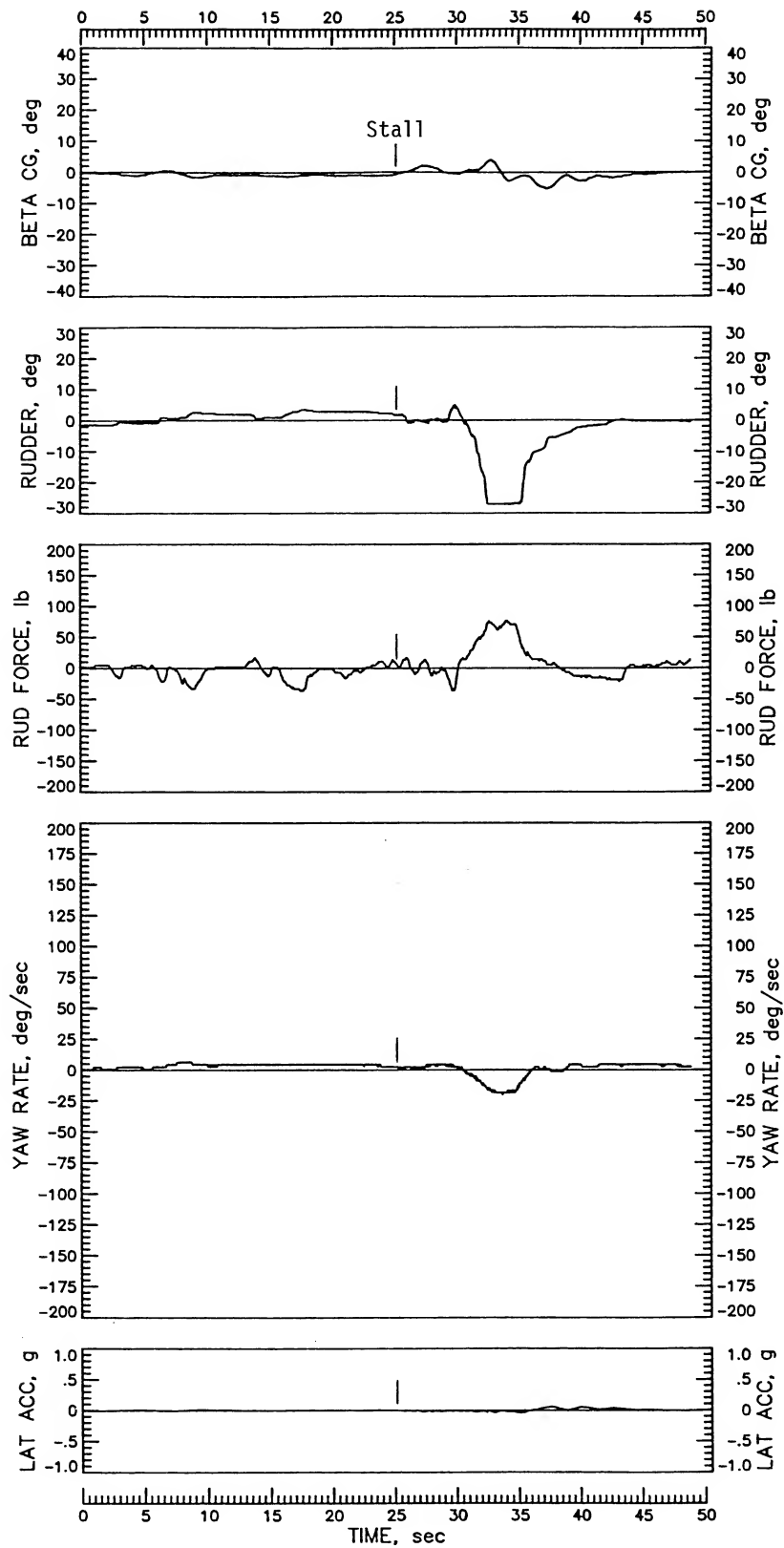


Figure 8. Continued.

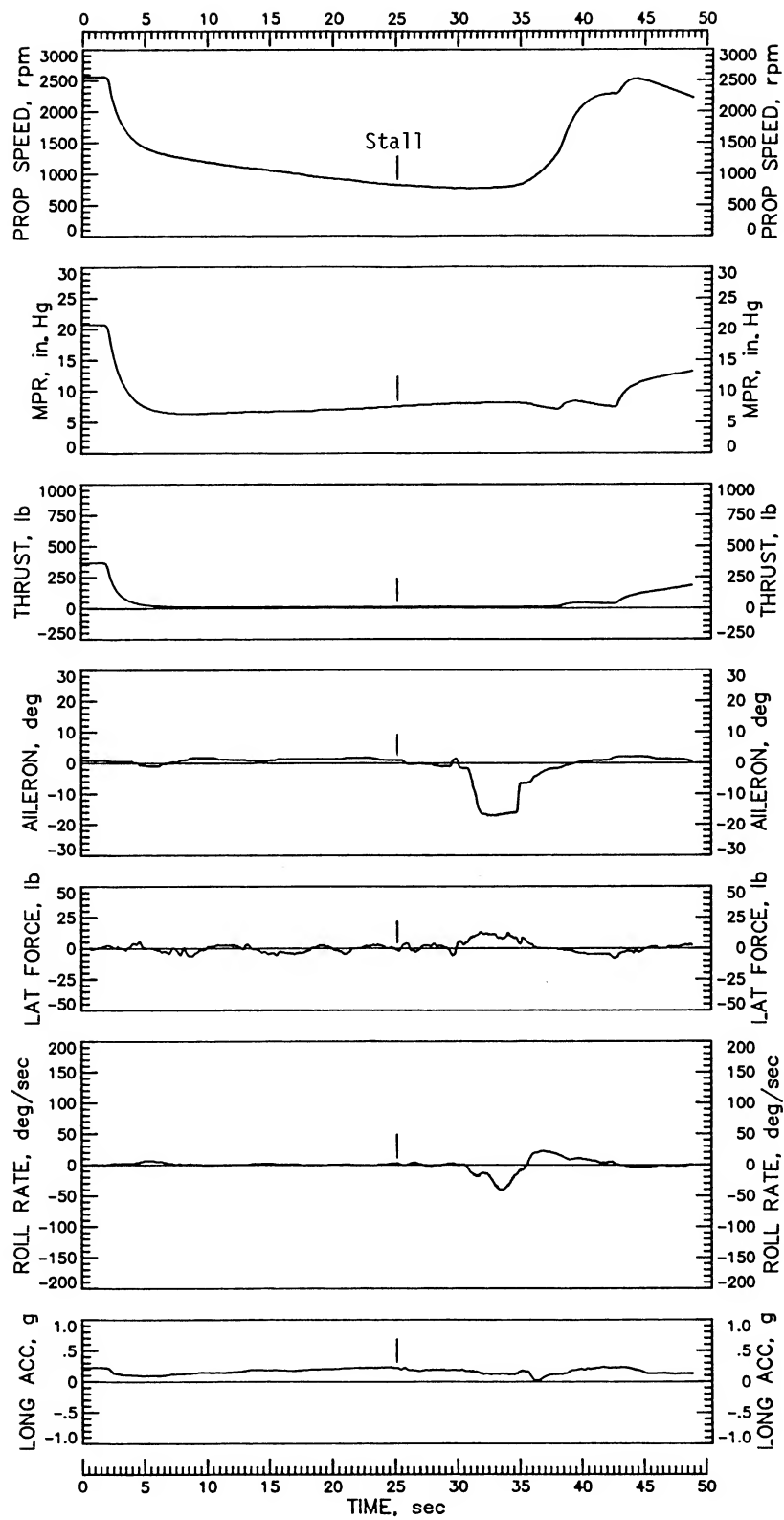


Figure 8. Continued.

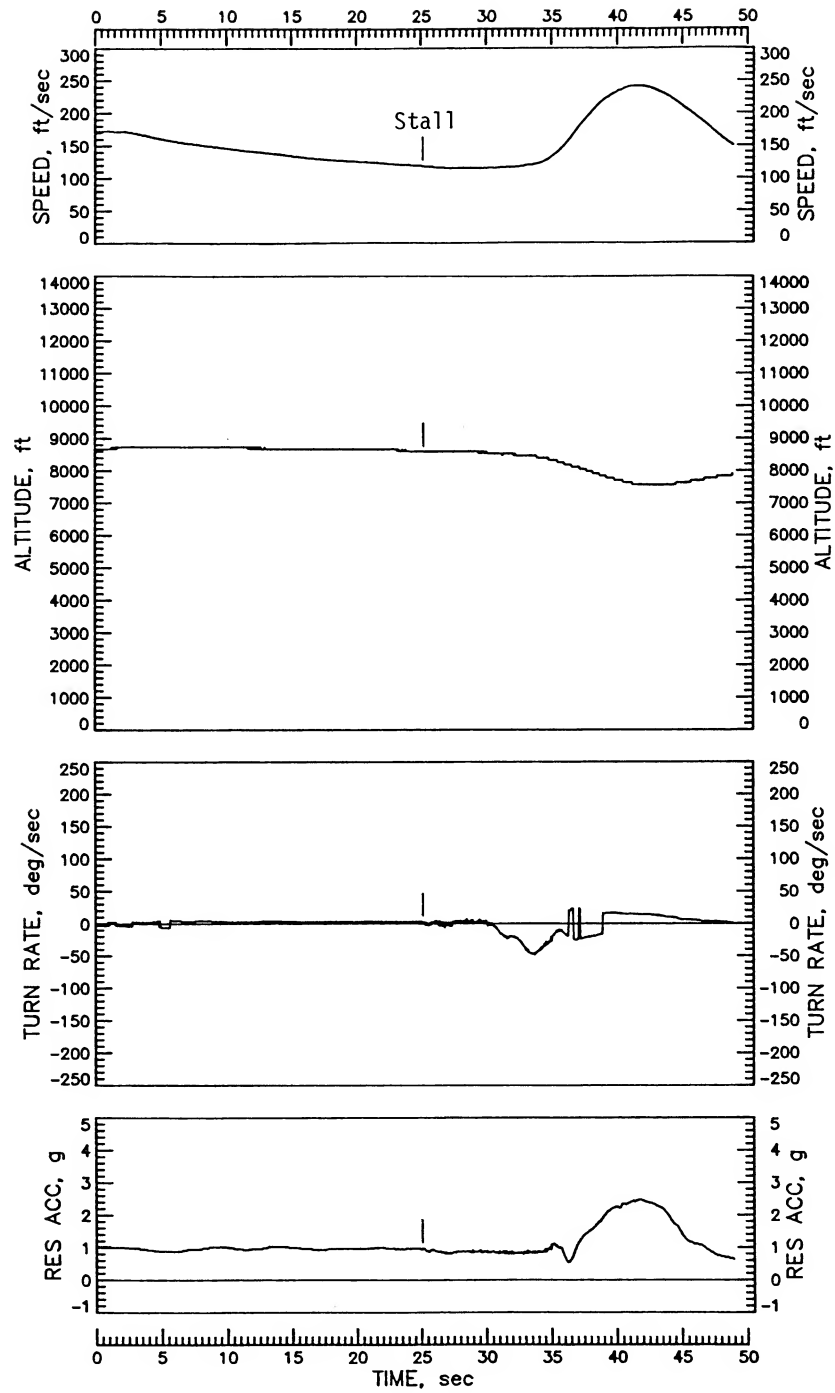


Figure 8. Concluded.

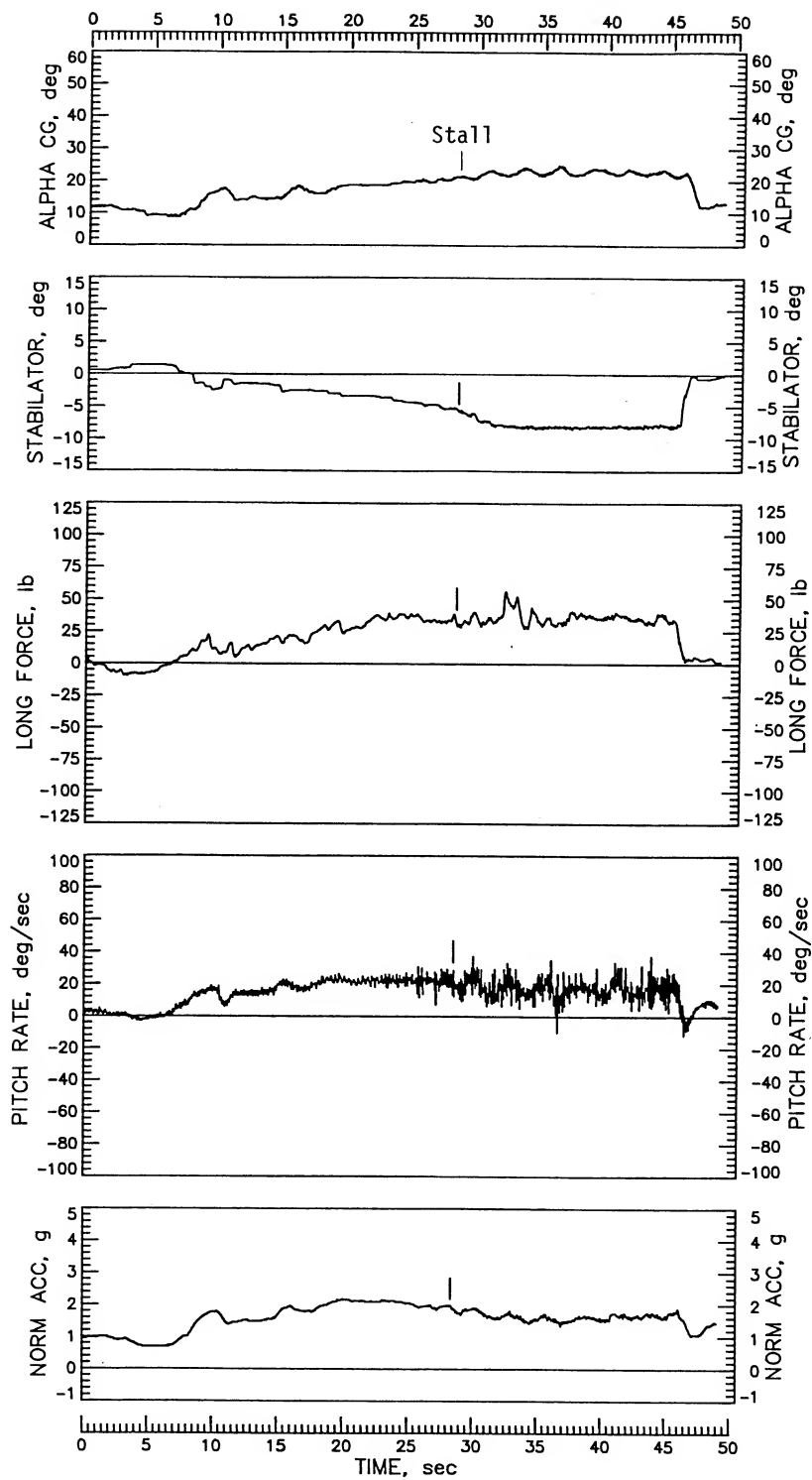


Figure 9. Idle-power stall from 60° banked left turn with flaps and gear retracted.

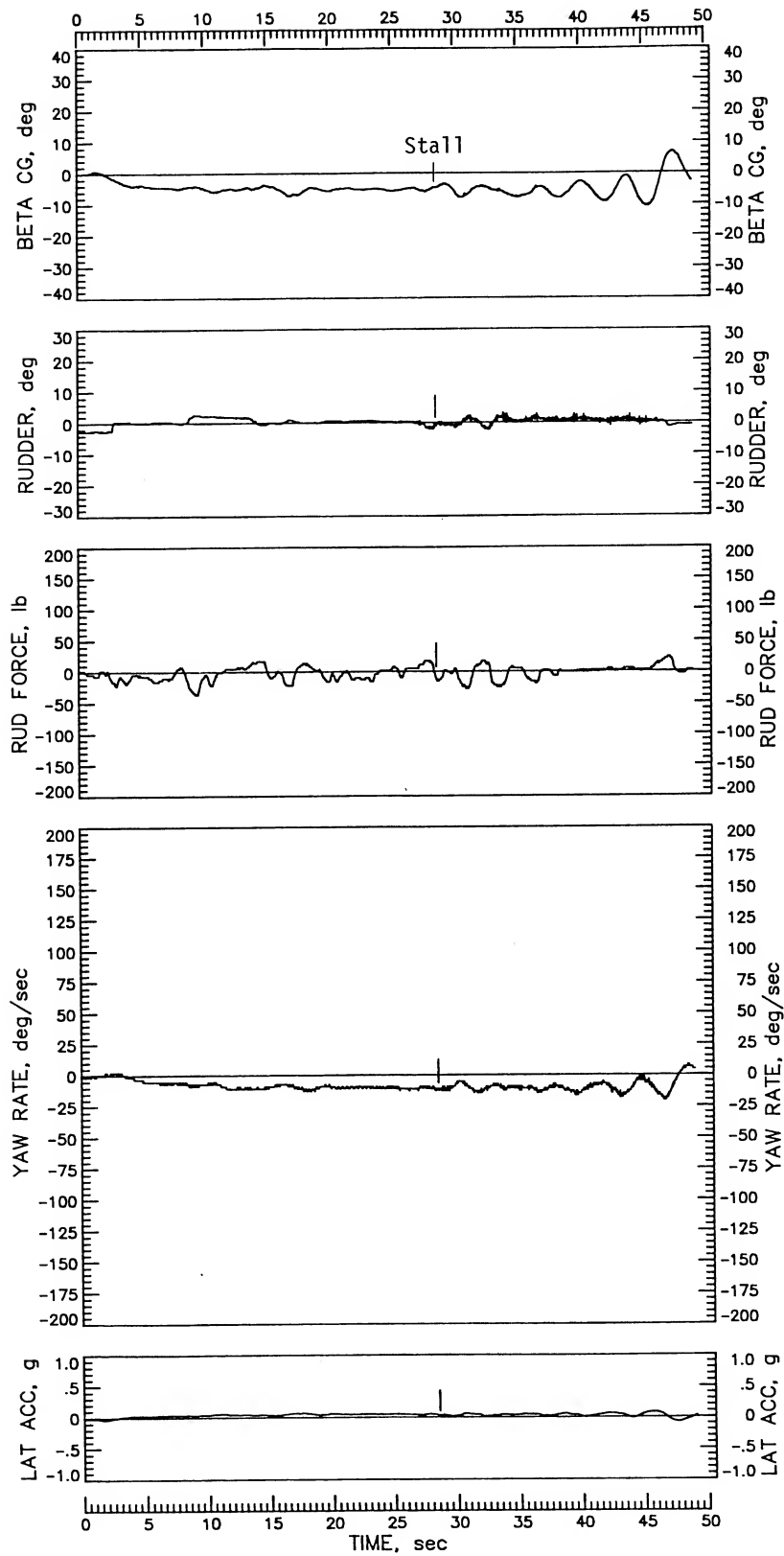


Figure 9. Continued.

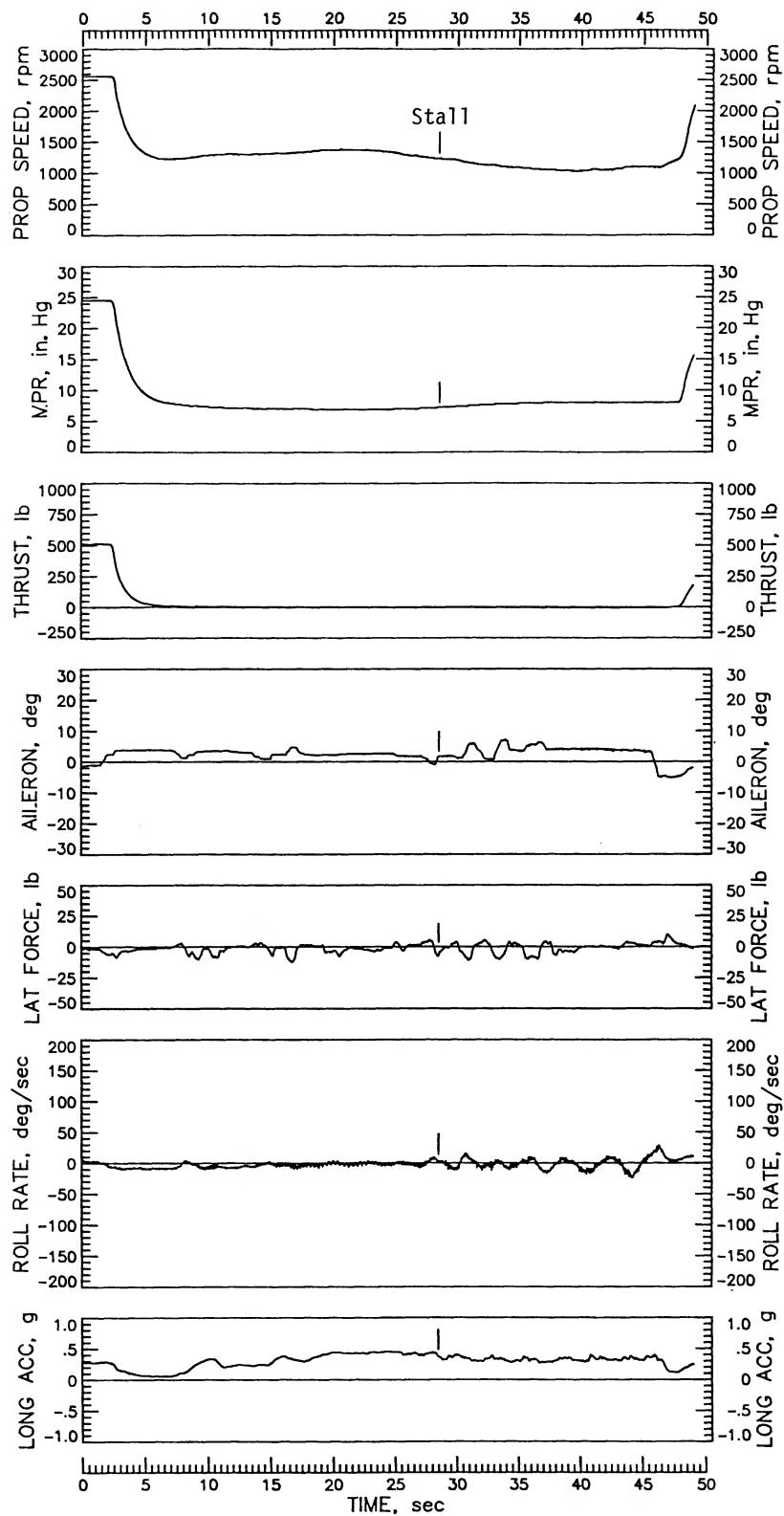


Figure 9. Continued.

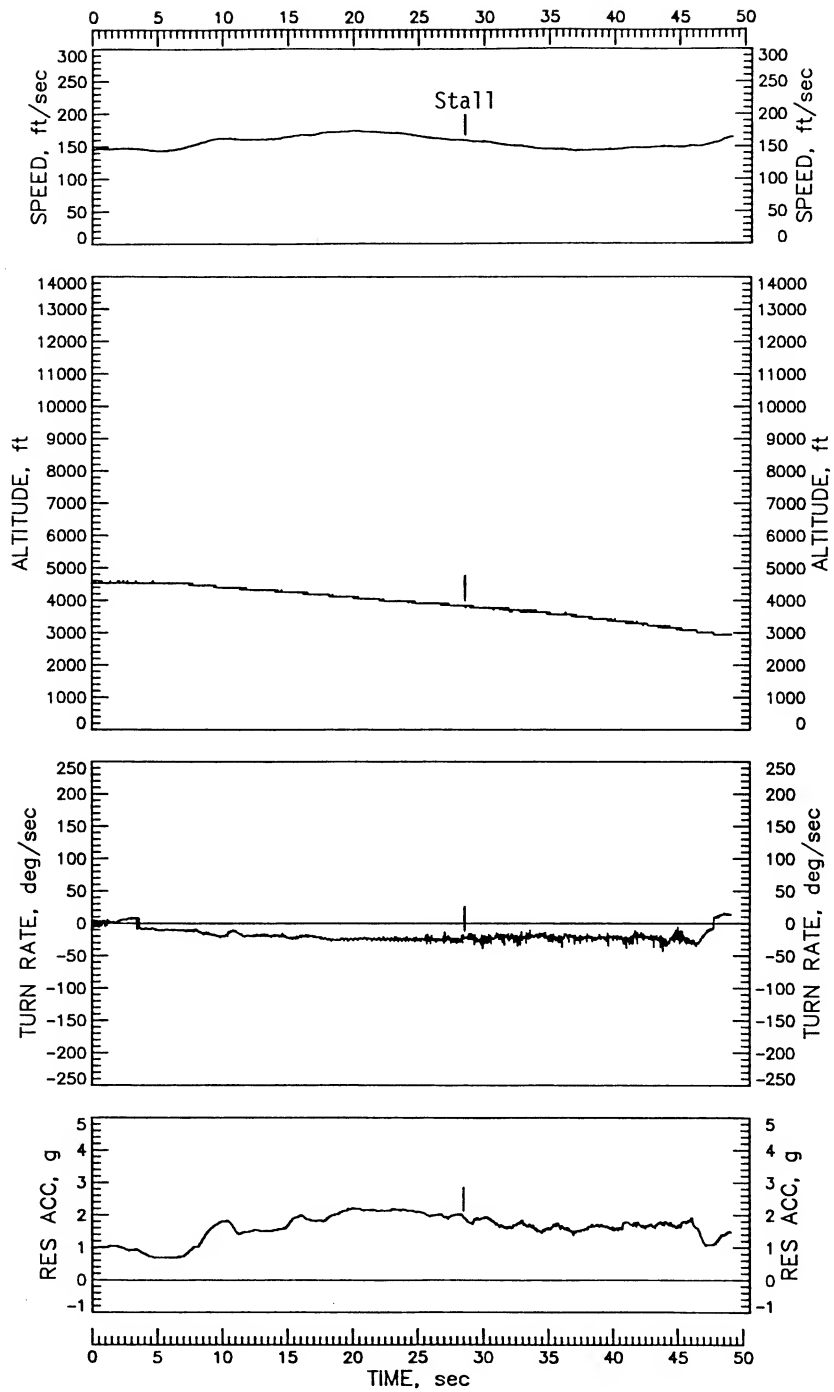


Figure 9. Concluded.

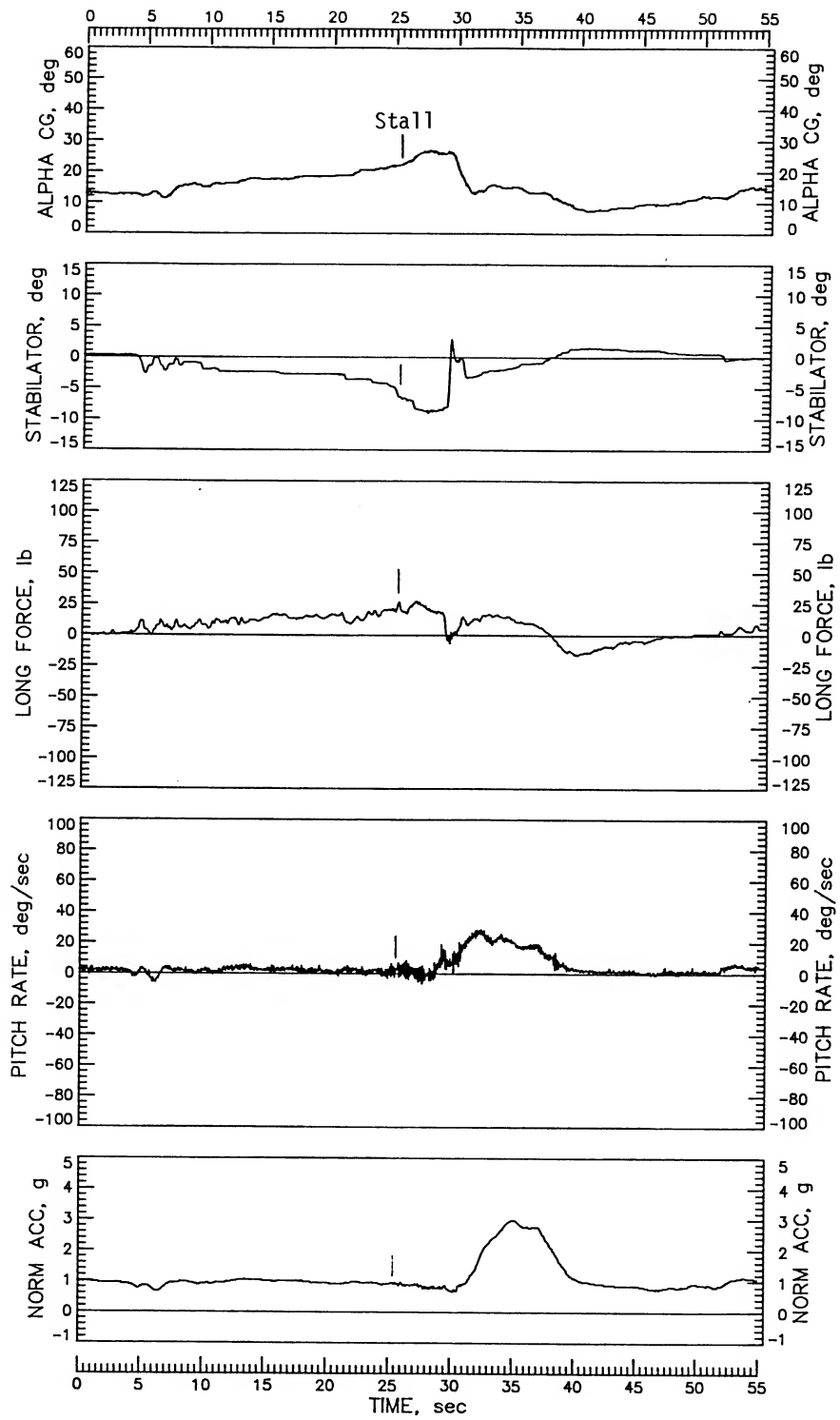


Figure 10. Idle-power stall from right slip with flaps and gear retracted.

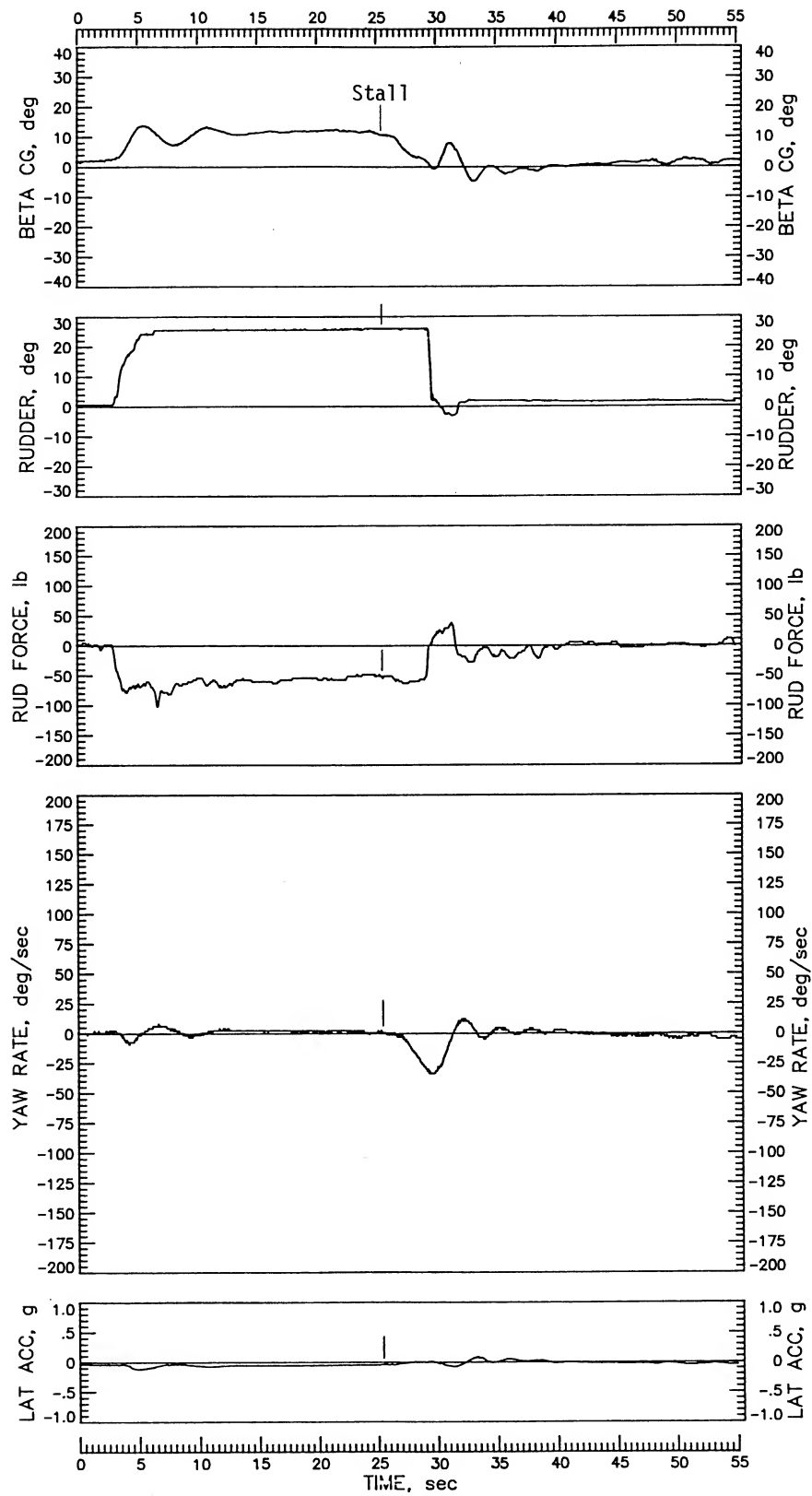


Figure 10. Continued.

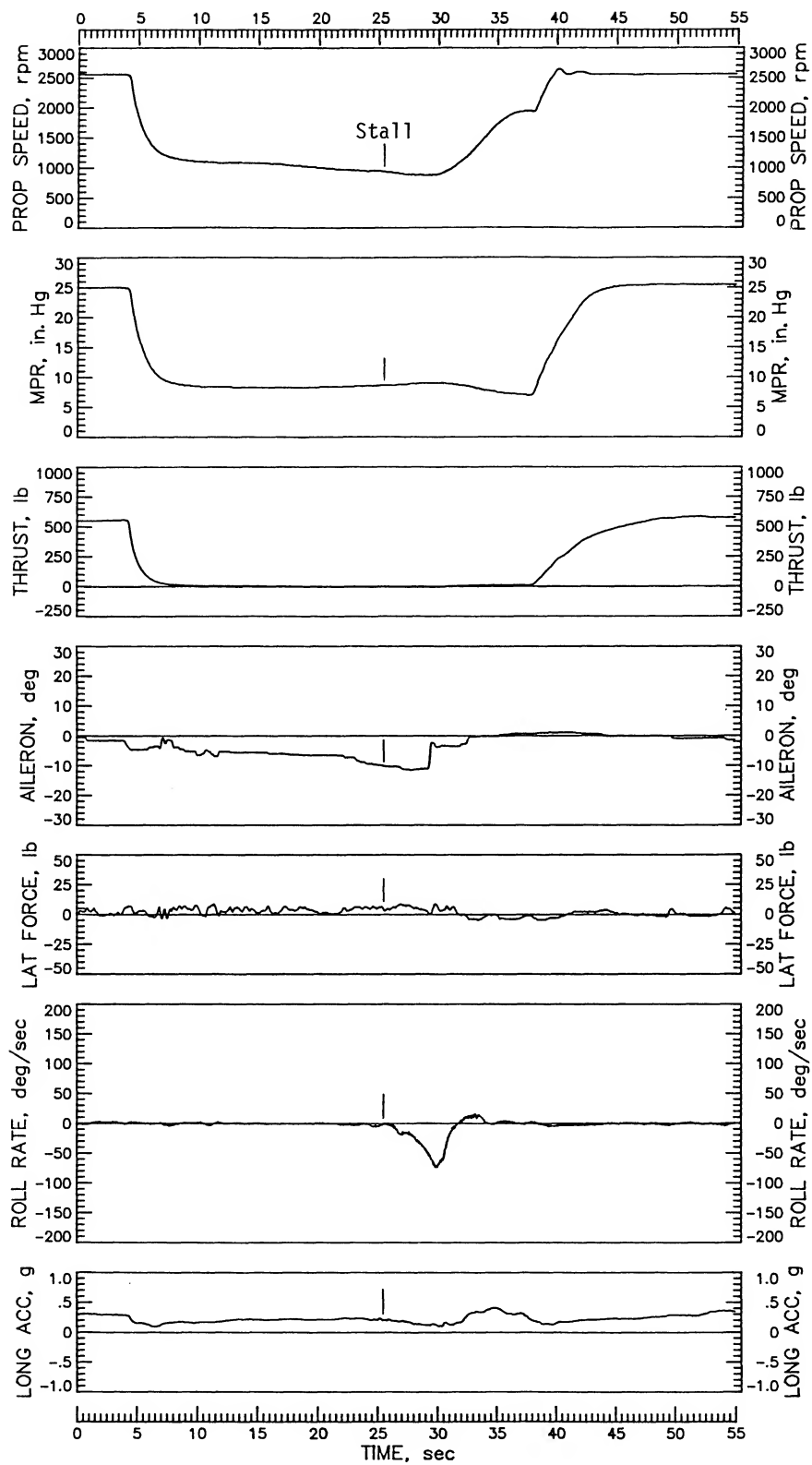


Figure 10. Continued.

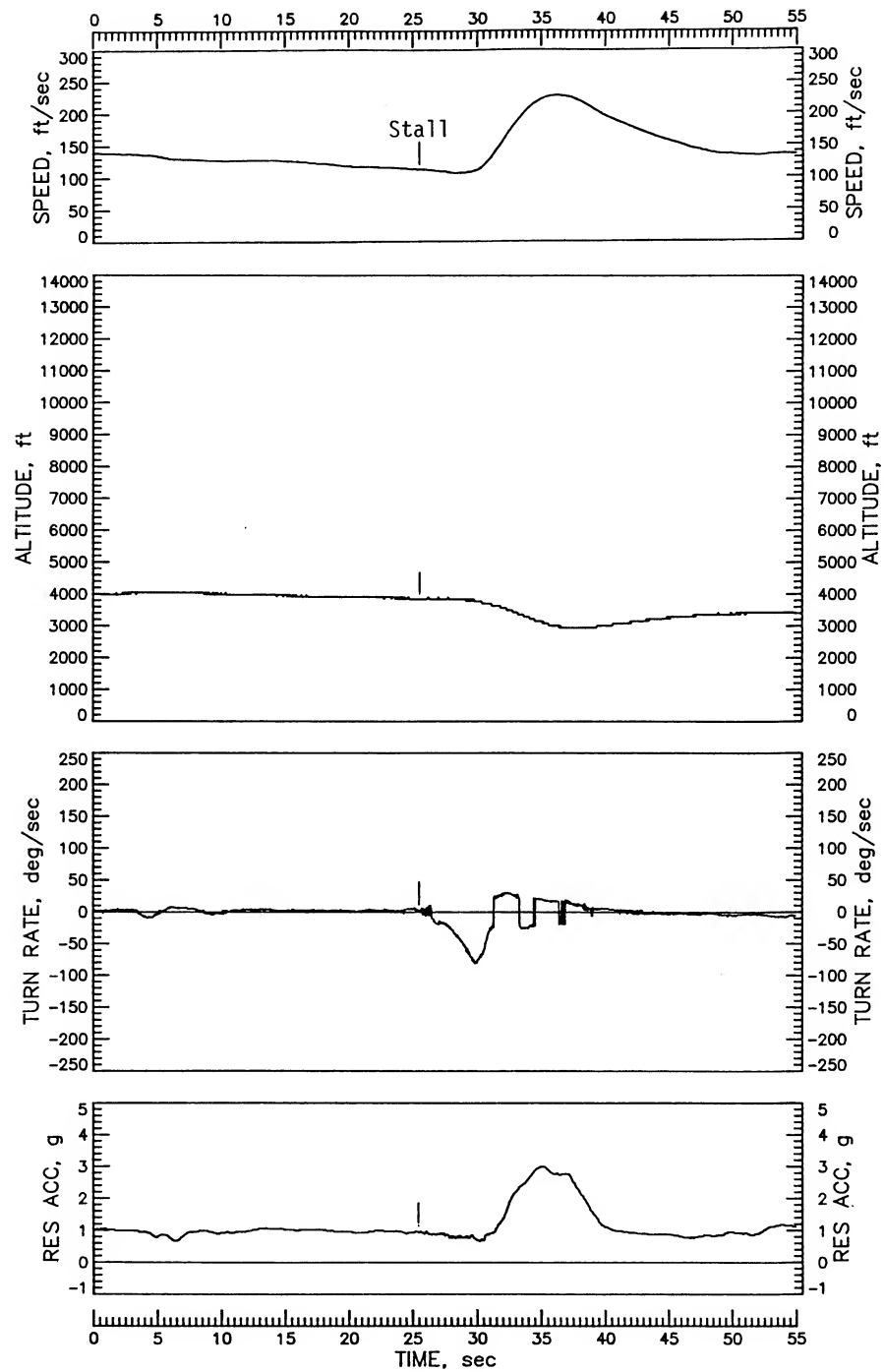


Figure 10. Concluded.

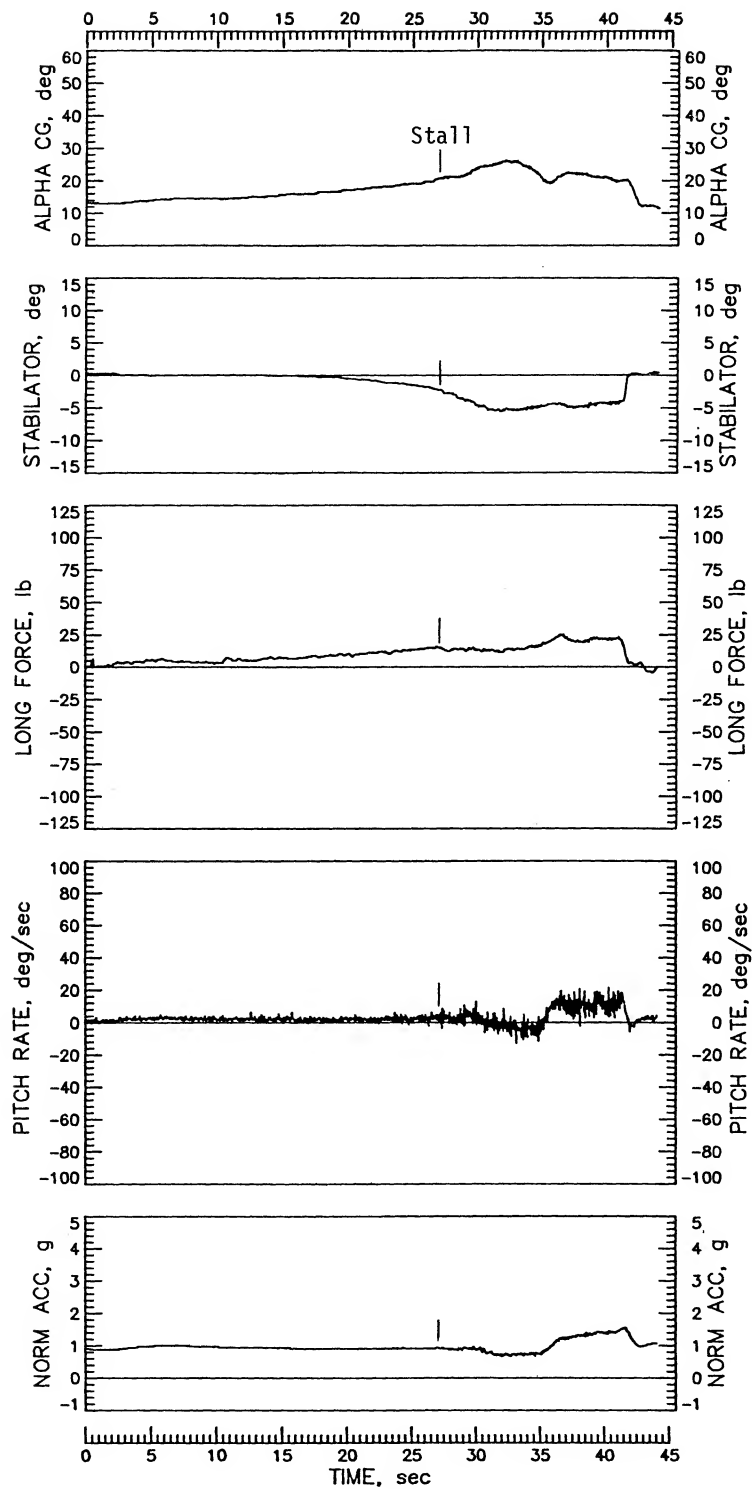


Figure 11. Slow deceleration to maximum-power, 1g, wings-level stall with flaps and gear retracted.

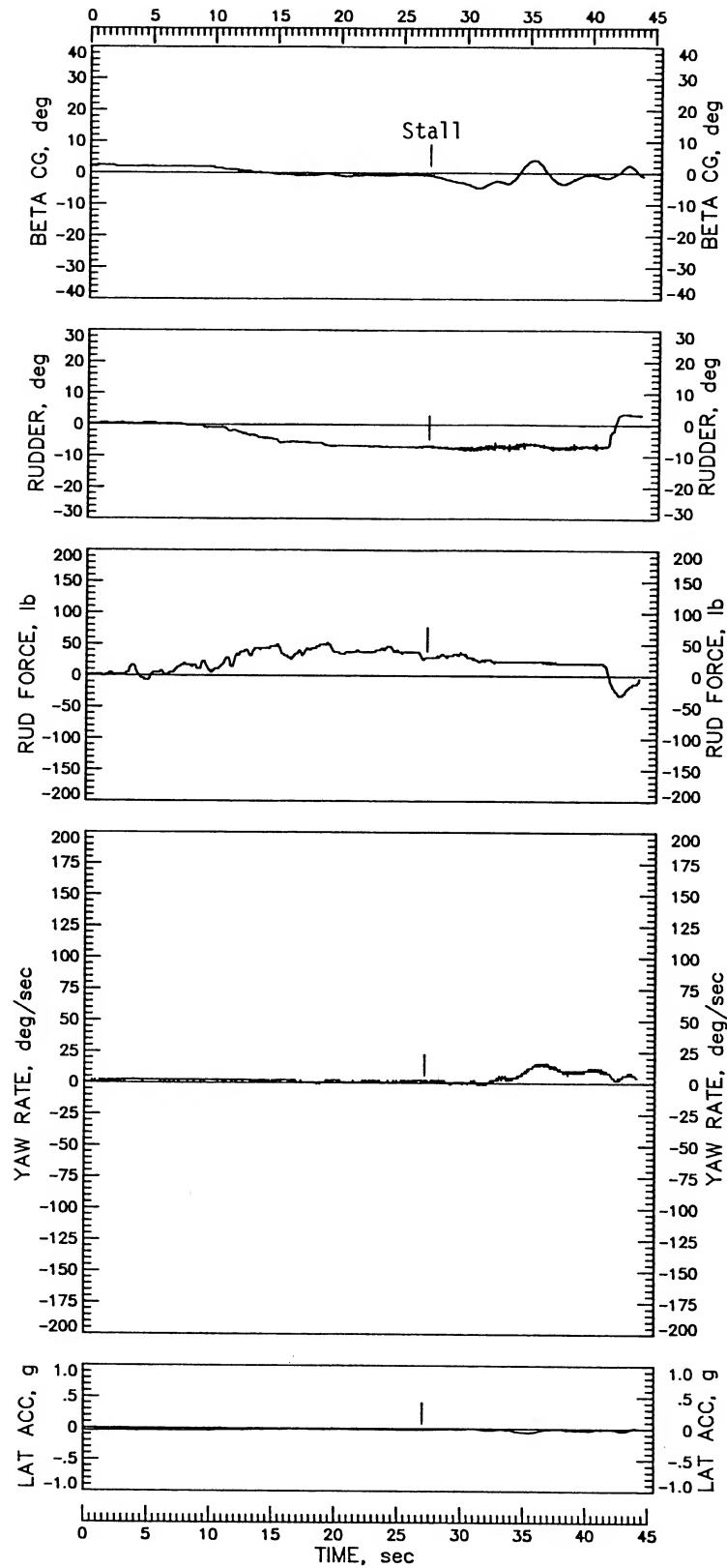


Figure 11. Continued.

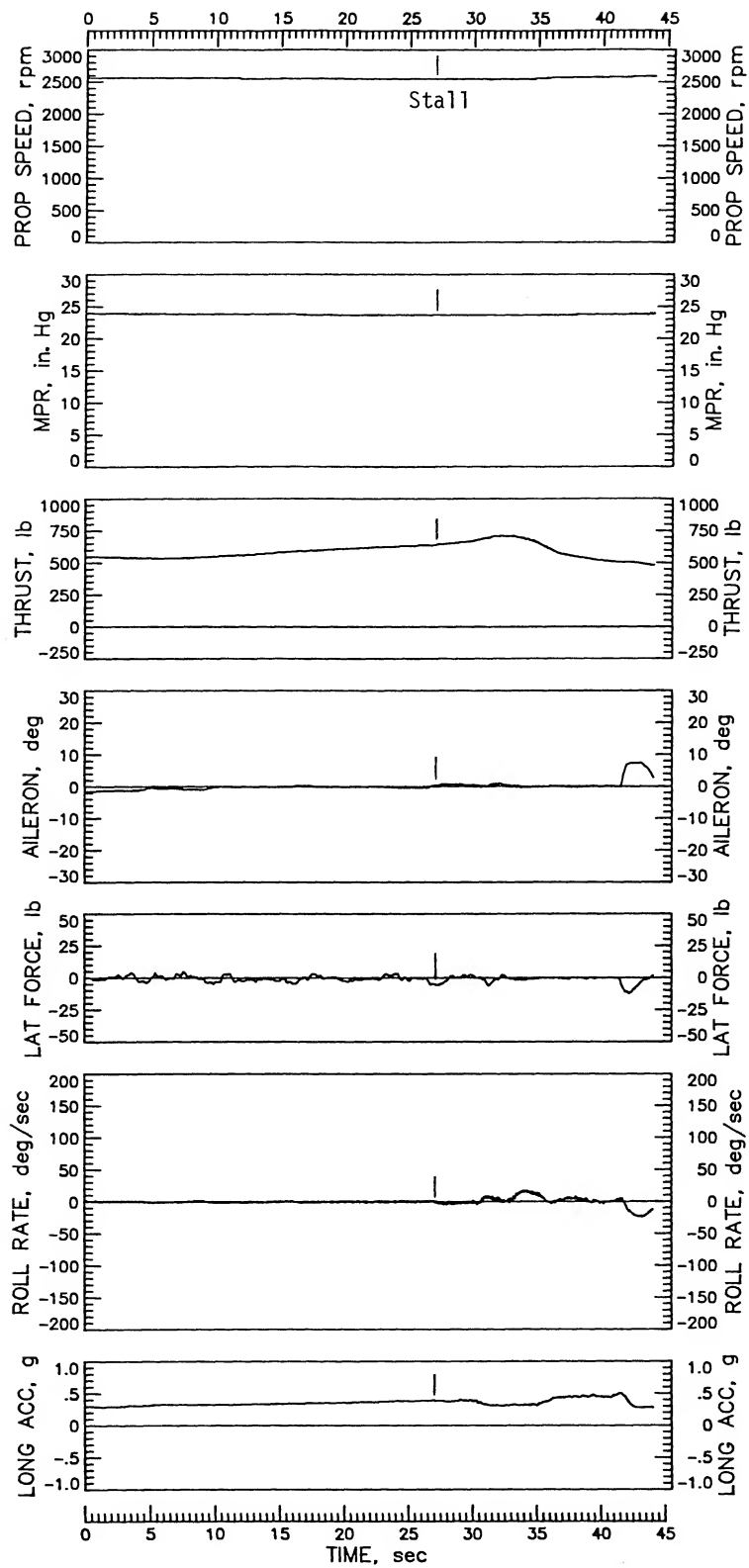


Figure 11. Continued.

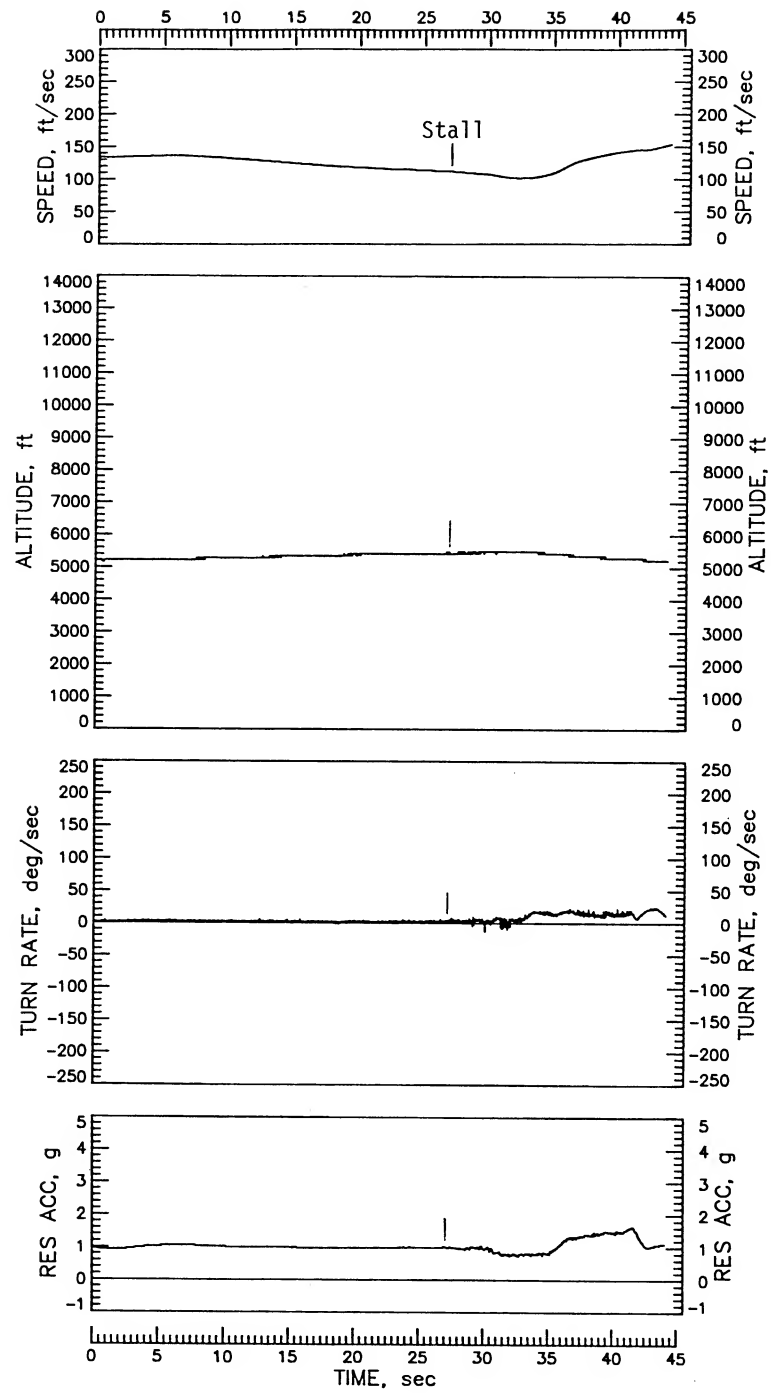


Figure 11. Concluded.

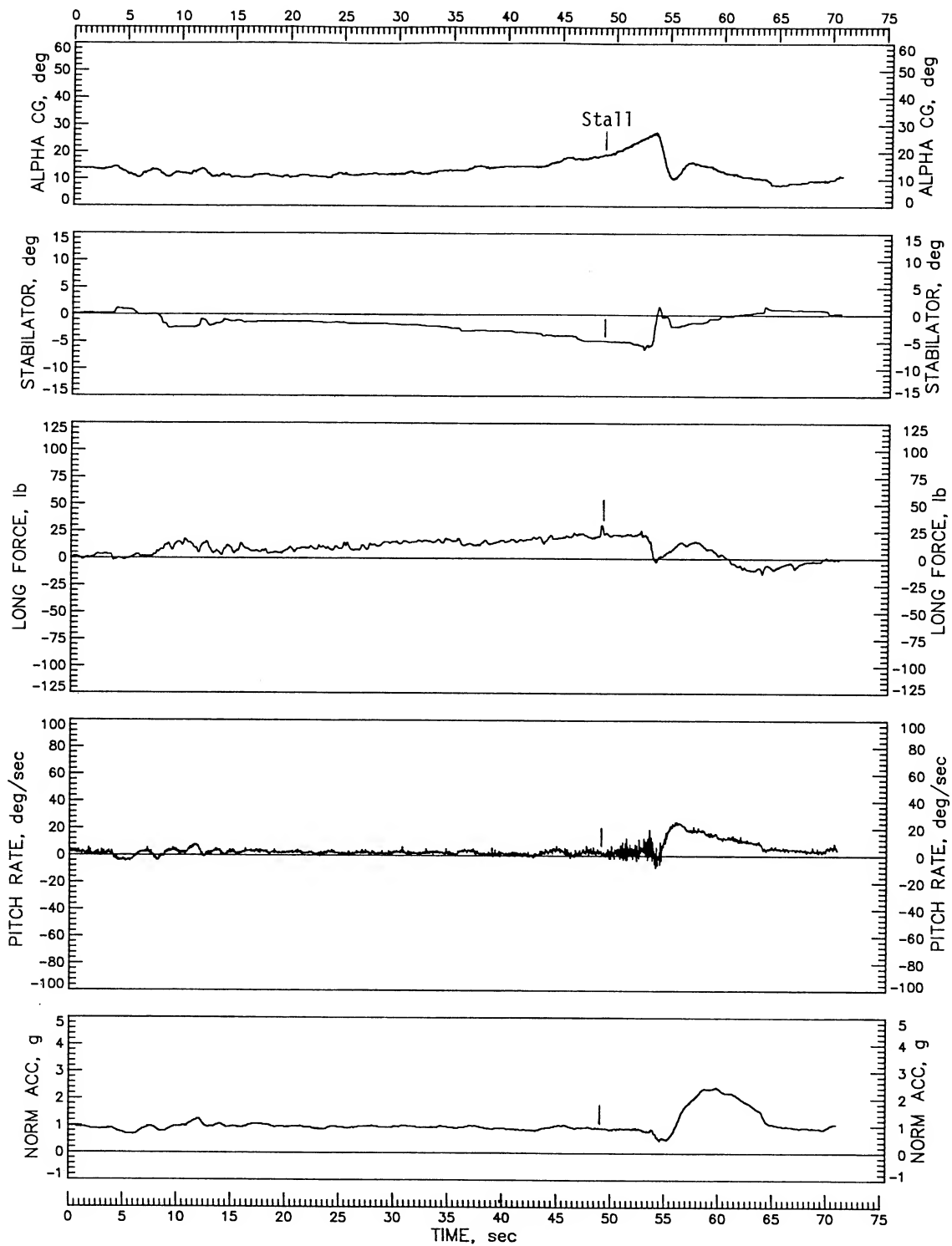


Figure 12. Maximum-power stall from right slip with flaps and gear retracted.

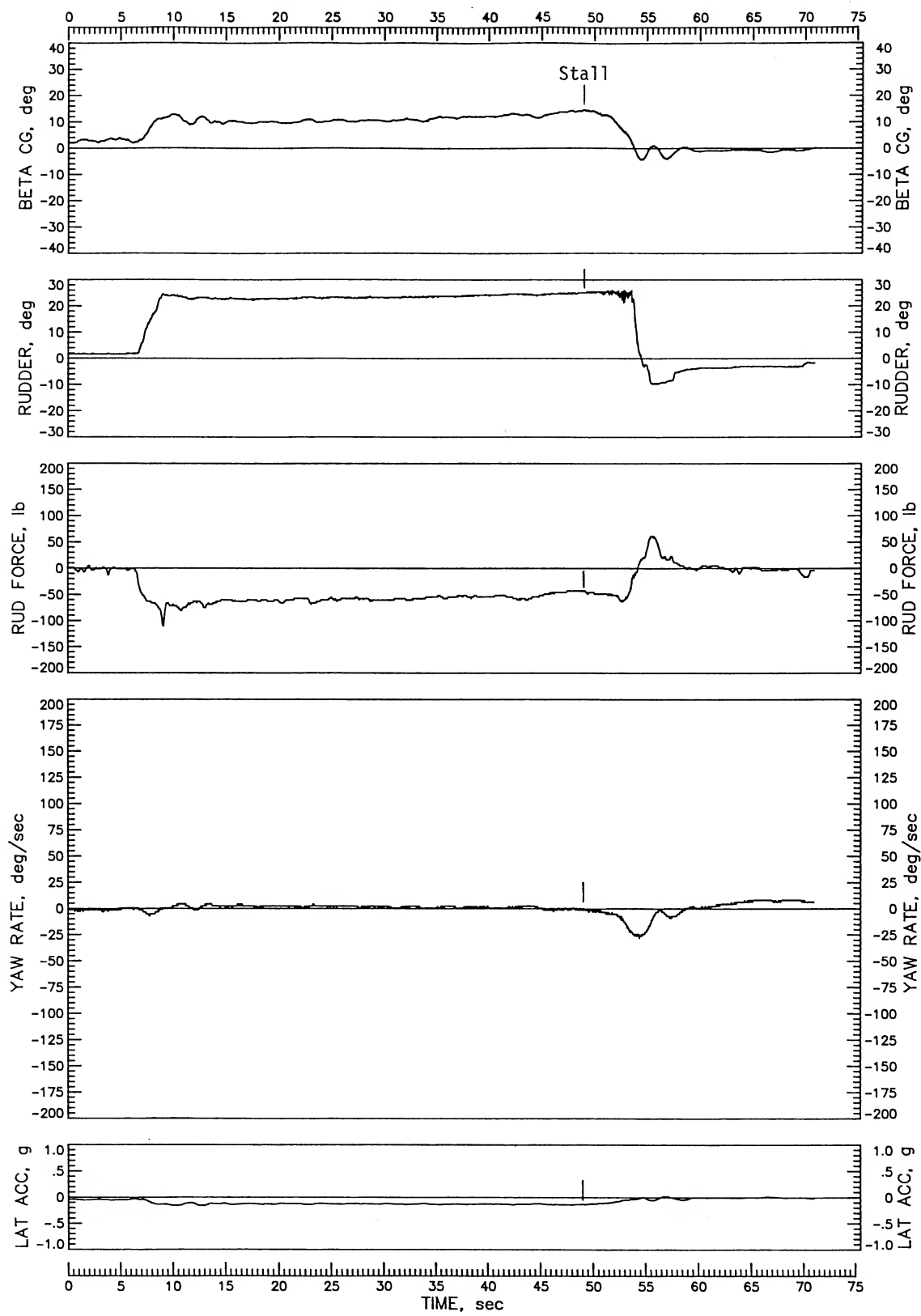


Figure 12. Continued.

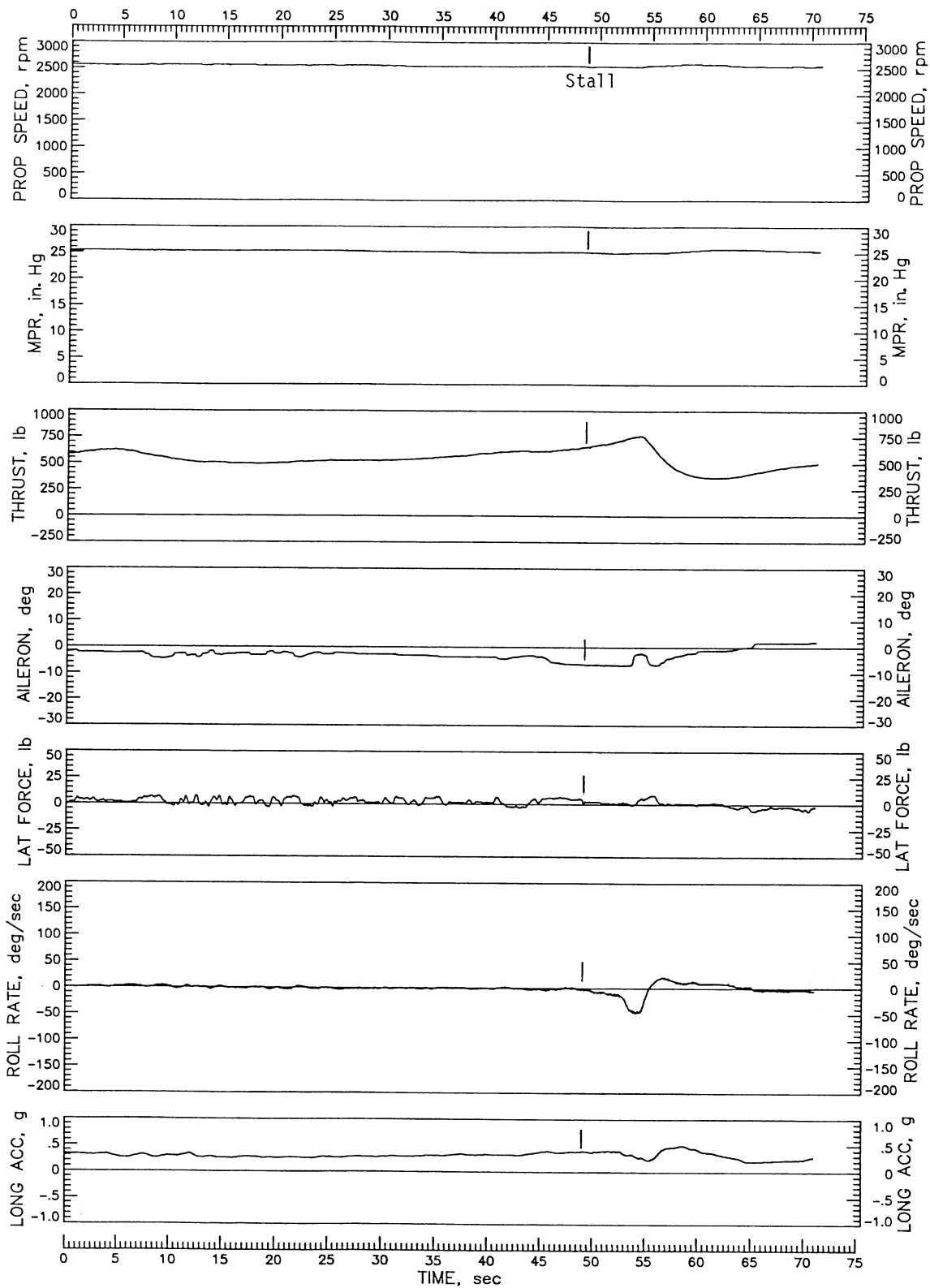


Figure 12. Continued.

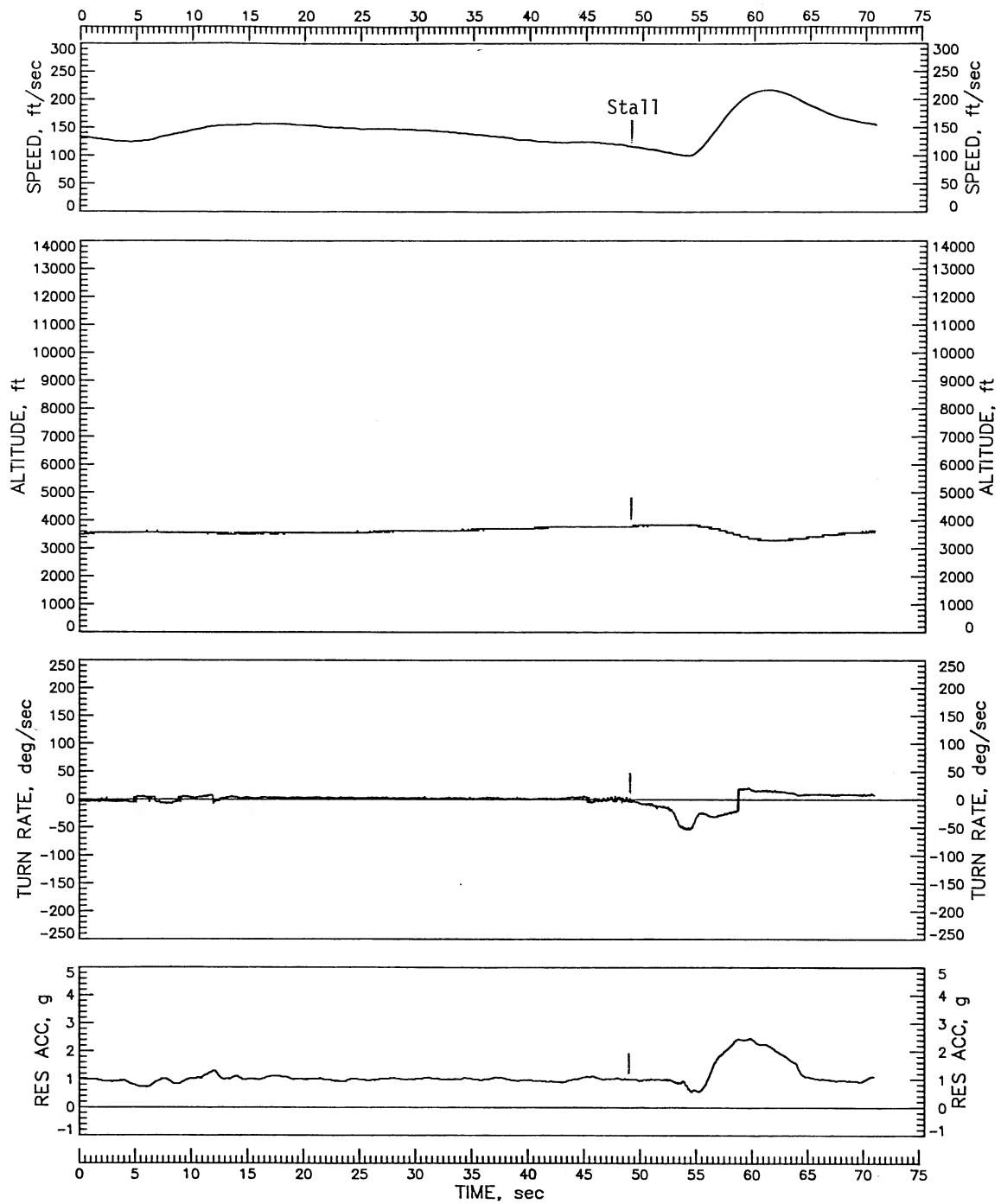


Figure 12. Concluded.

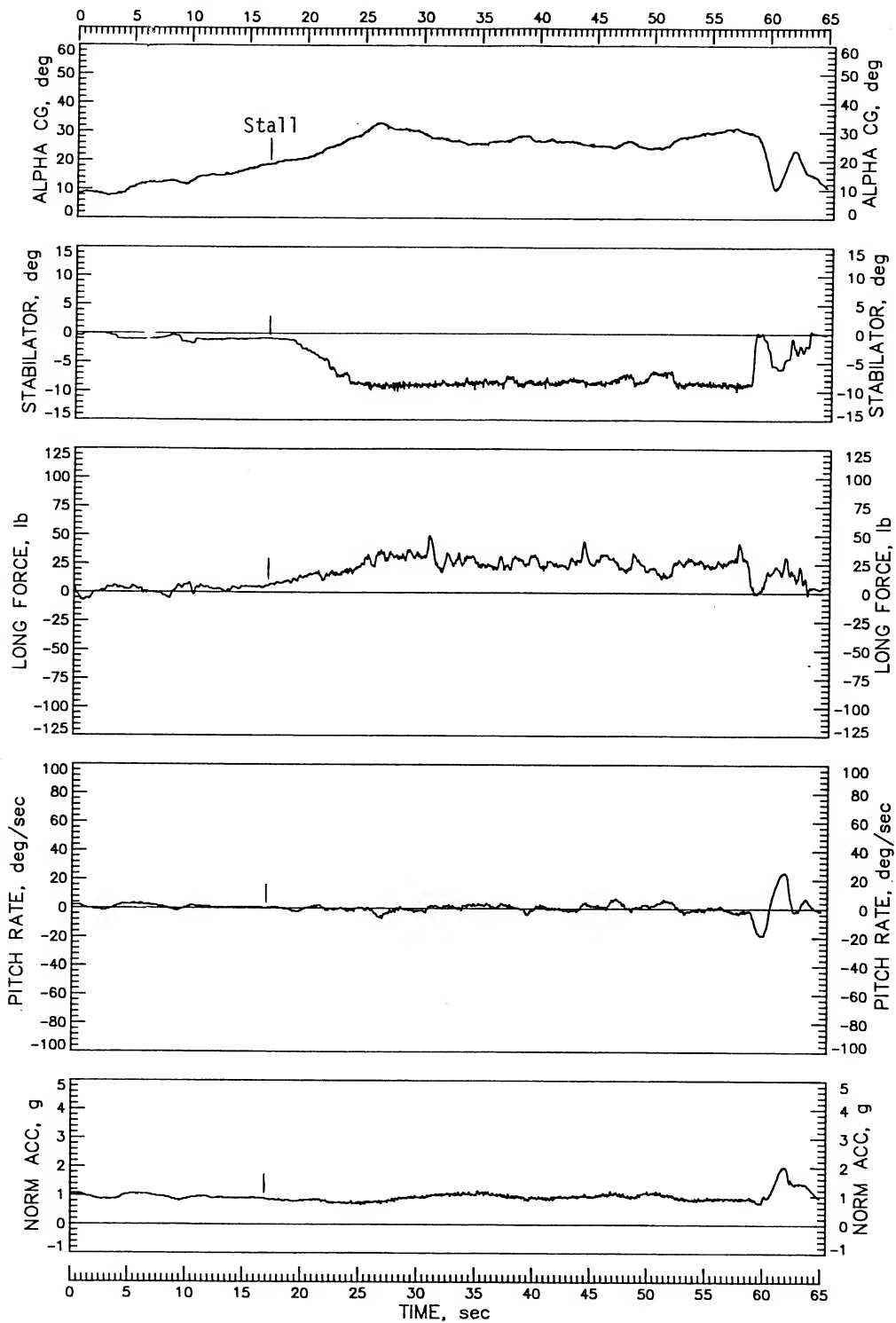


Figure 13. Maximum-power stall with flaps extended 40° and gear retracted.

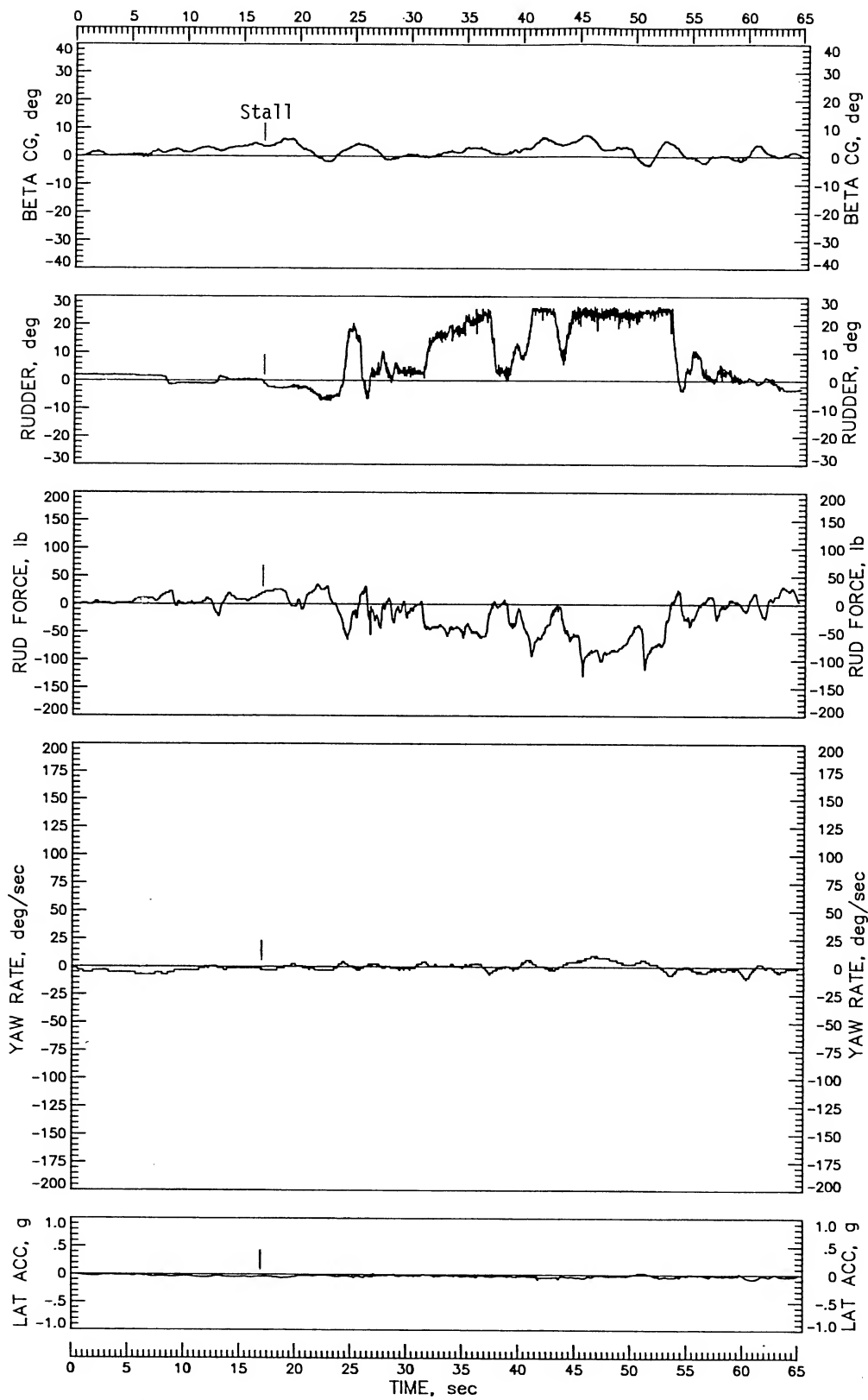


Figure 13. Continued.

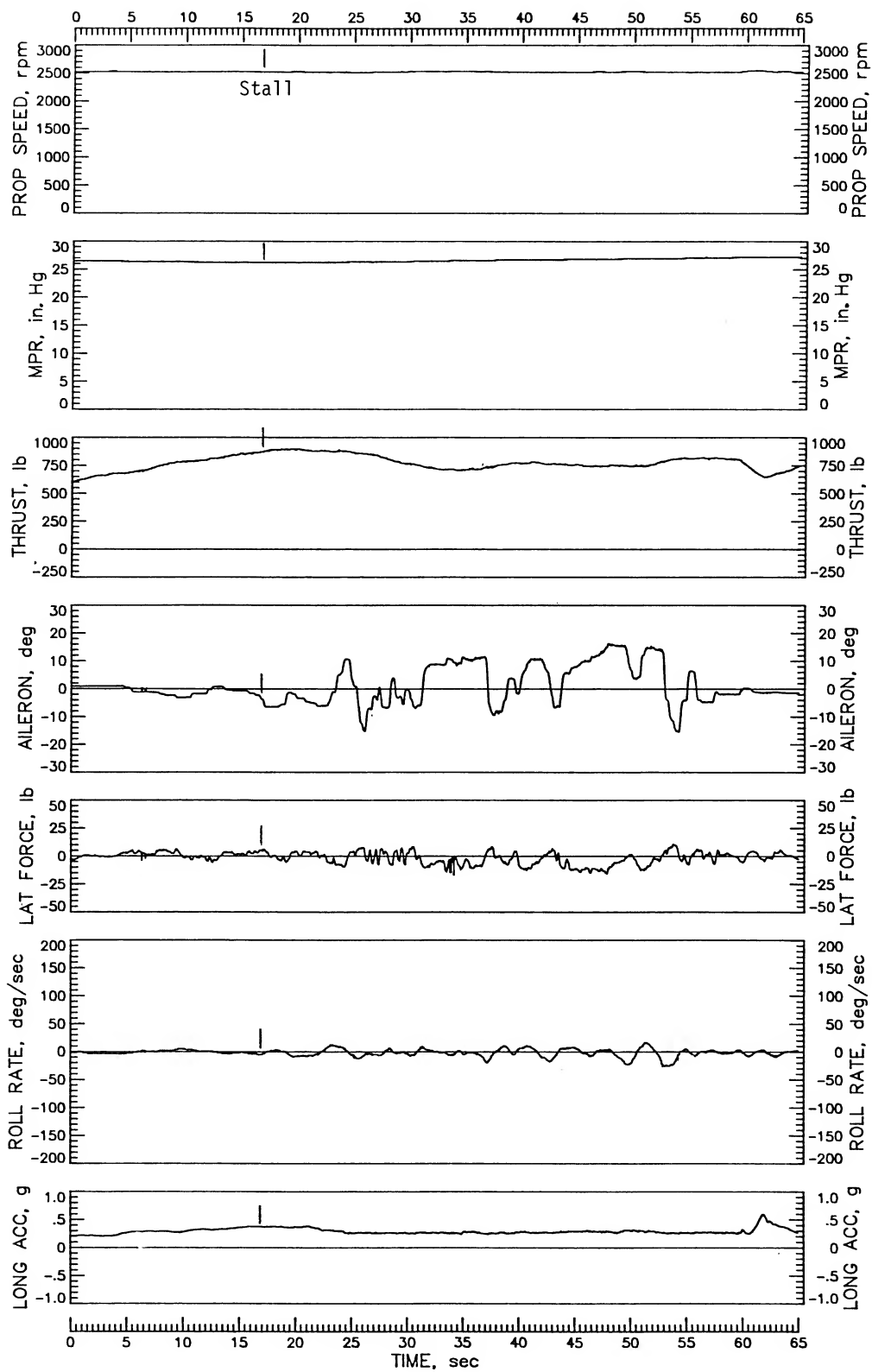


Figure 13. Continued.

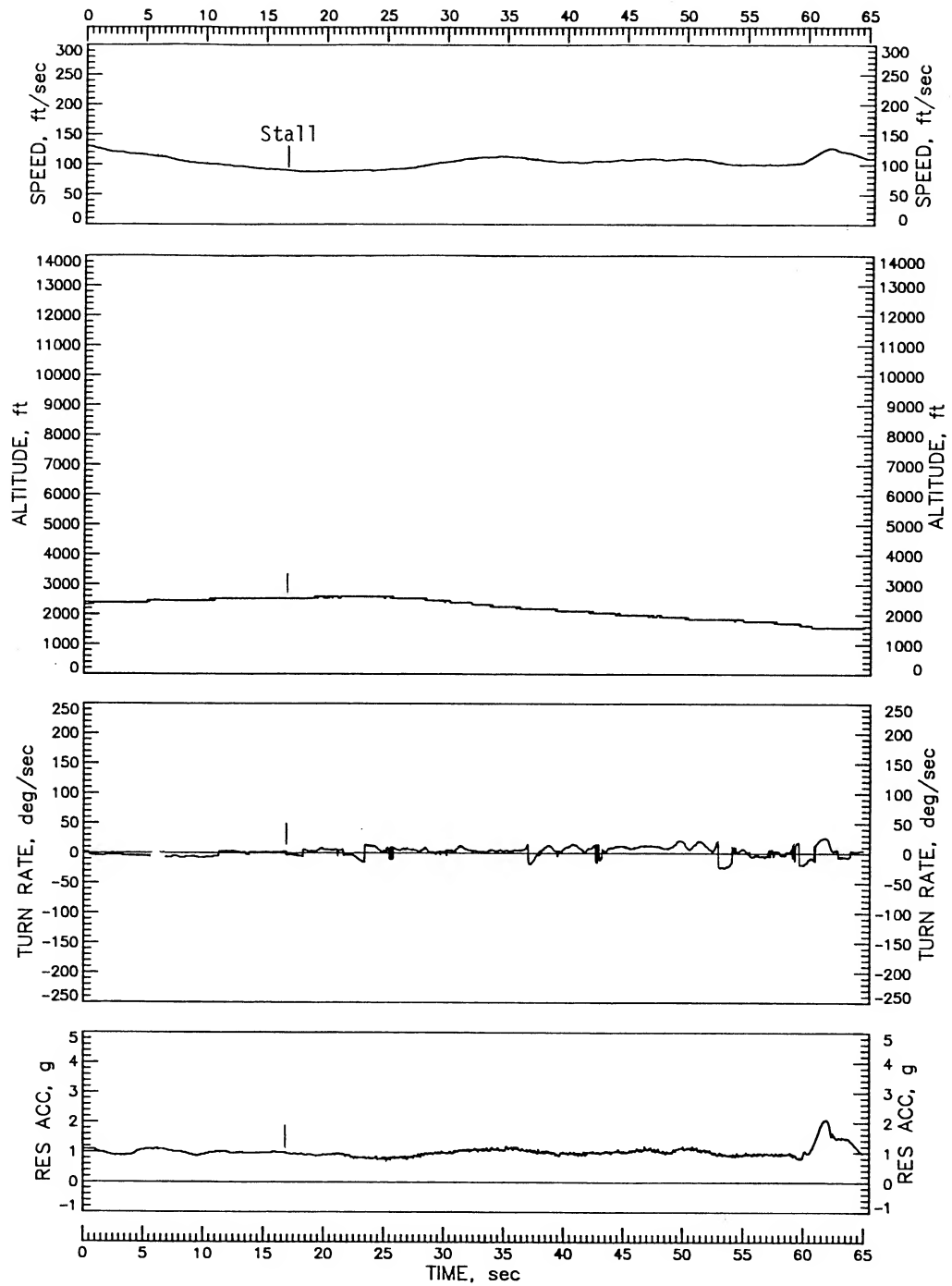


Figure 13. Concluded.

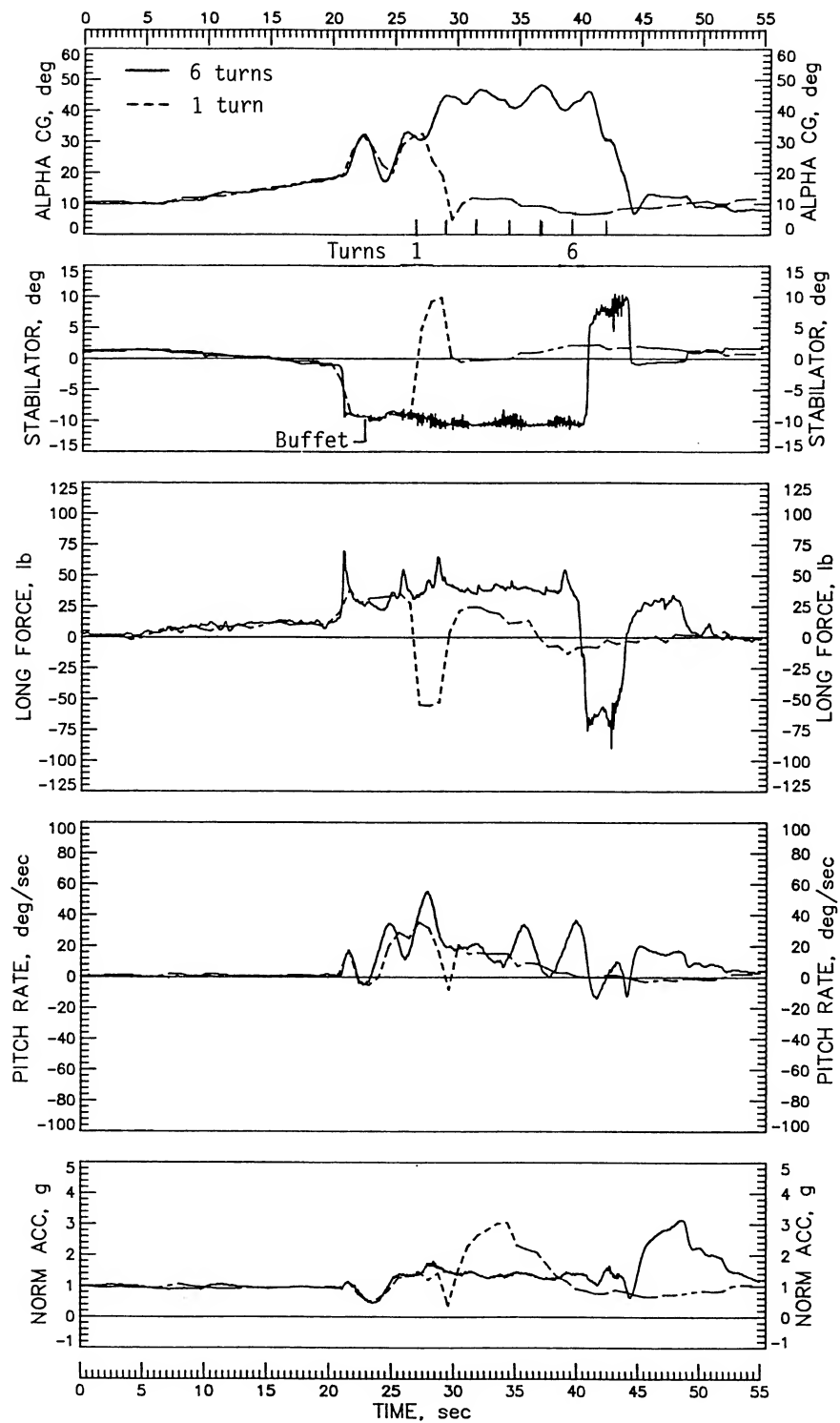


Figure 14. One- and six-turn right spins at idle power with ailerons neutral, flaps and gear retracted. Normal recovery controls.

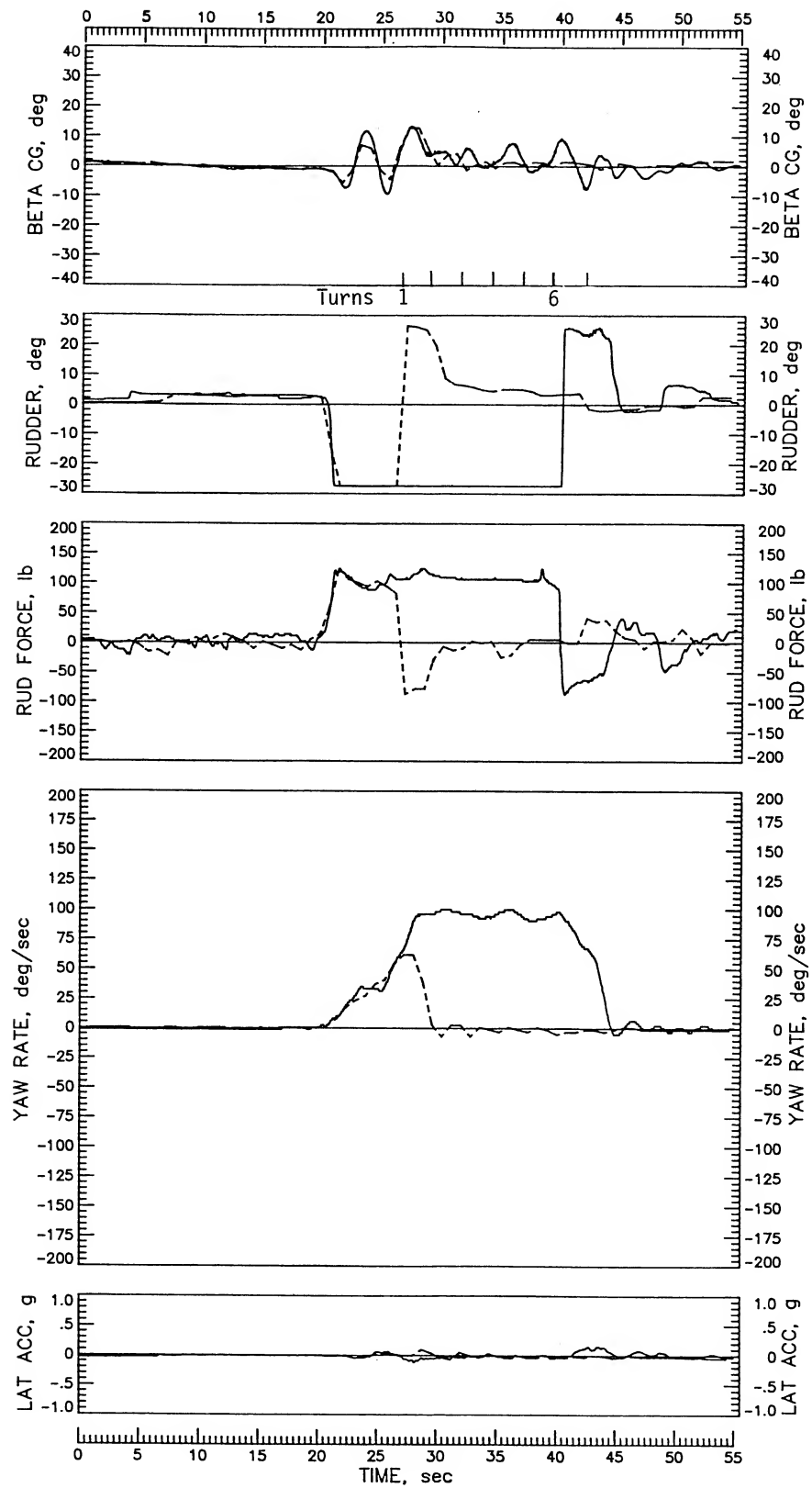


Figure 14. Continued.

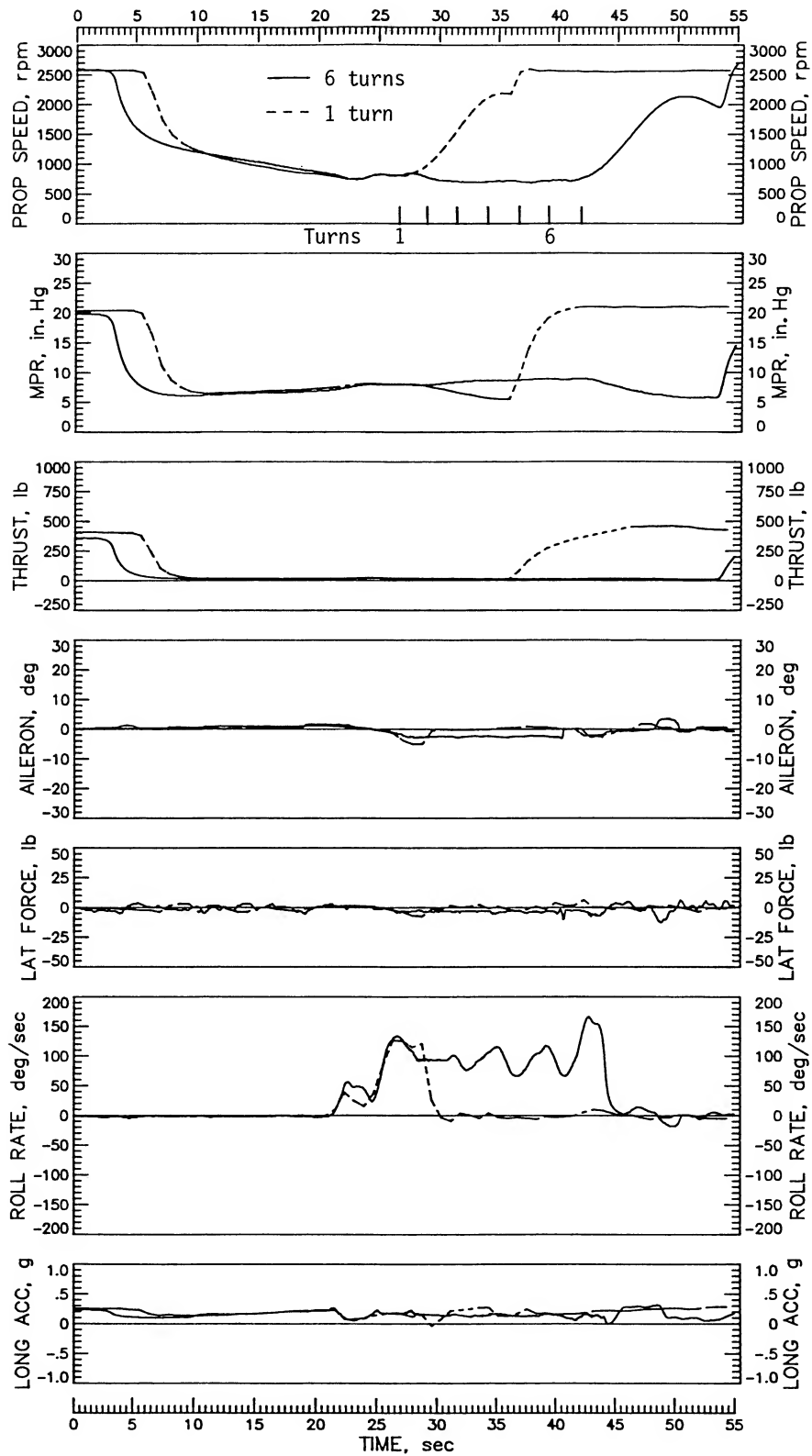


Figure 14. Continued.

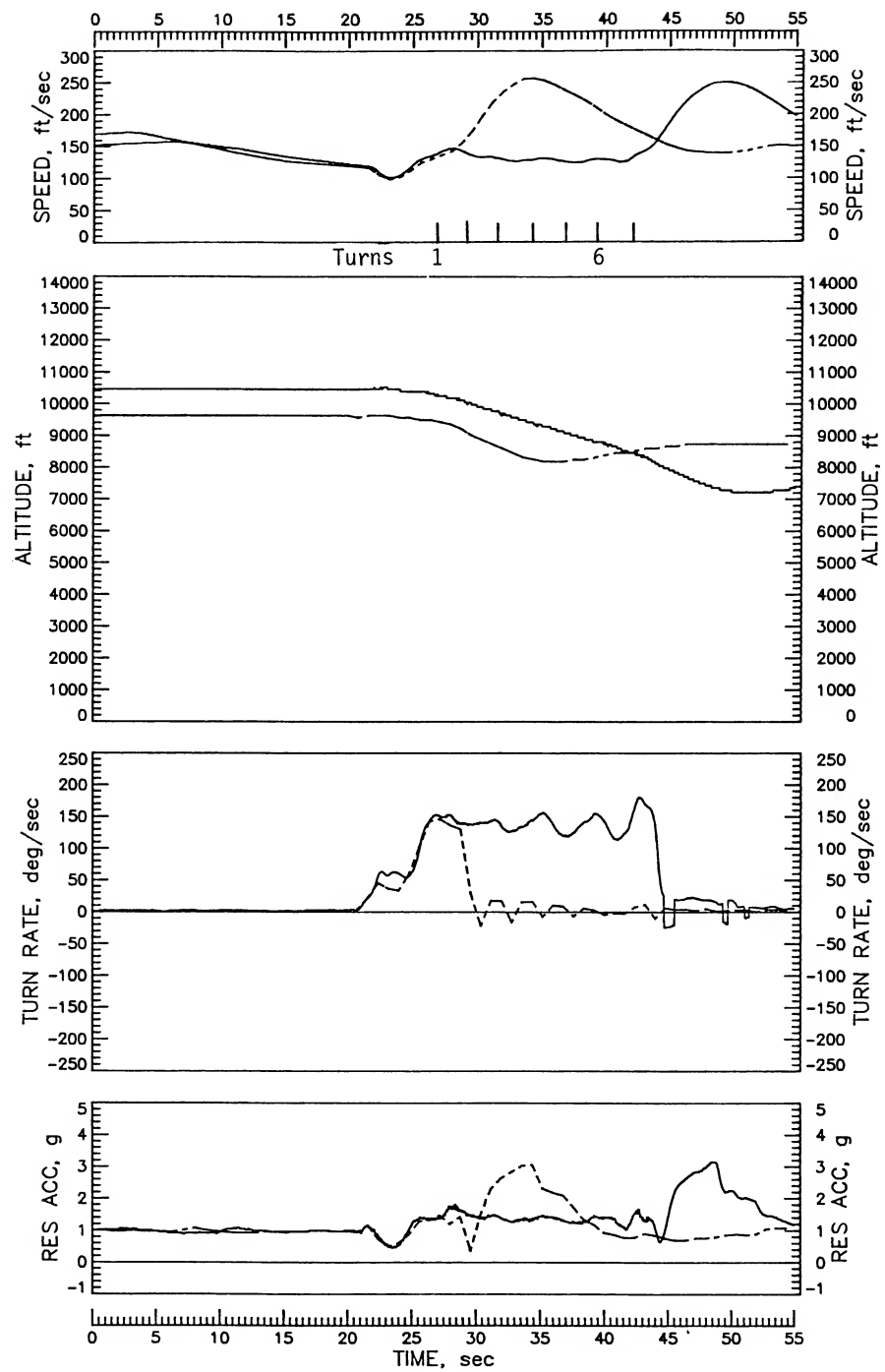


Figure 14. Concluded.

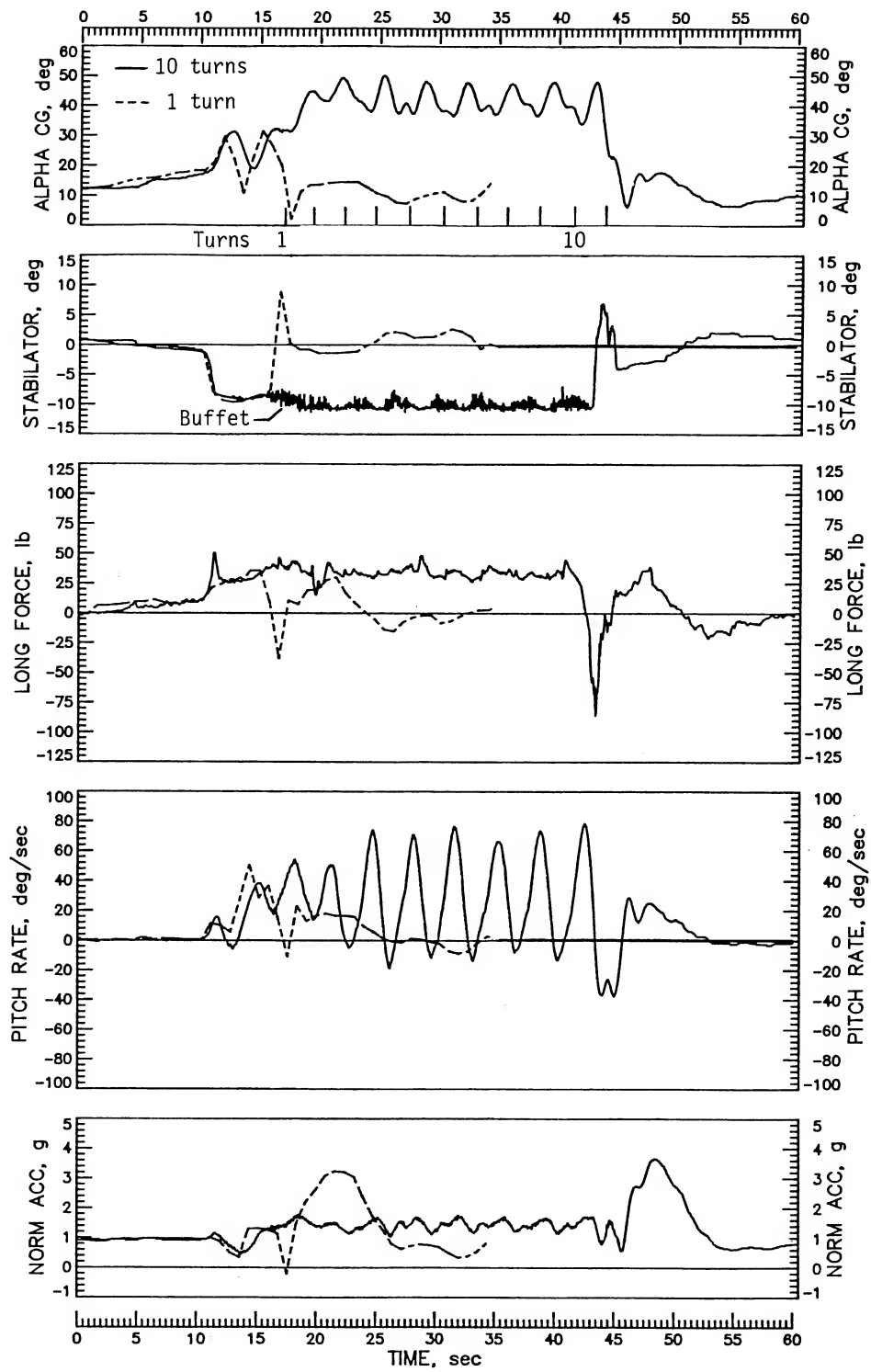


Figure 15. One- and ten-turn left spins at idle power, ailerons with the spin, flaps and gear retracted. Normal recovery controls.

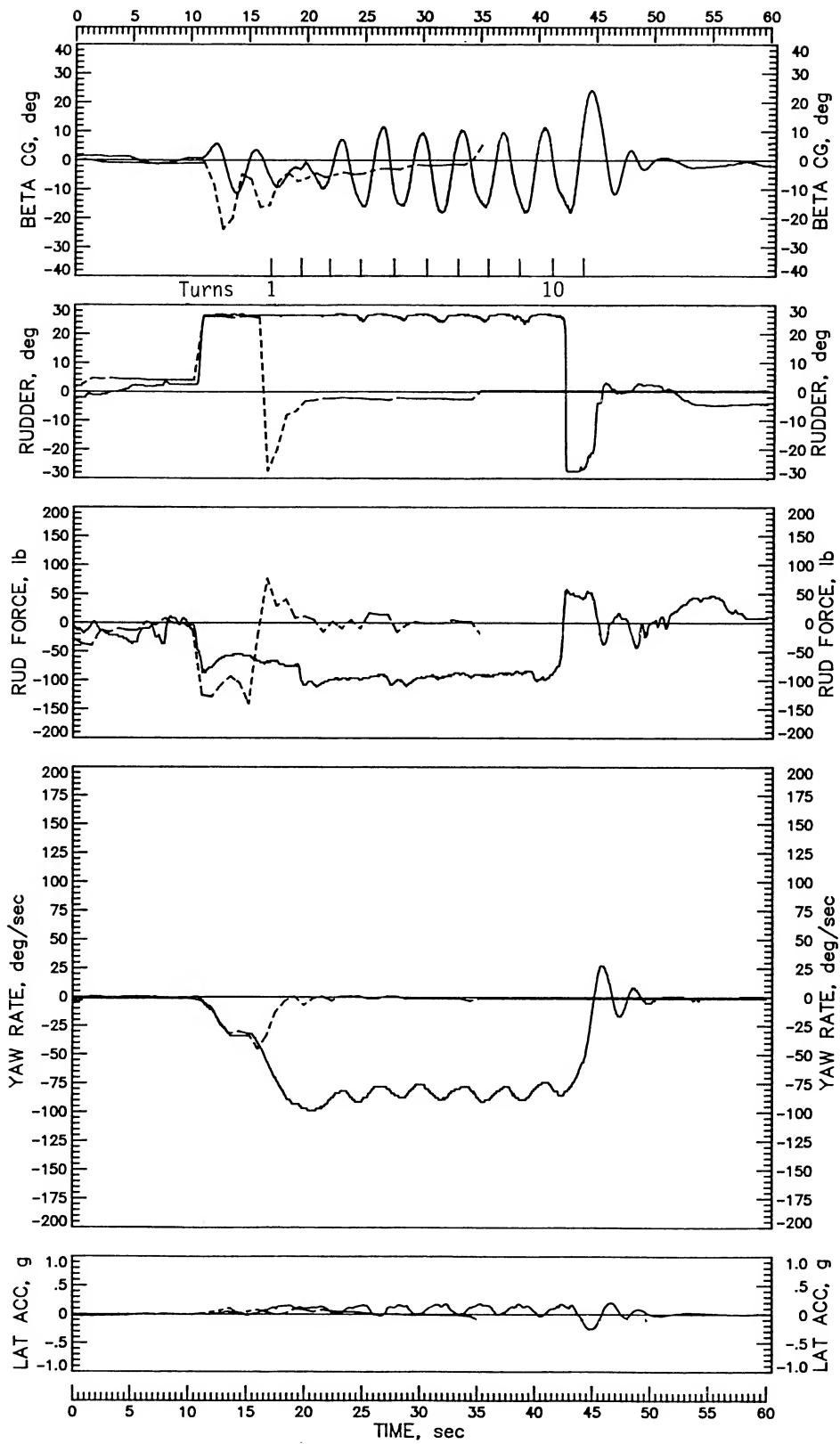


Figure 15. Continued.

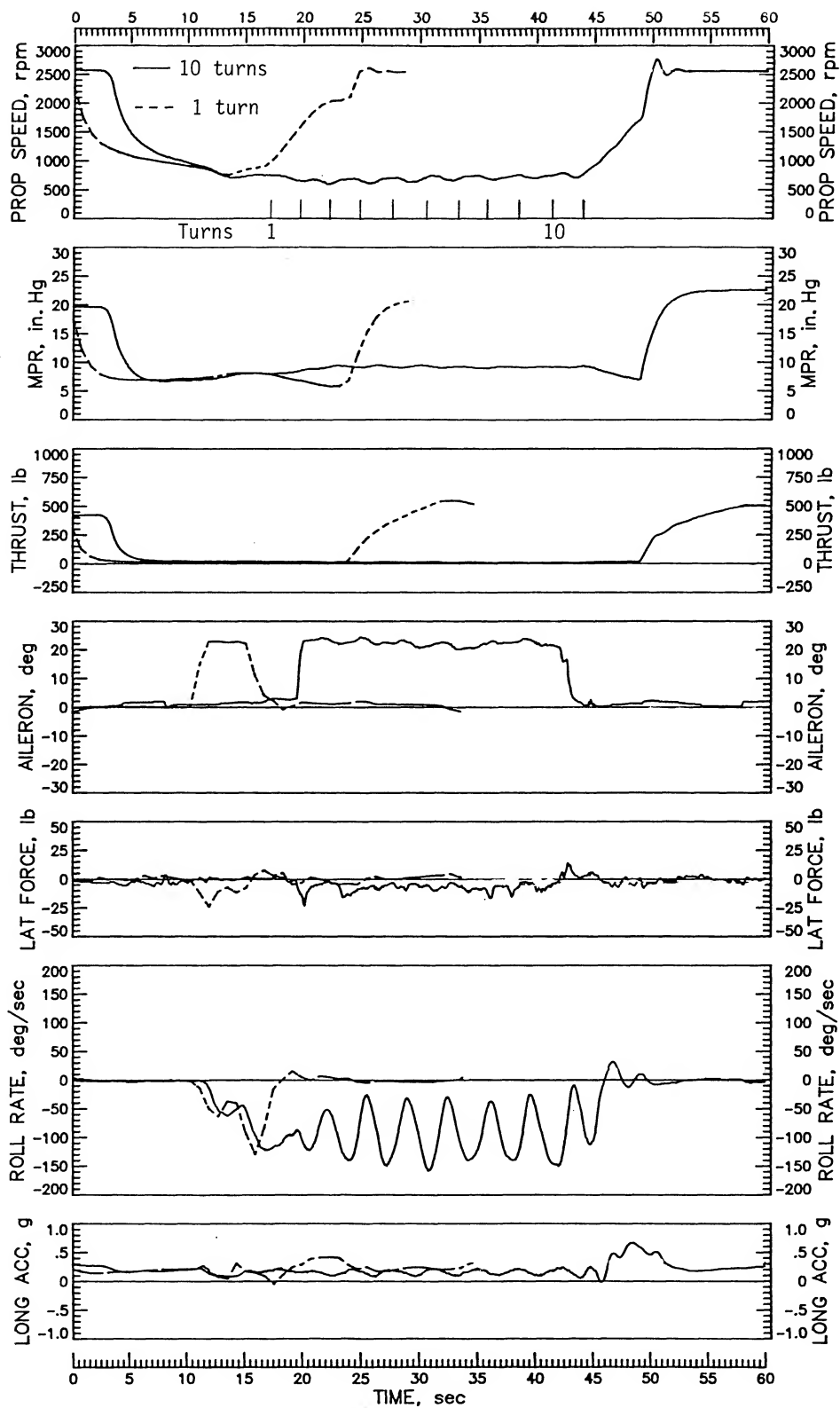


Figure 15. Continued.

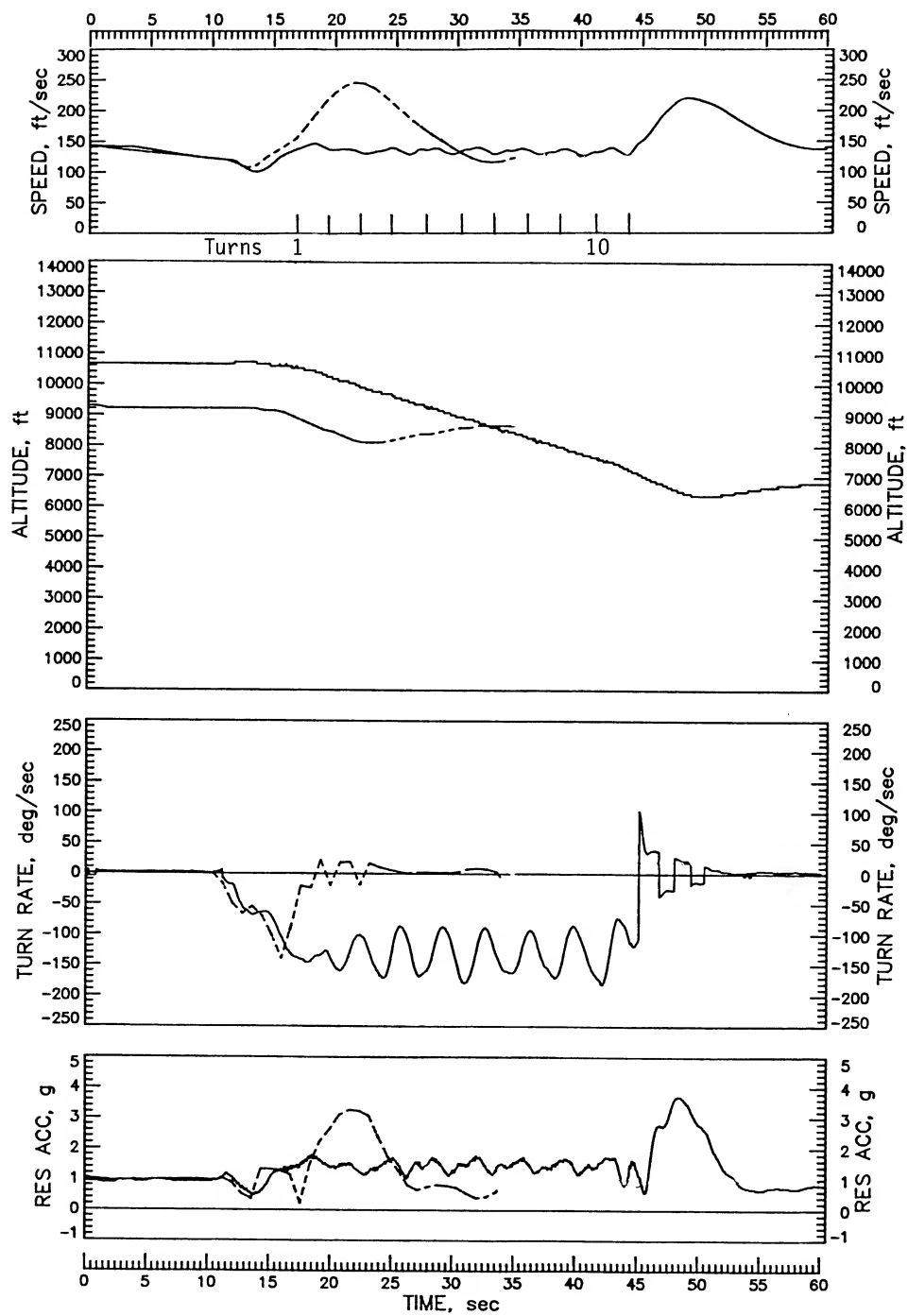


Figure 15. Concluded.

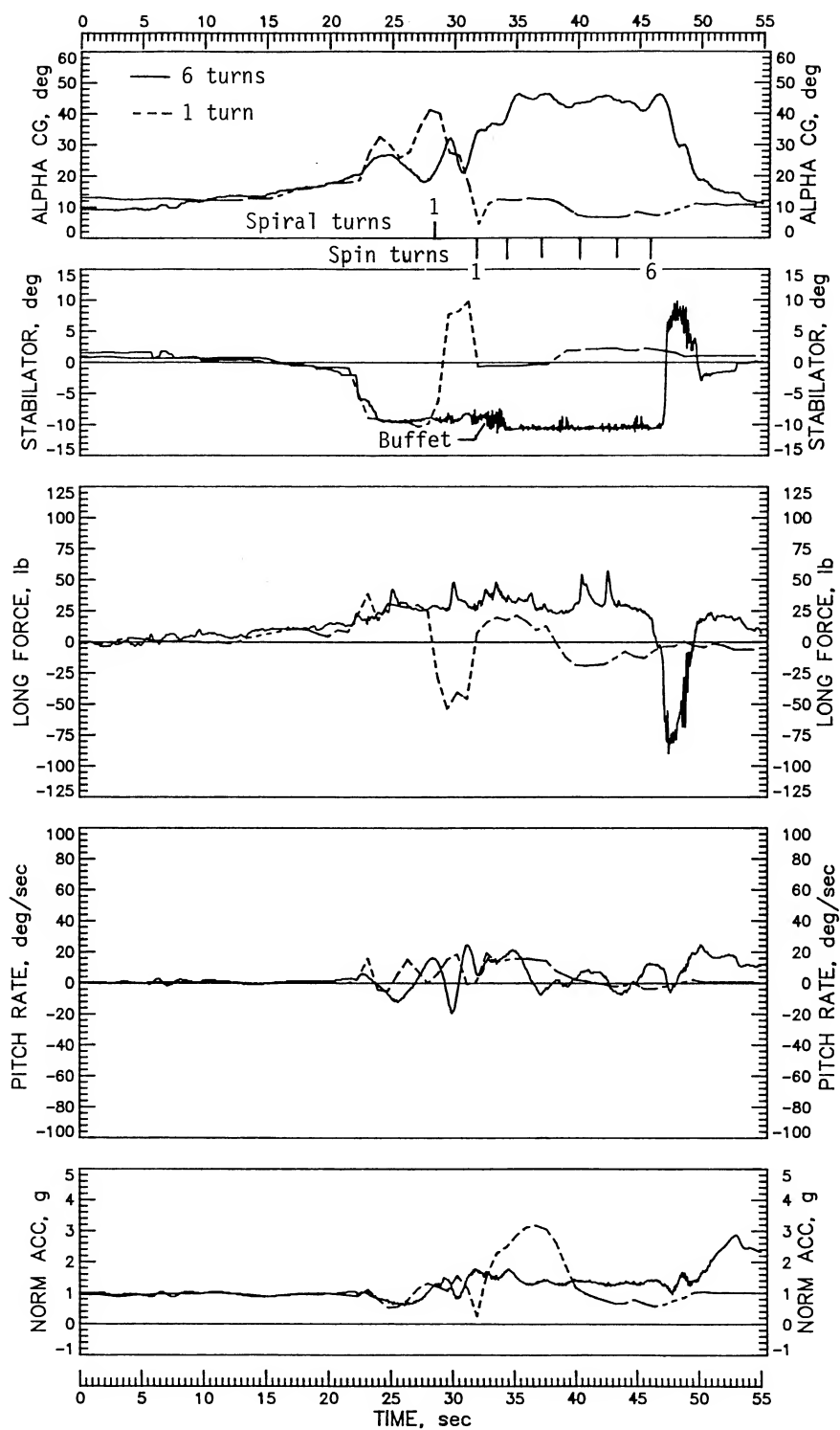


Figure 16. One- and six-turn right spins at idle power, ailerons against the spin, flaps and gear retracted. Normal recovery controls.

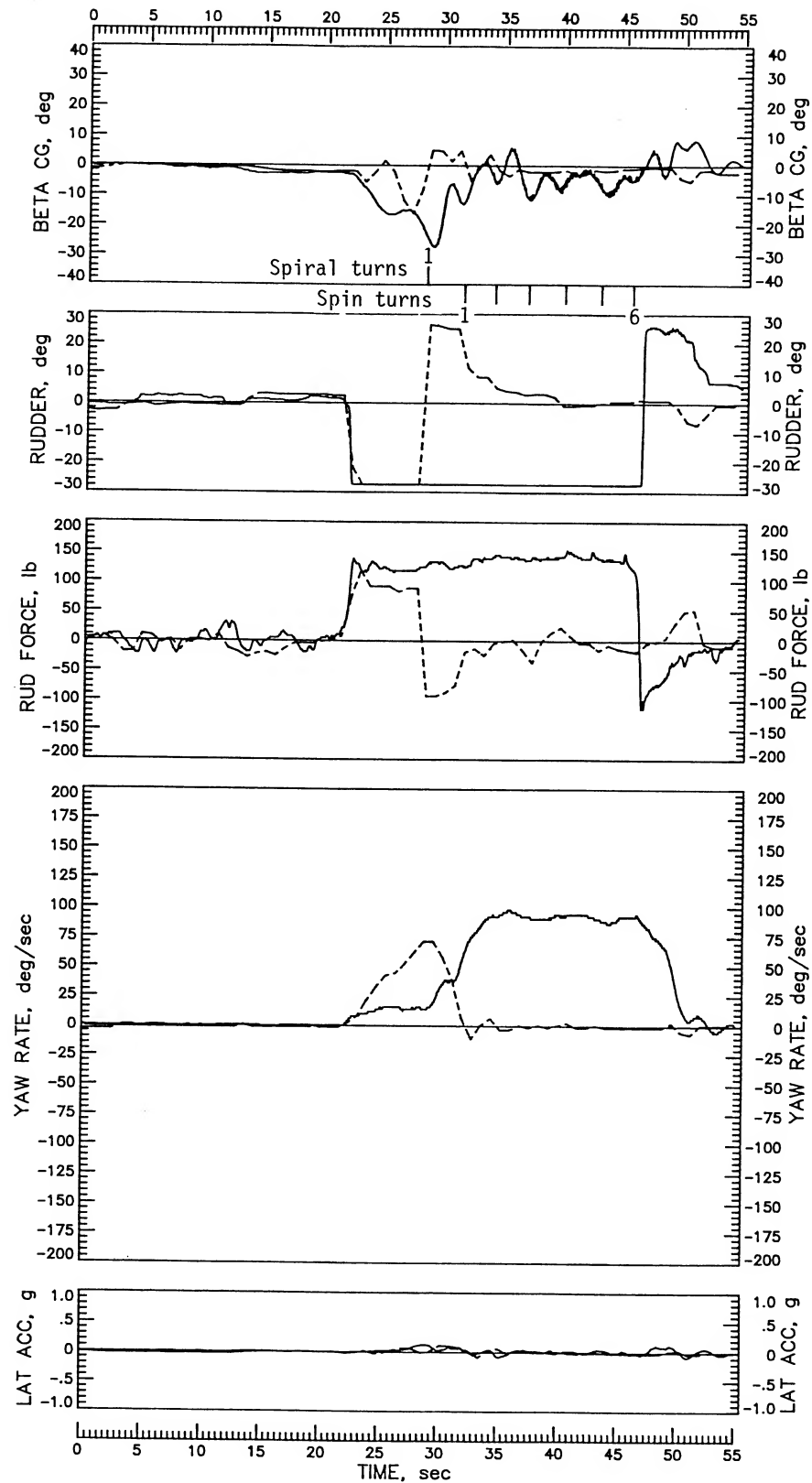


Figure 16. Continued.

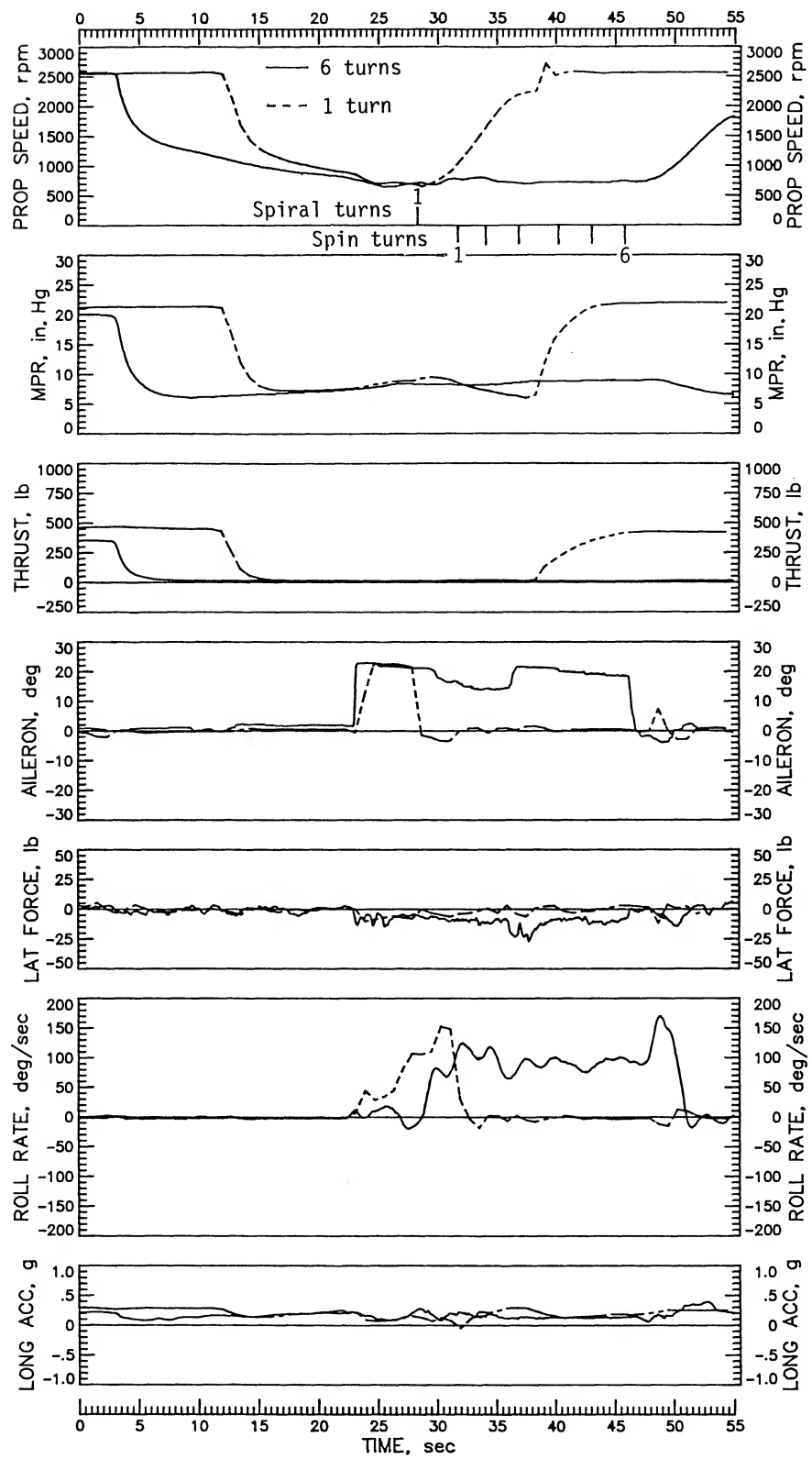


Figure 16. Continued.

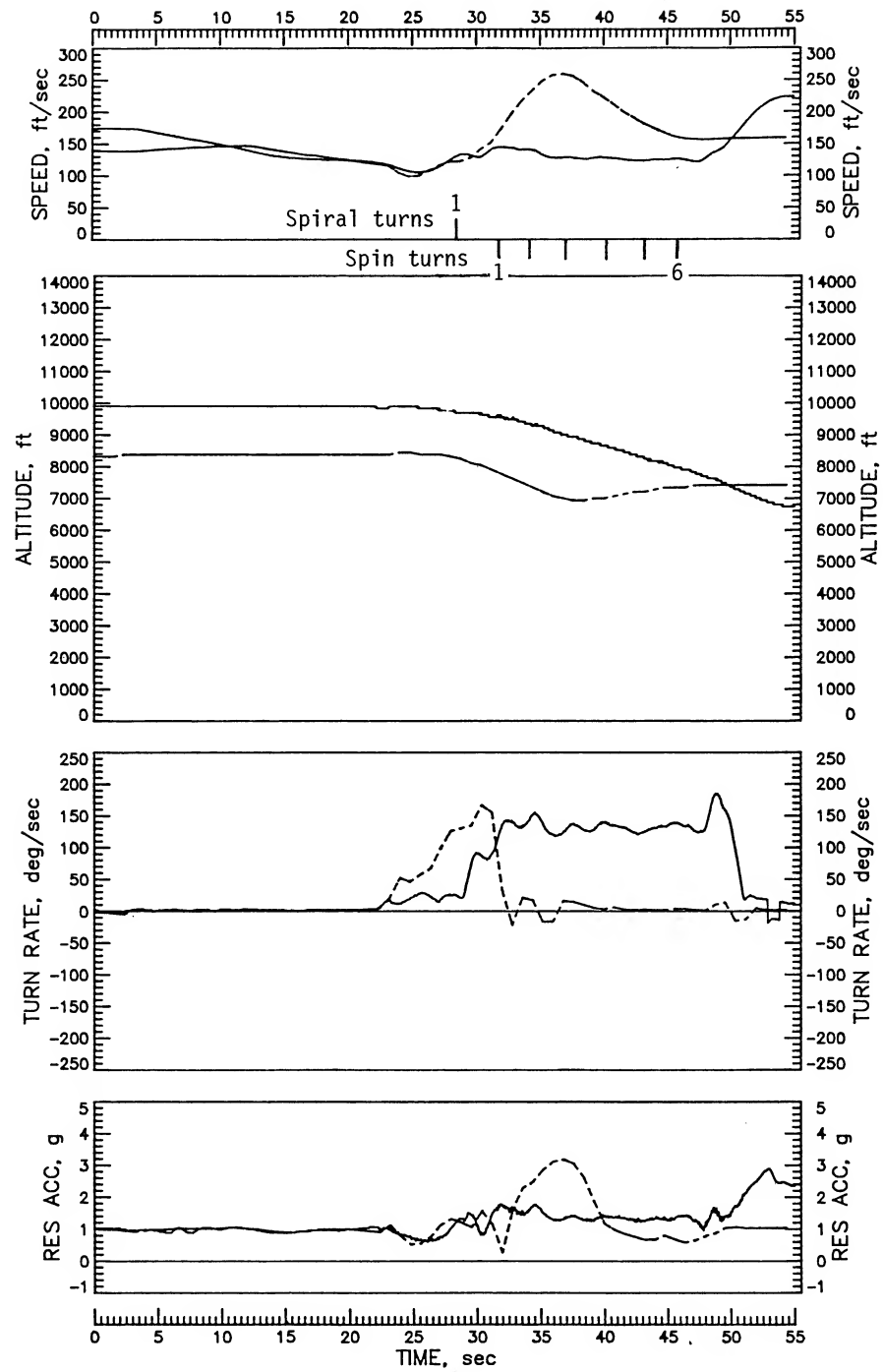


Figure 16. Concluded.

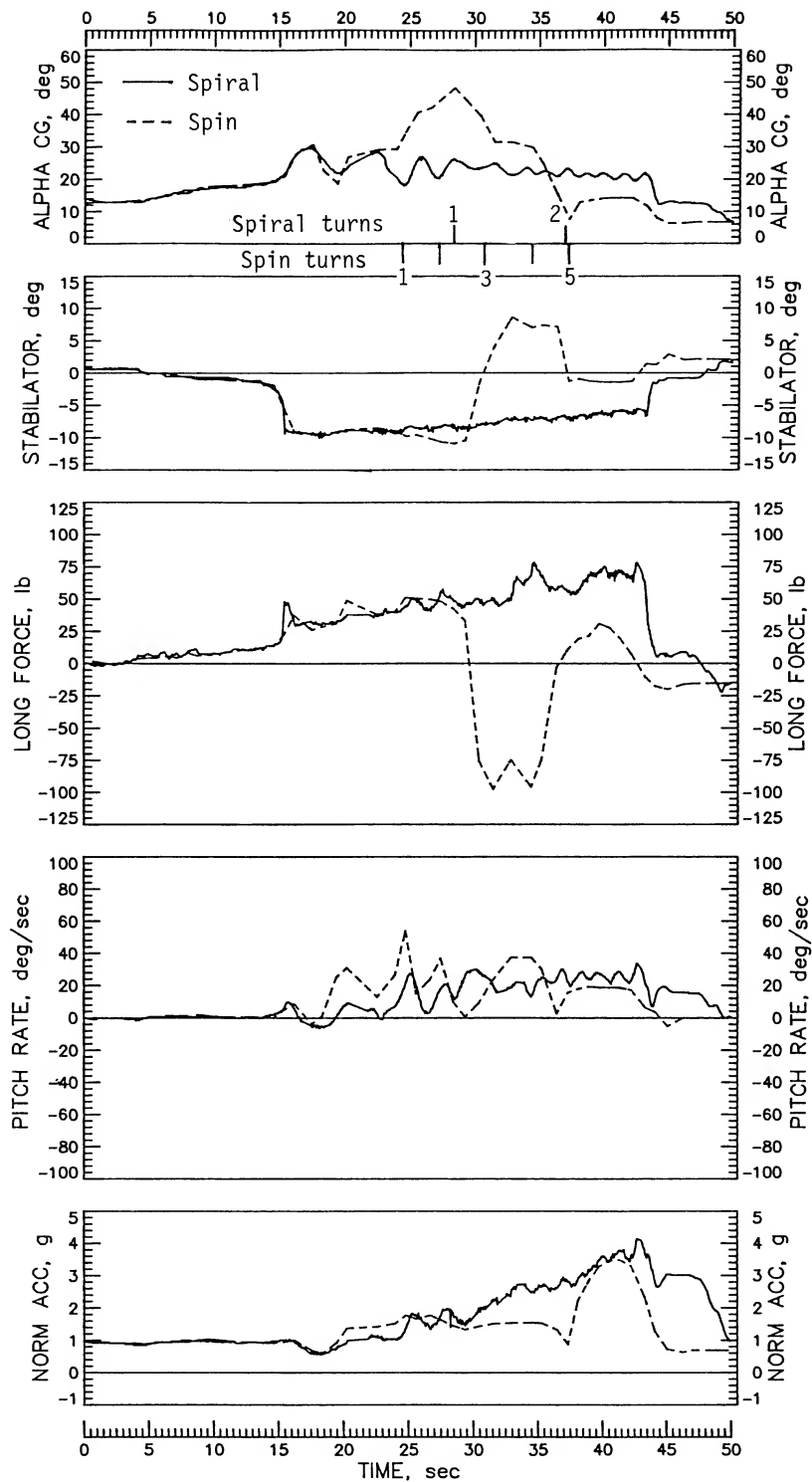


Figure 17. Comparison of spiral and spin entered from idle-power, 1g stalls, flaps and gear retracted.

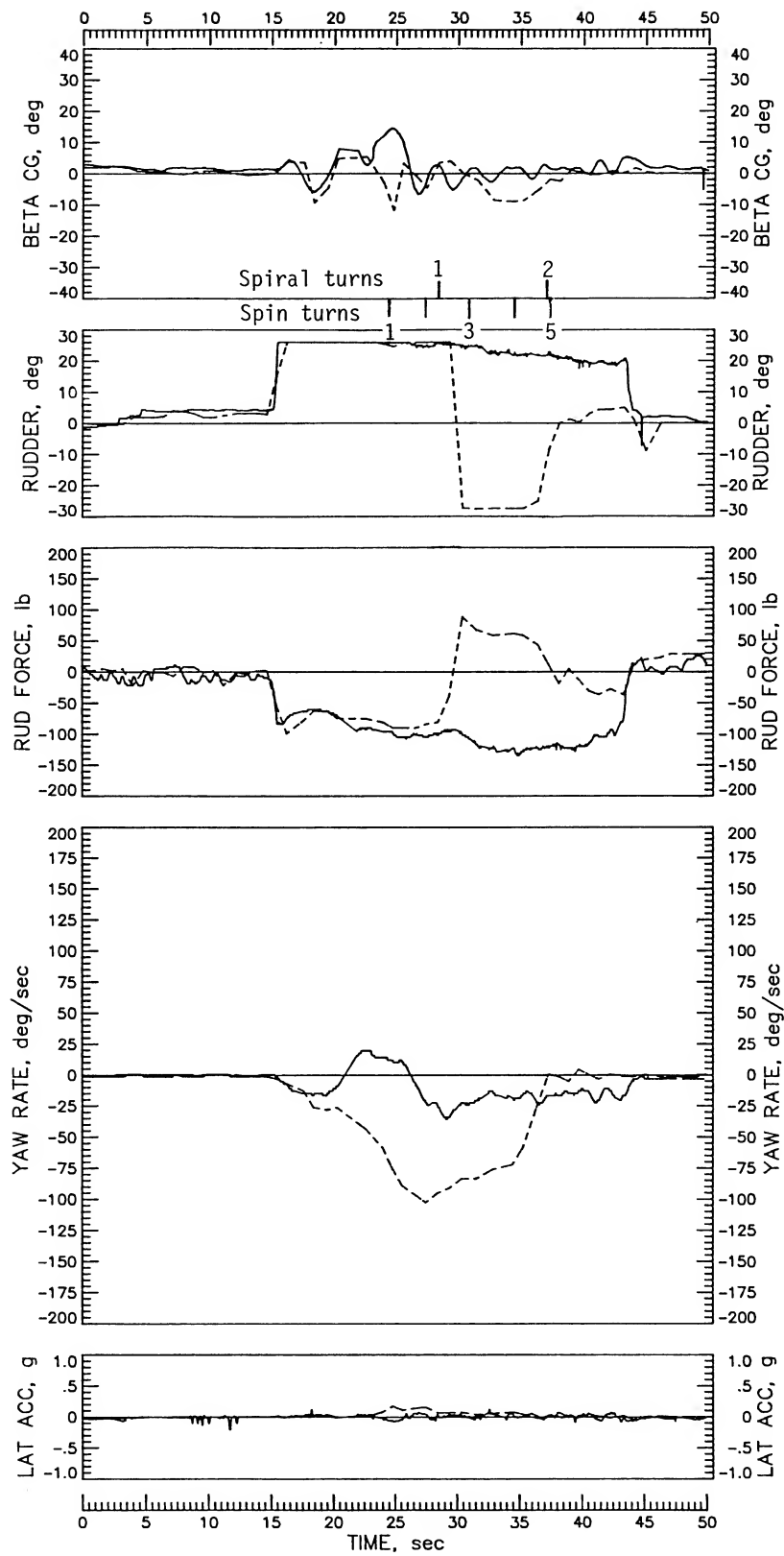


Figure 17. Continued.

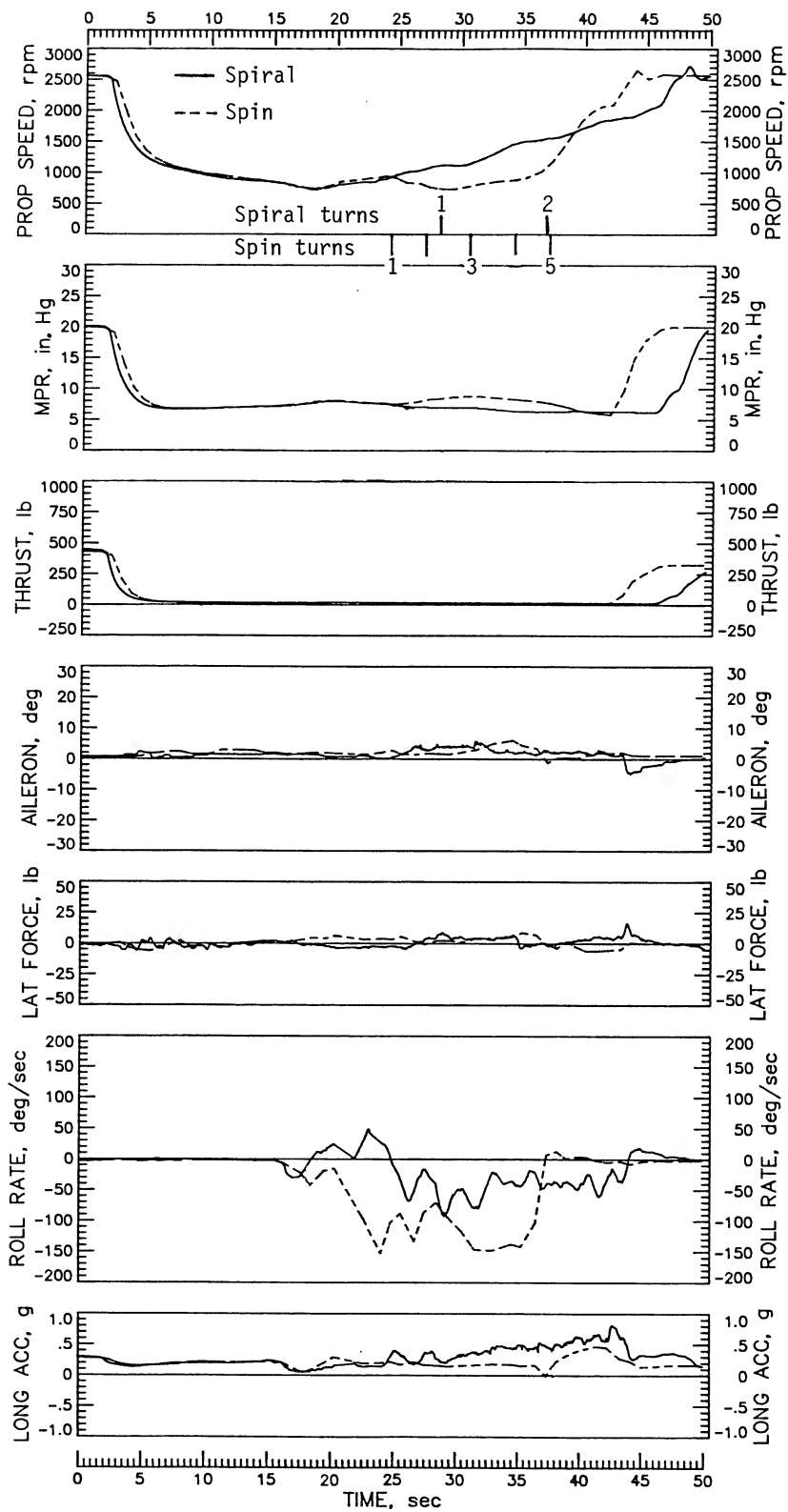


Figure 17. Continued.

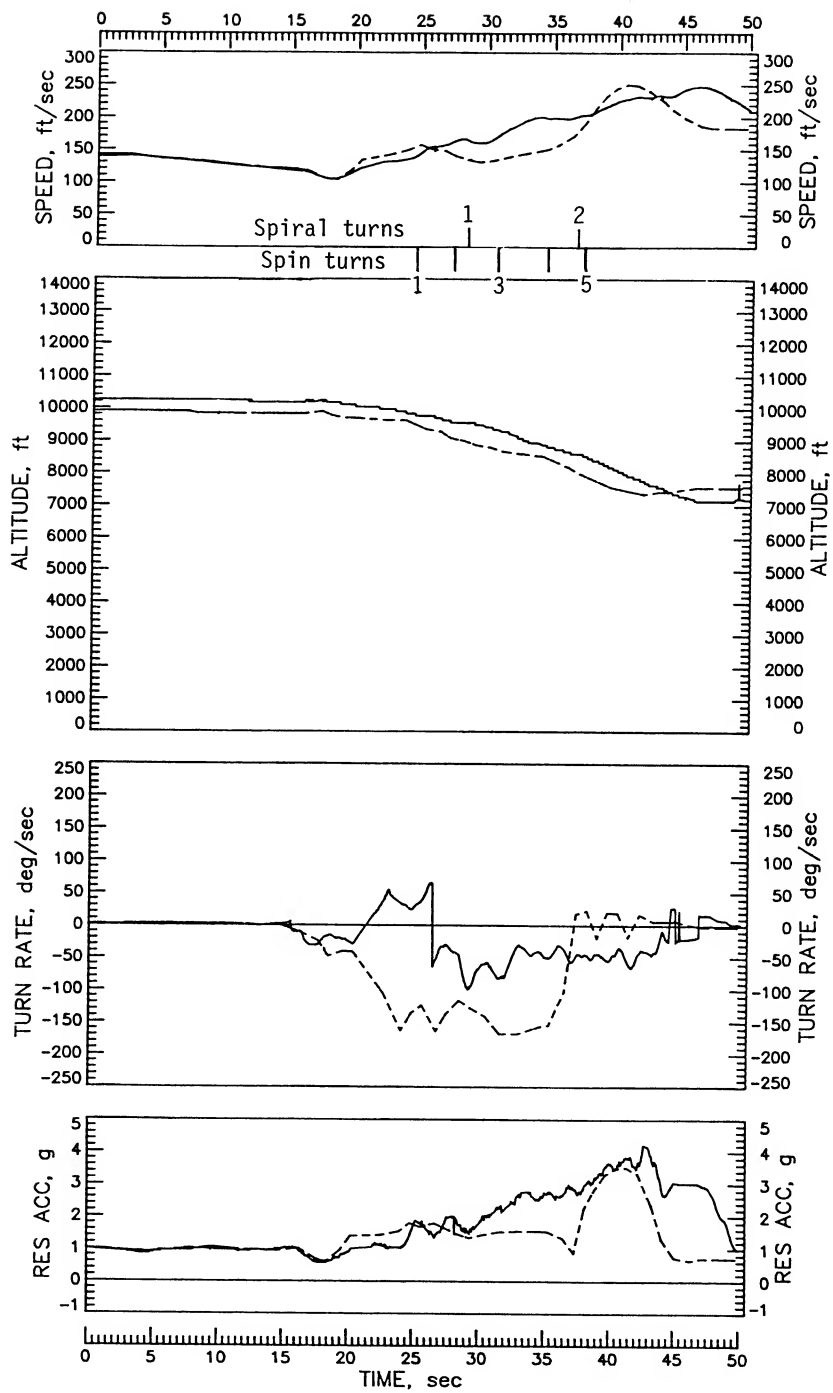


Figure 17. Concluded.

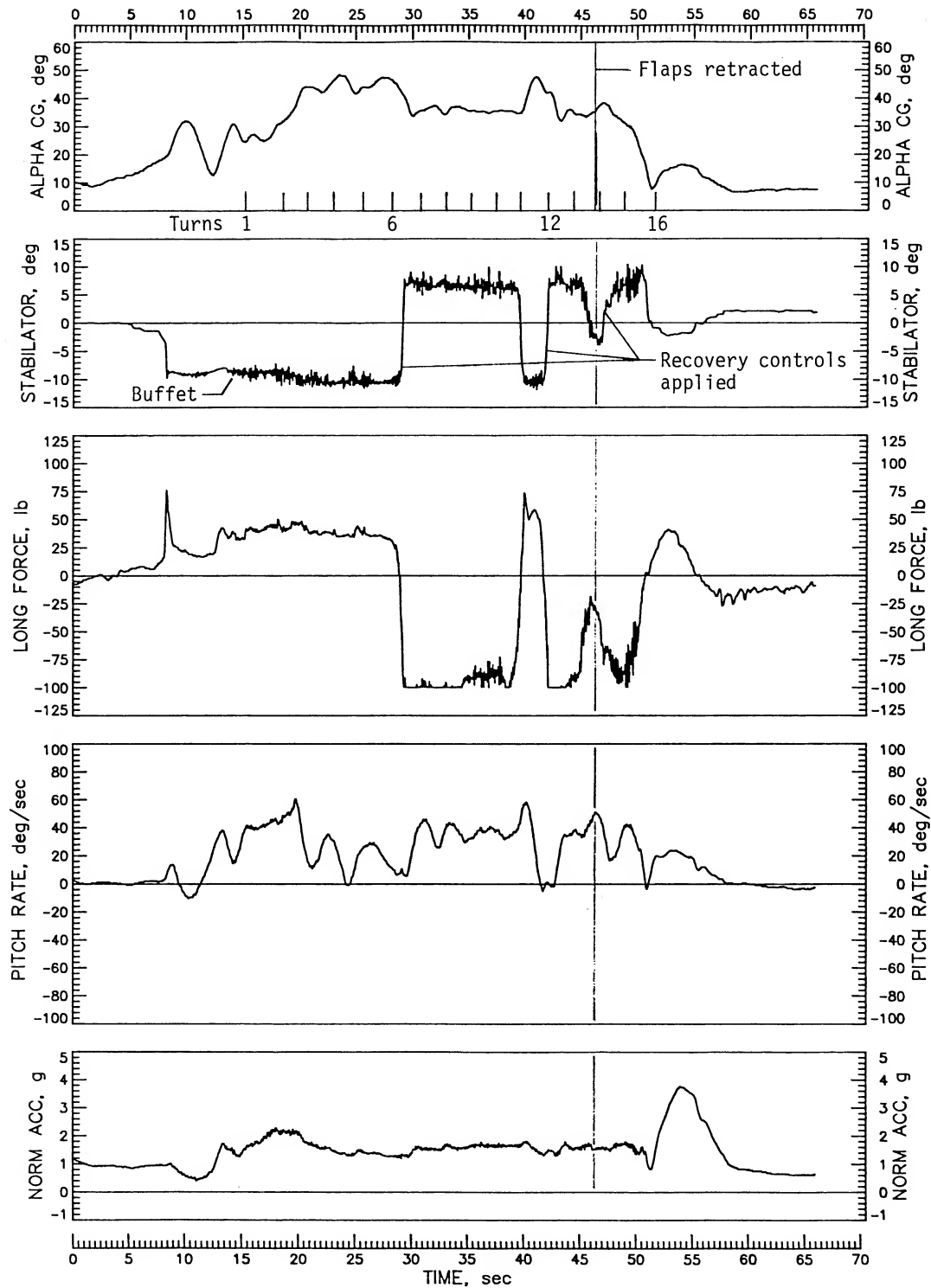


Figure 18. Left spin at idle power, ailerons neutral, flaps extended 40°, gear retracted. Normal recovery controls were unable to stop the spin until flaps were retracted.

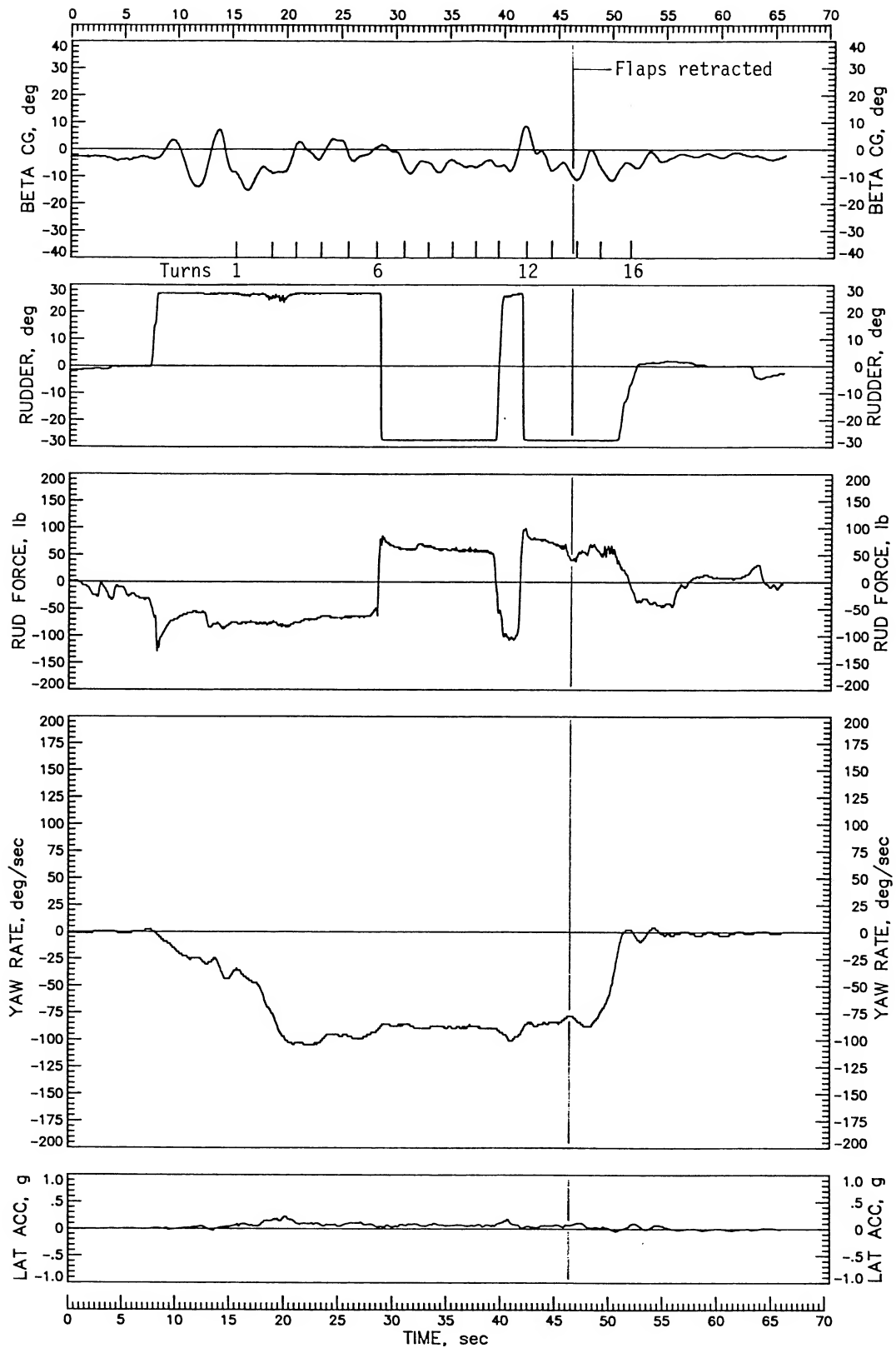


Figure 18. Continued.

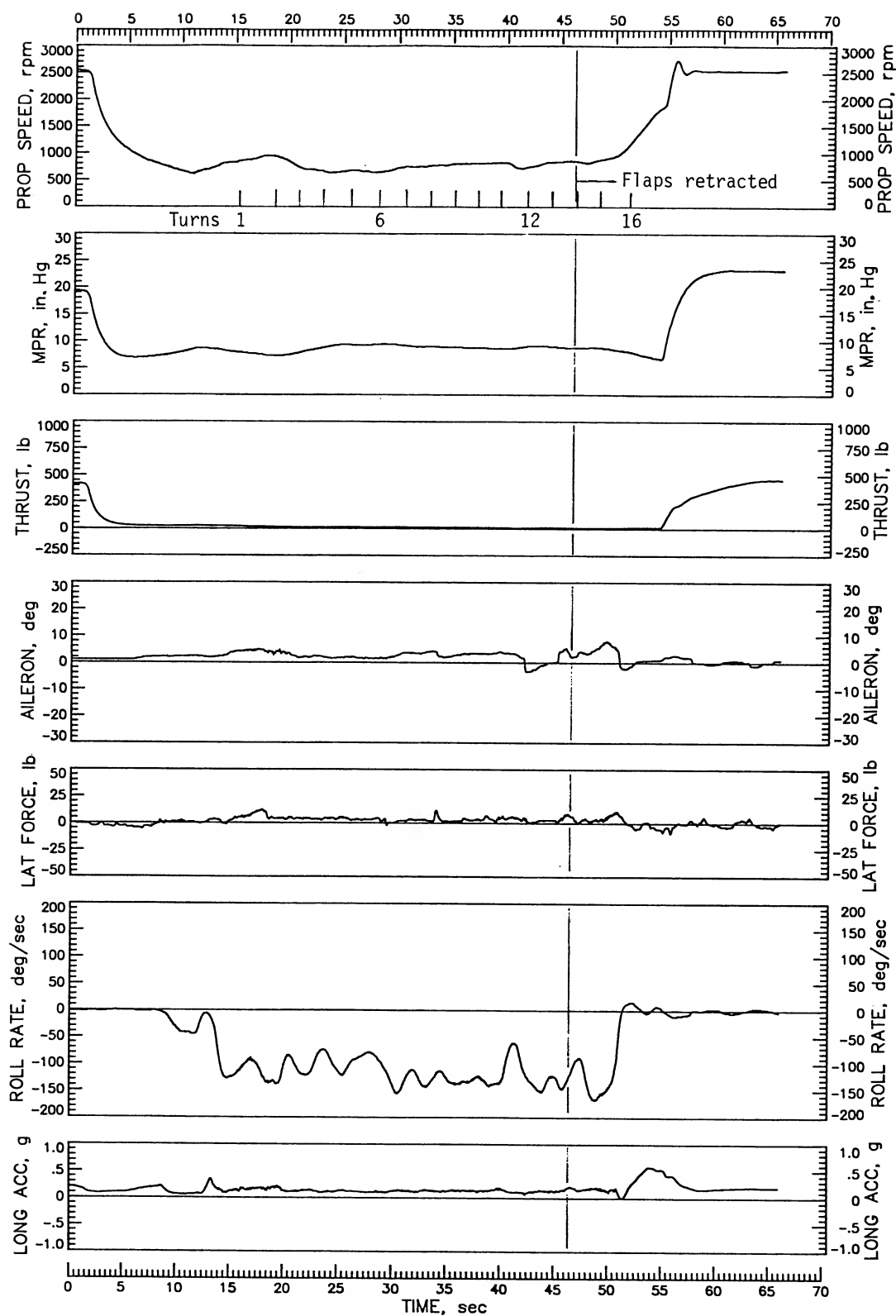


Figure 18. Continued.

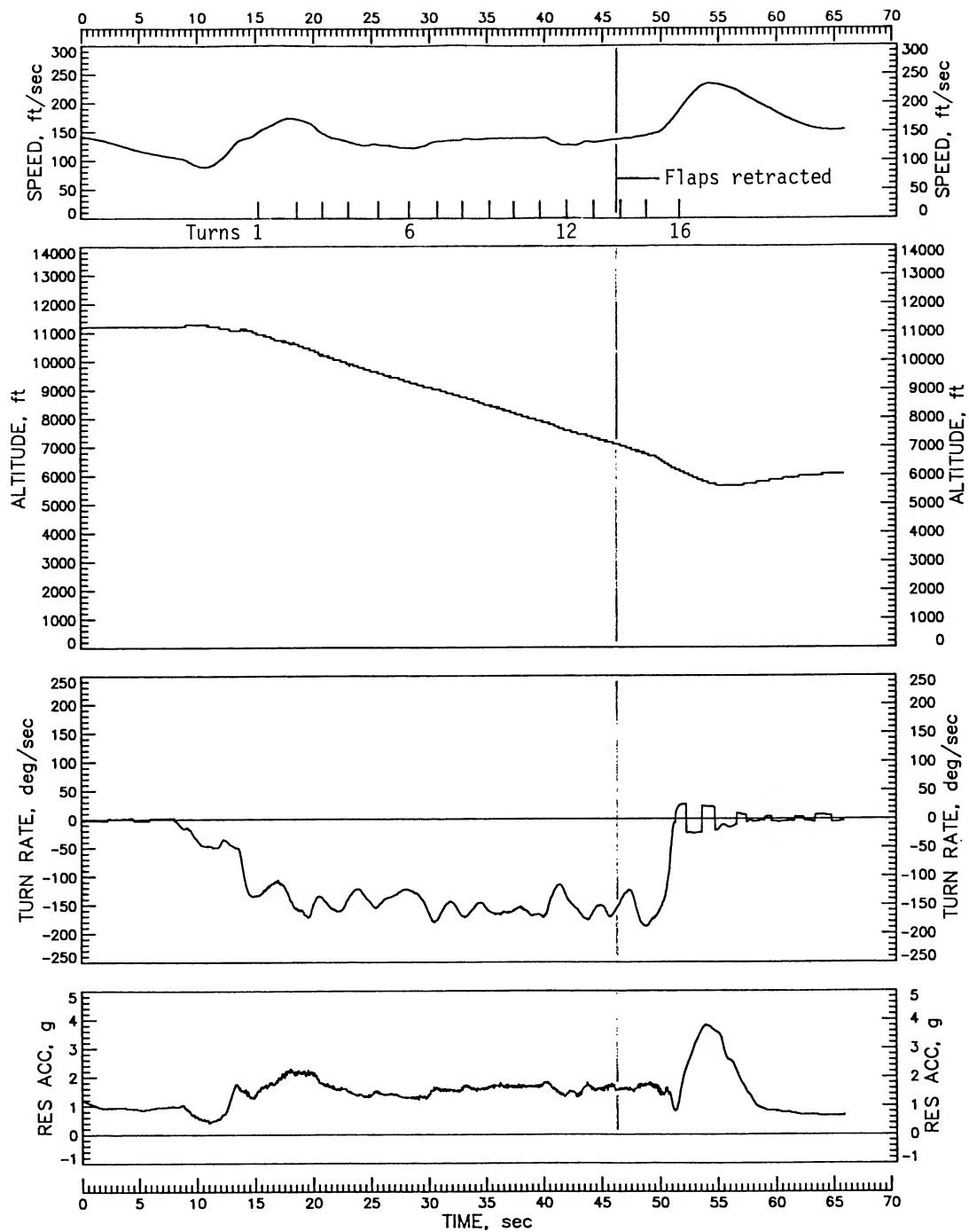


Figure 18. Concluded.

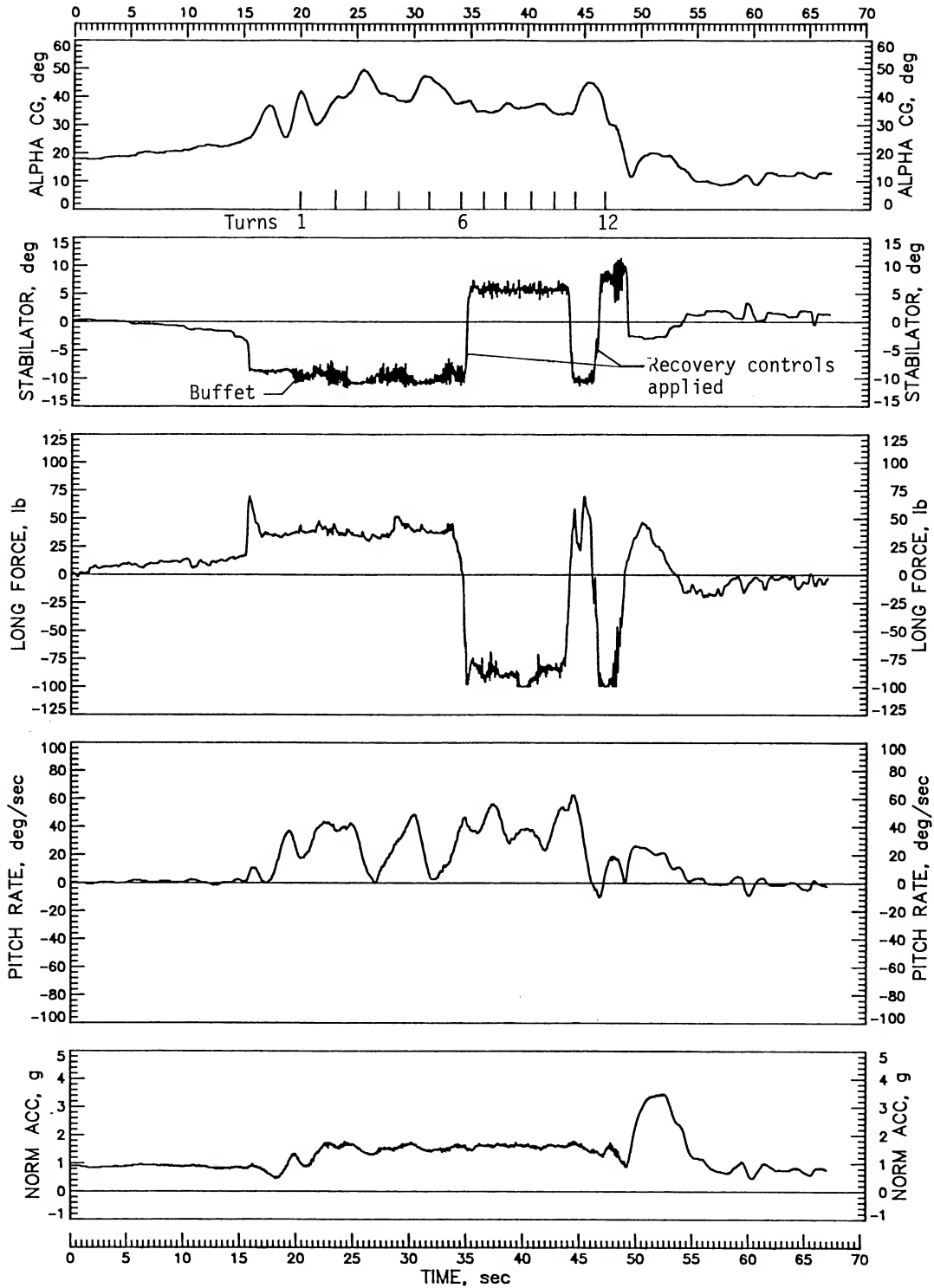


Figure 19. Right spin at maximum power, ailerons neutral, flaps and gear retracted. Initial application of normal recovery controls failed to stop spin.

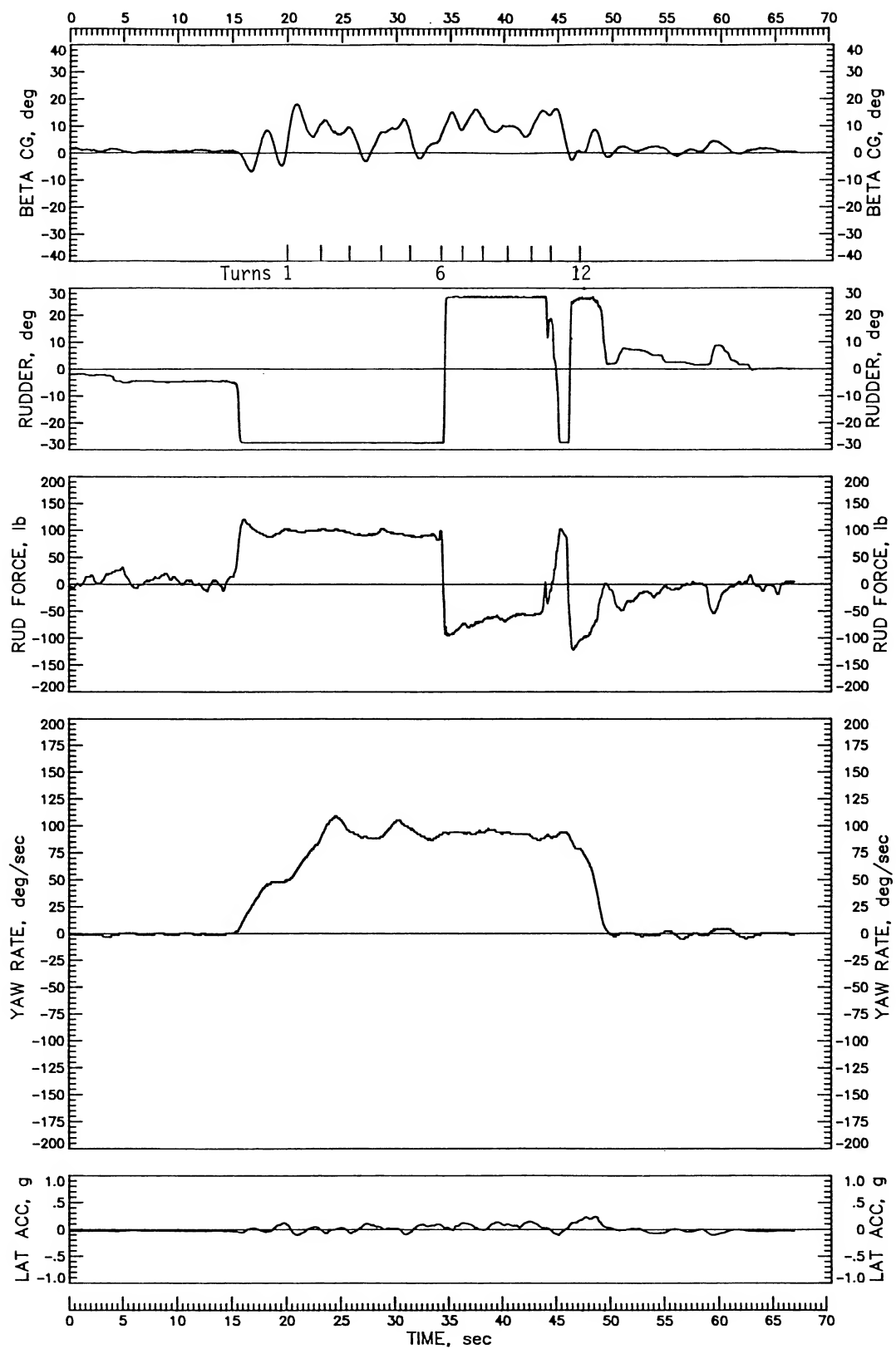


Figure 19. Continued.

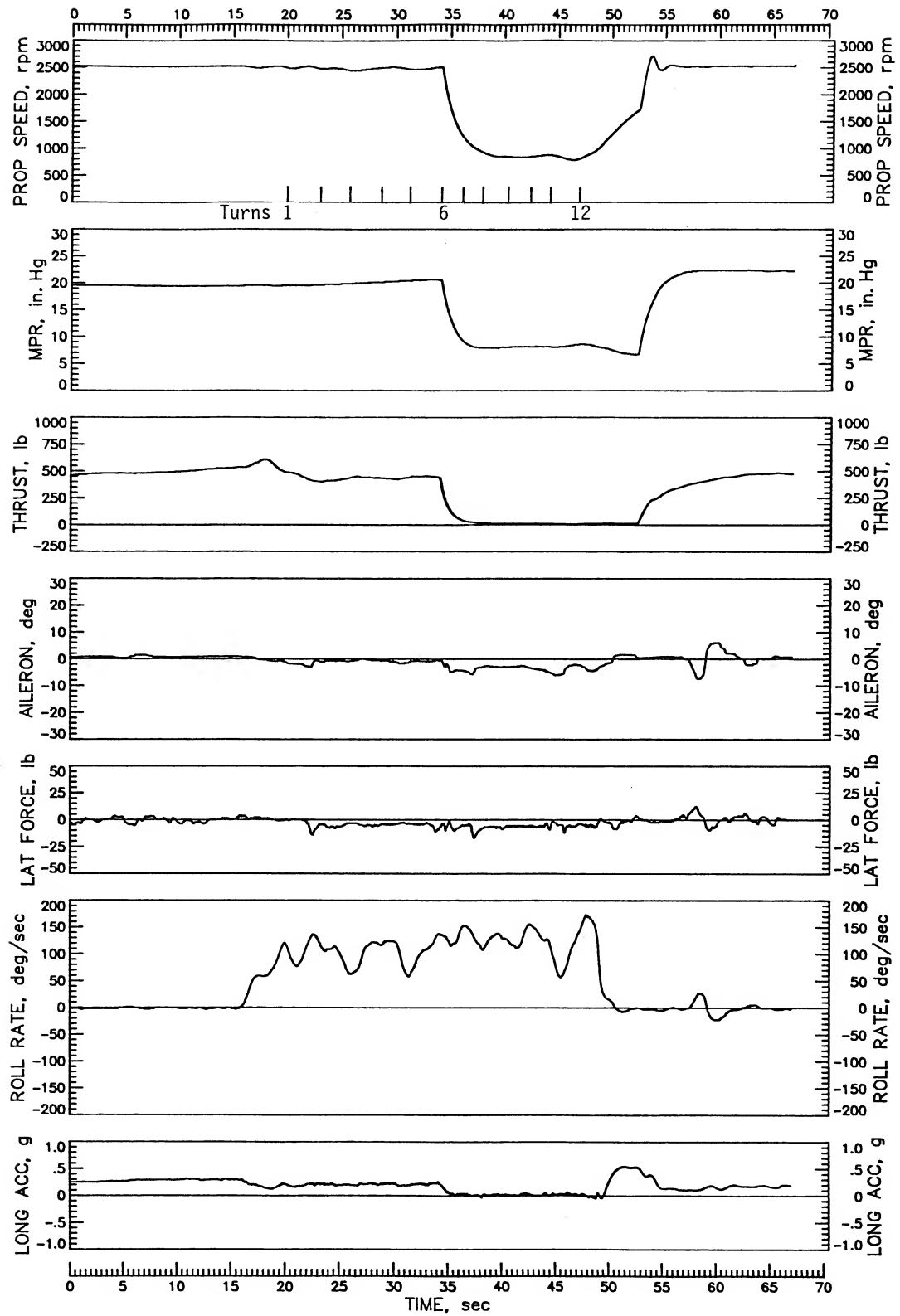


Figure 19. Continued.

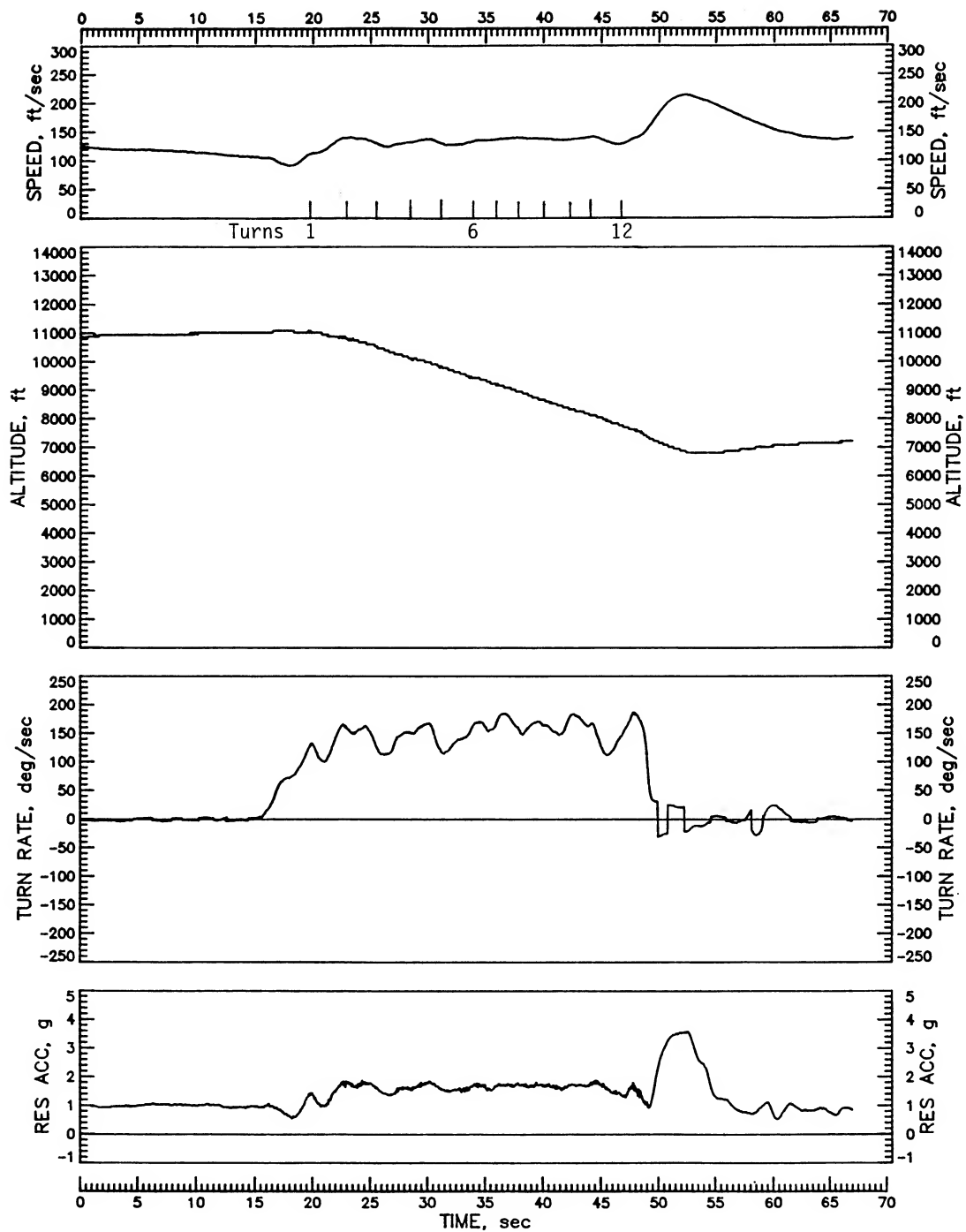


Figure 19. Concluded.

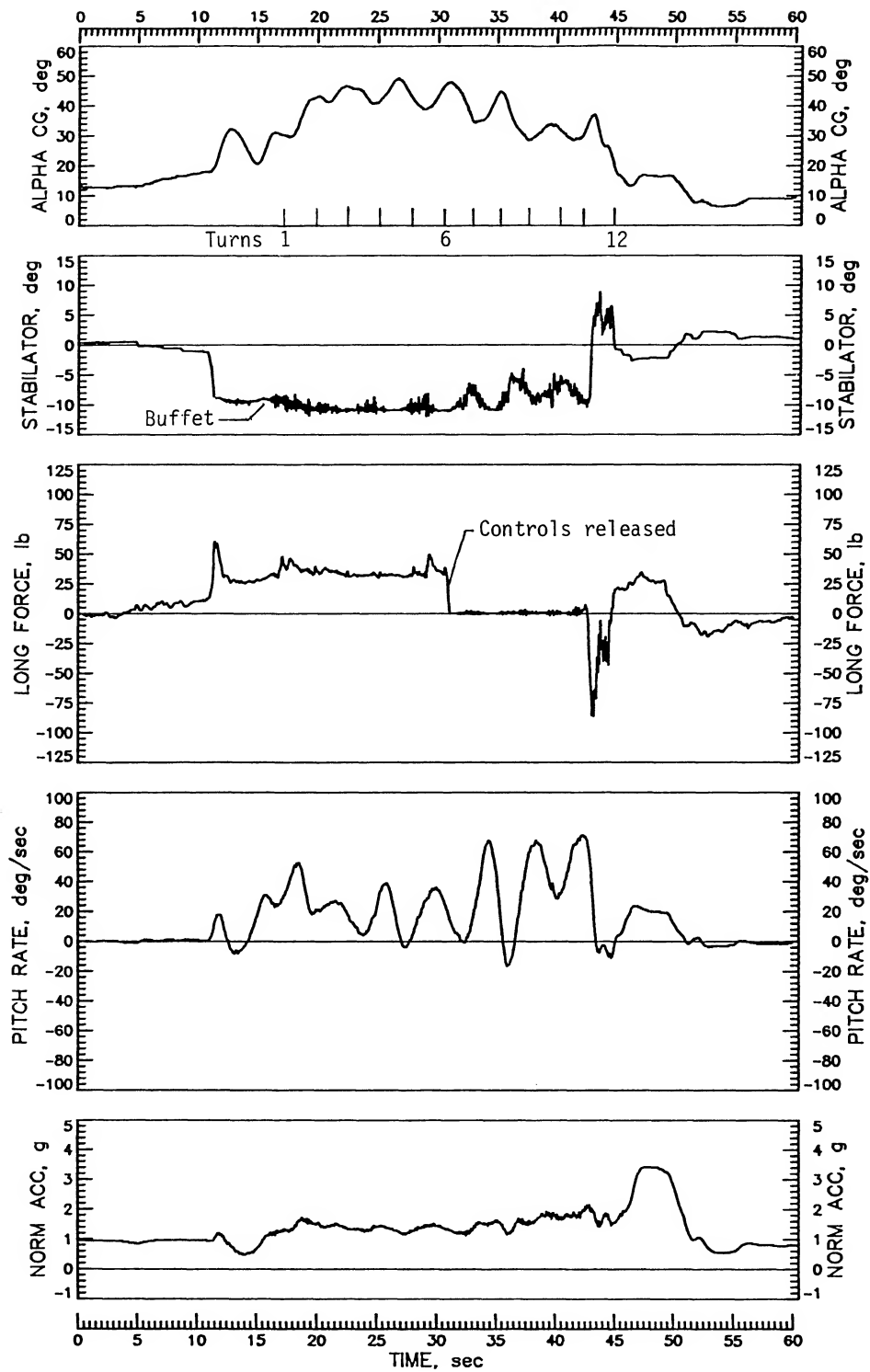


Figure 20. Right spin at idle power, ailerons neutral, flaps and gear retracted. Airplane stabilized in a steeper spin following release of controls.

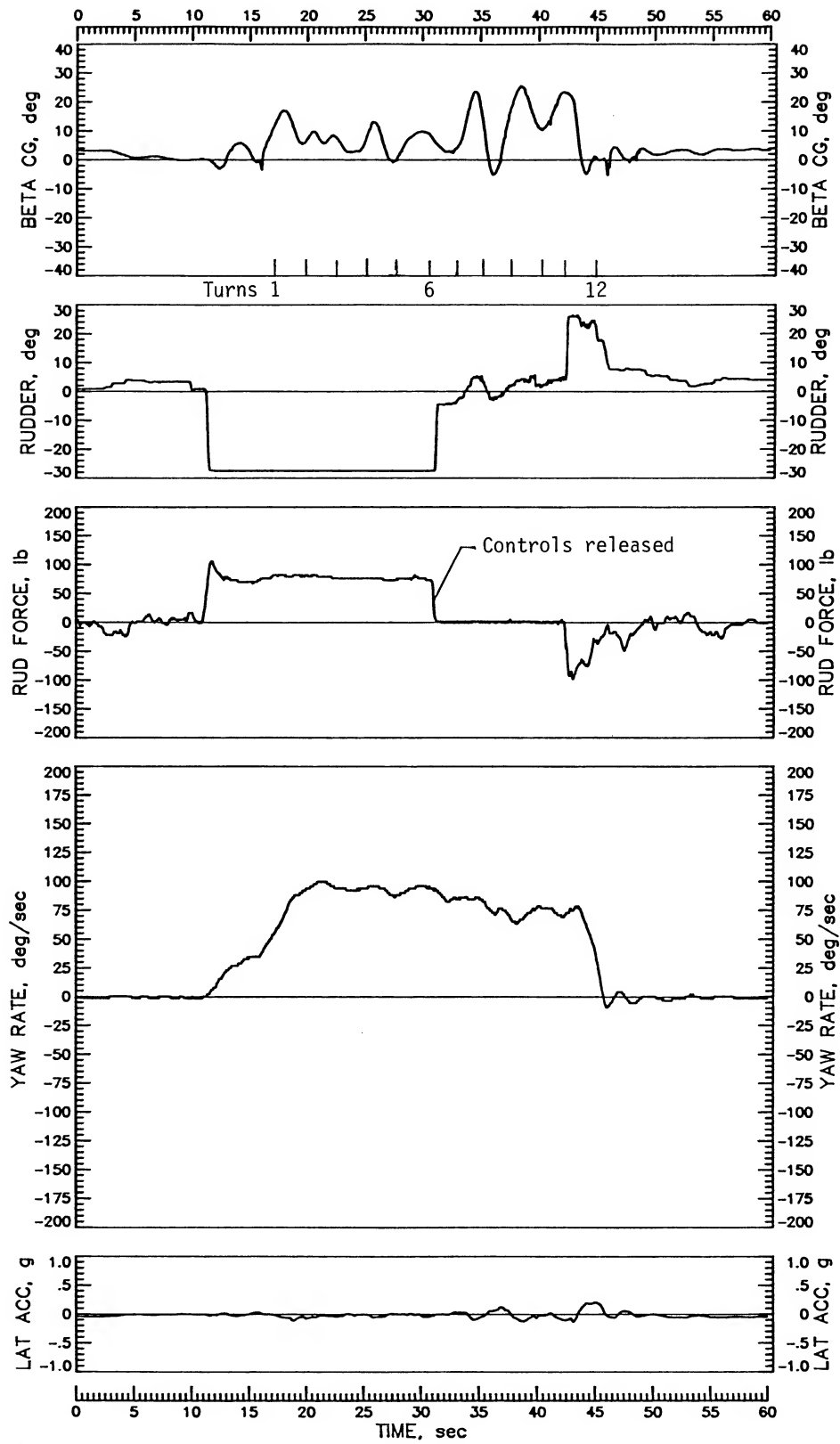


Figure 20. Continued.

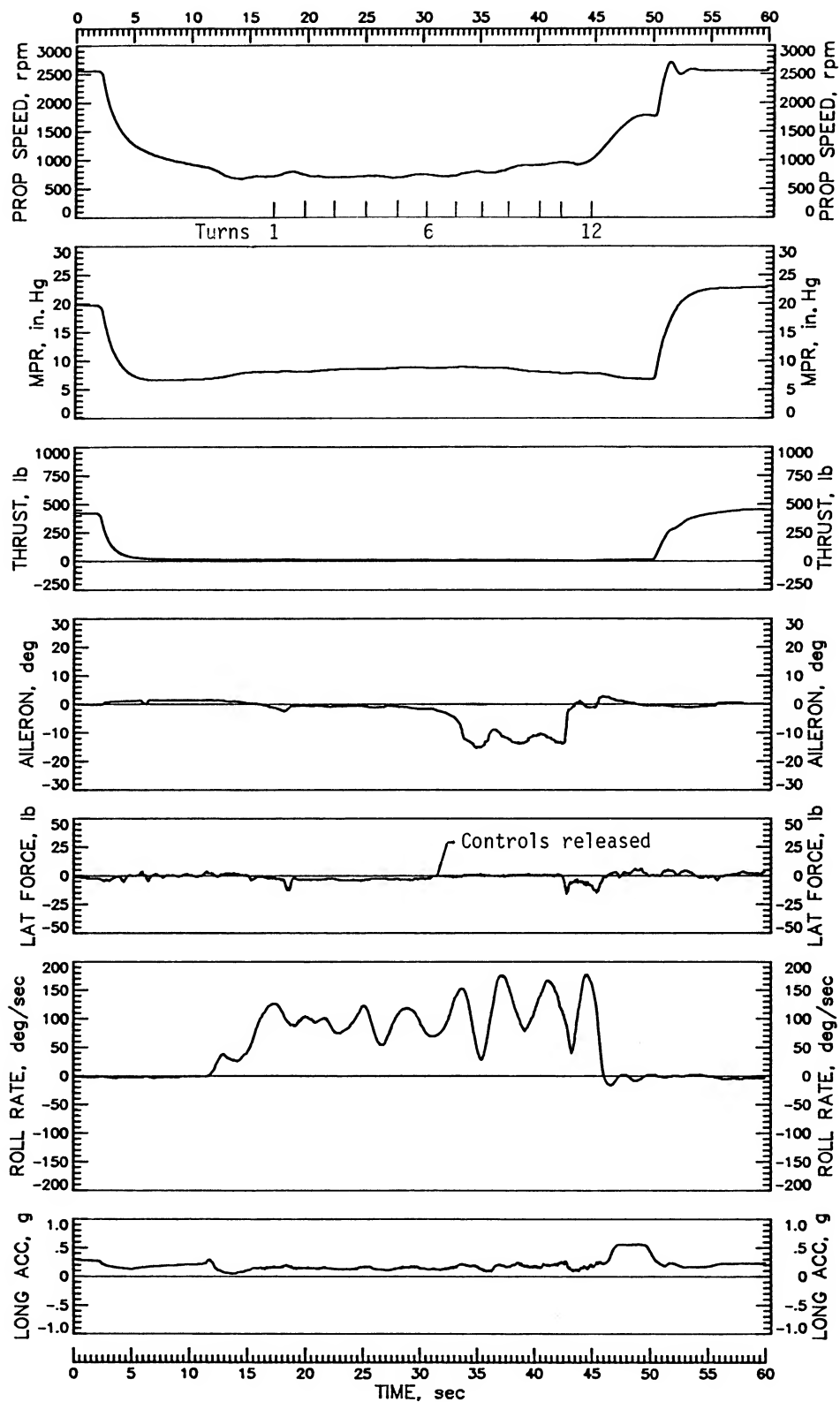


Figure 20. Continued.

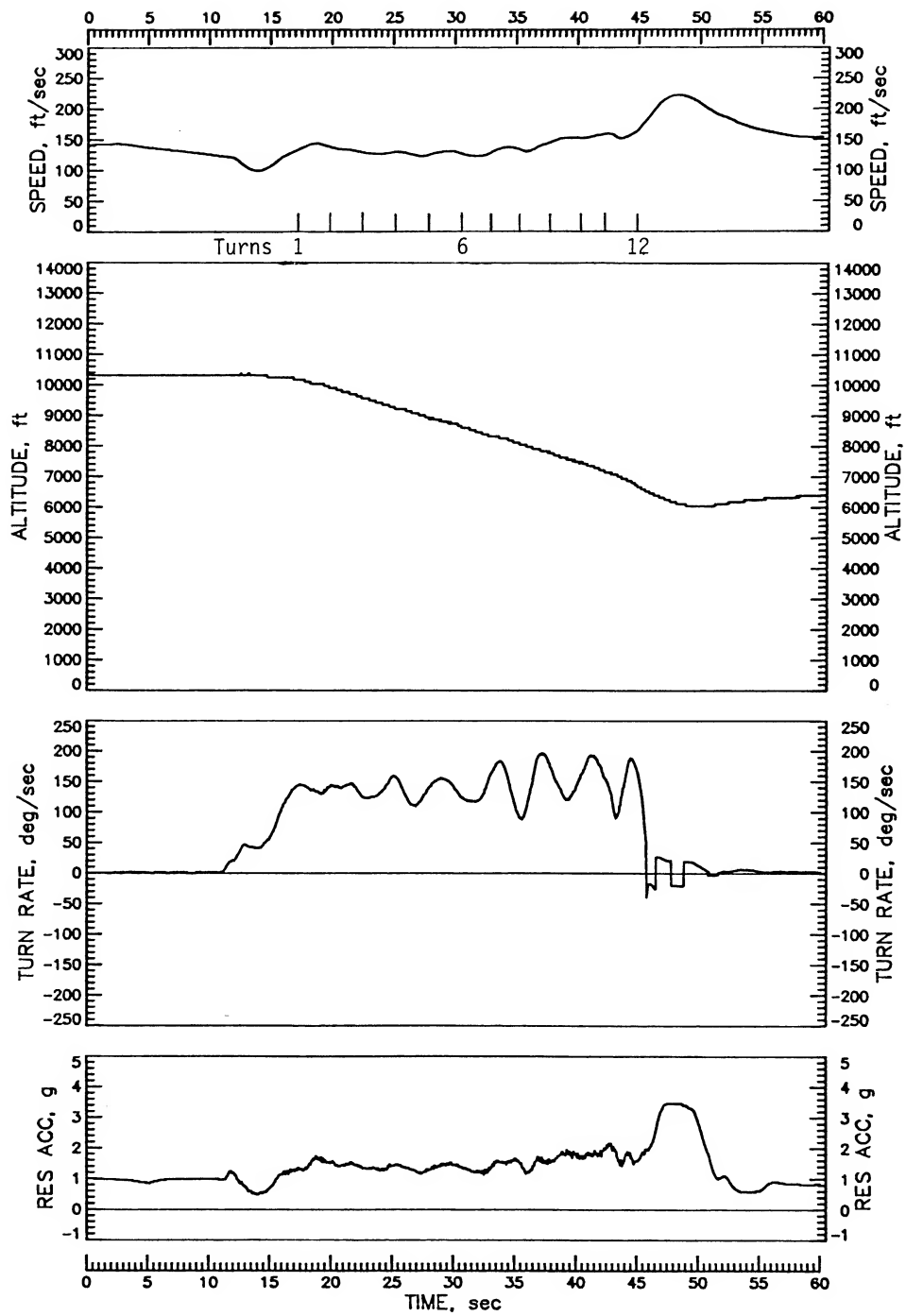


Figure 20. Concluded.

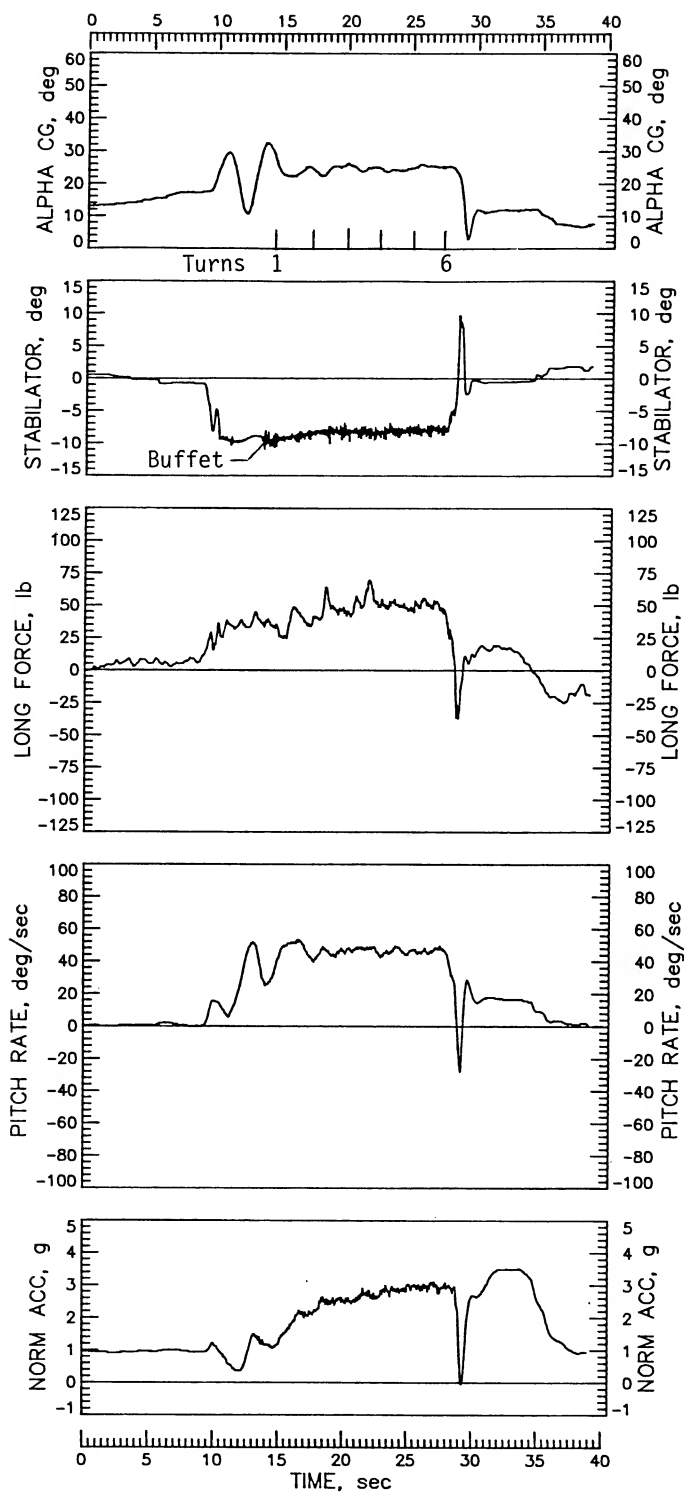


Figure 21. Very steep spin, bordering on spiral, at idle power, ailerons with the spin, flaps and gear retracted.

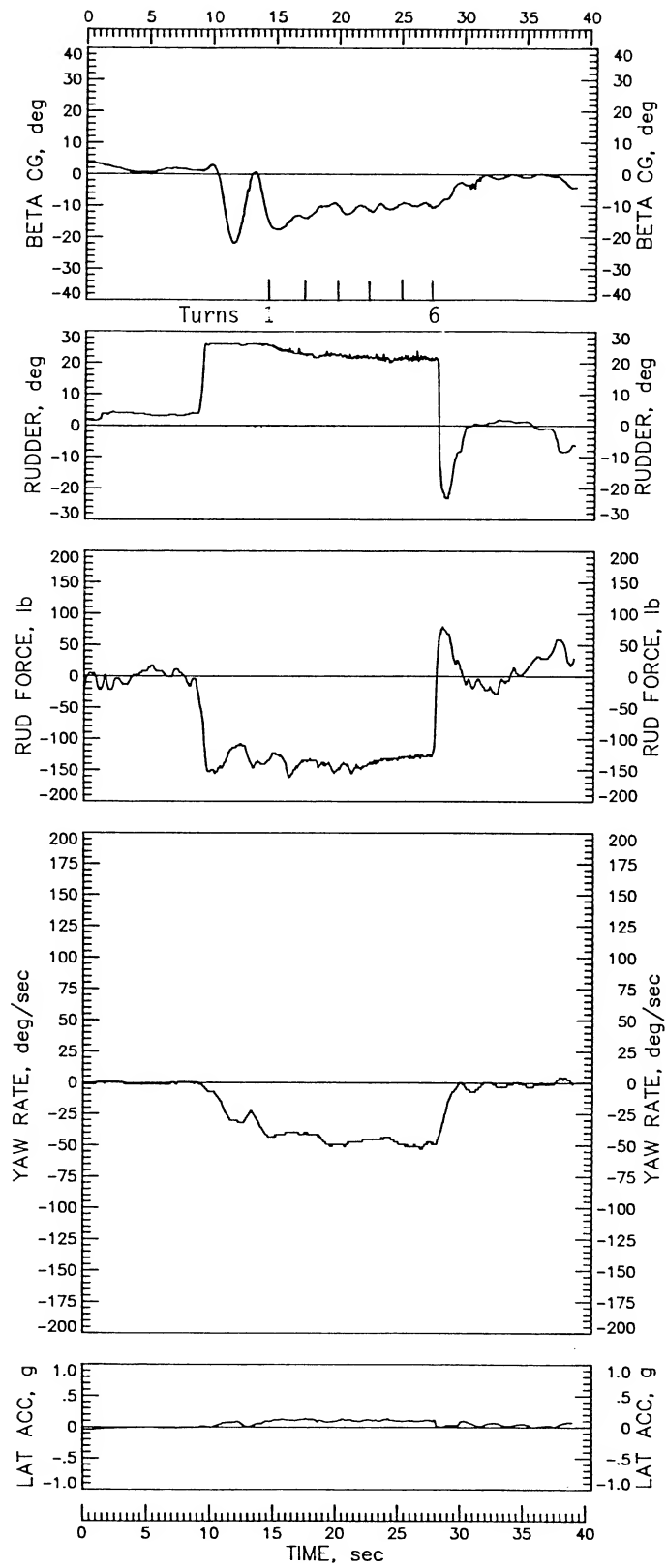


Figure 21. Continued.

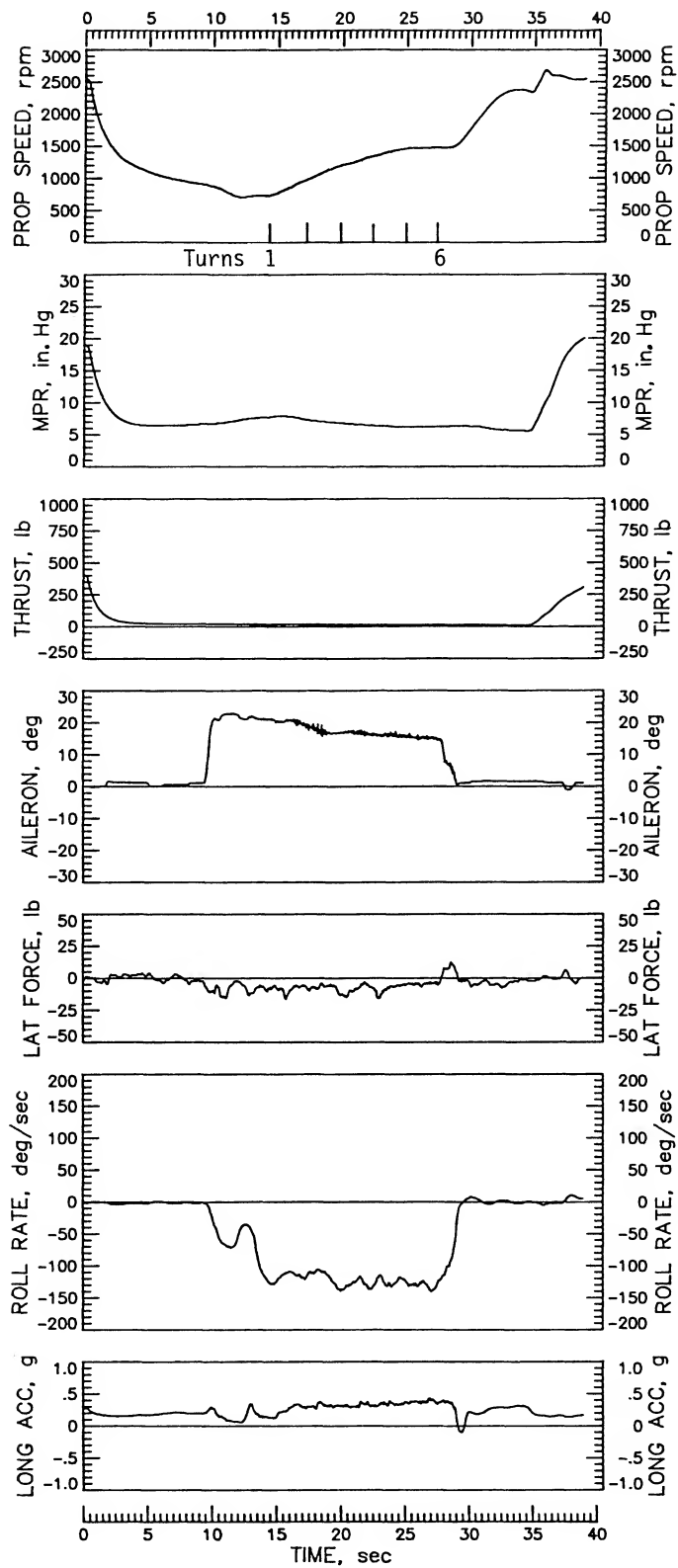


Figure 21. Continued.

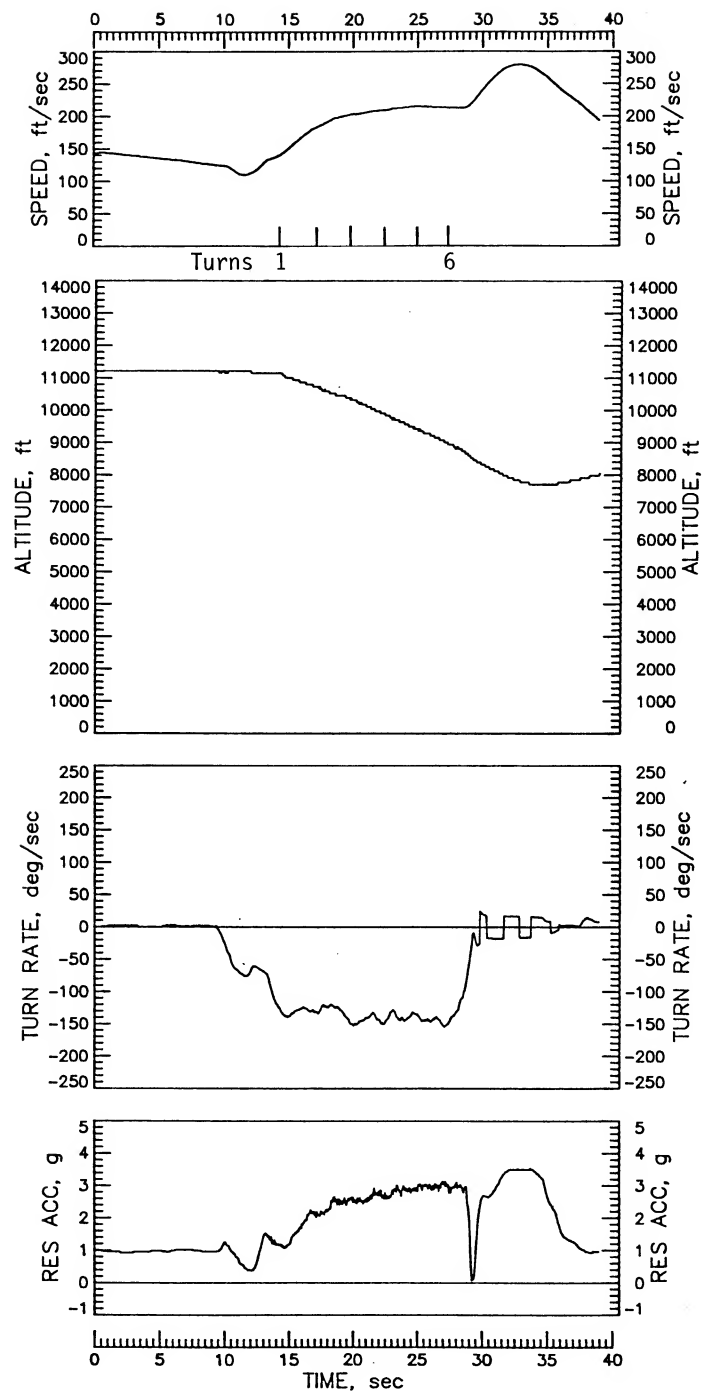


Figure 21. Concluded.

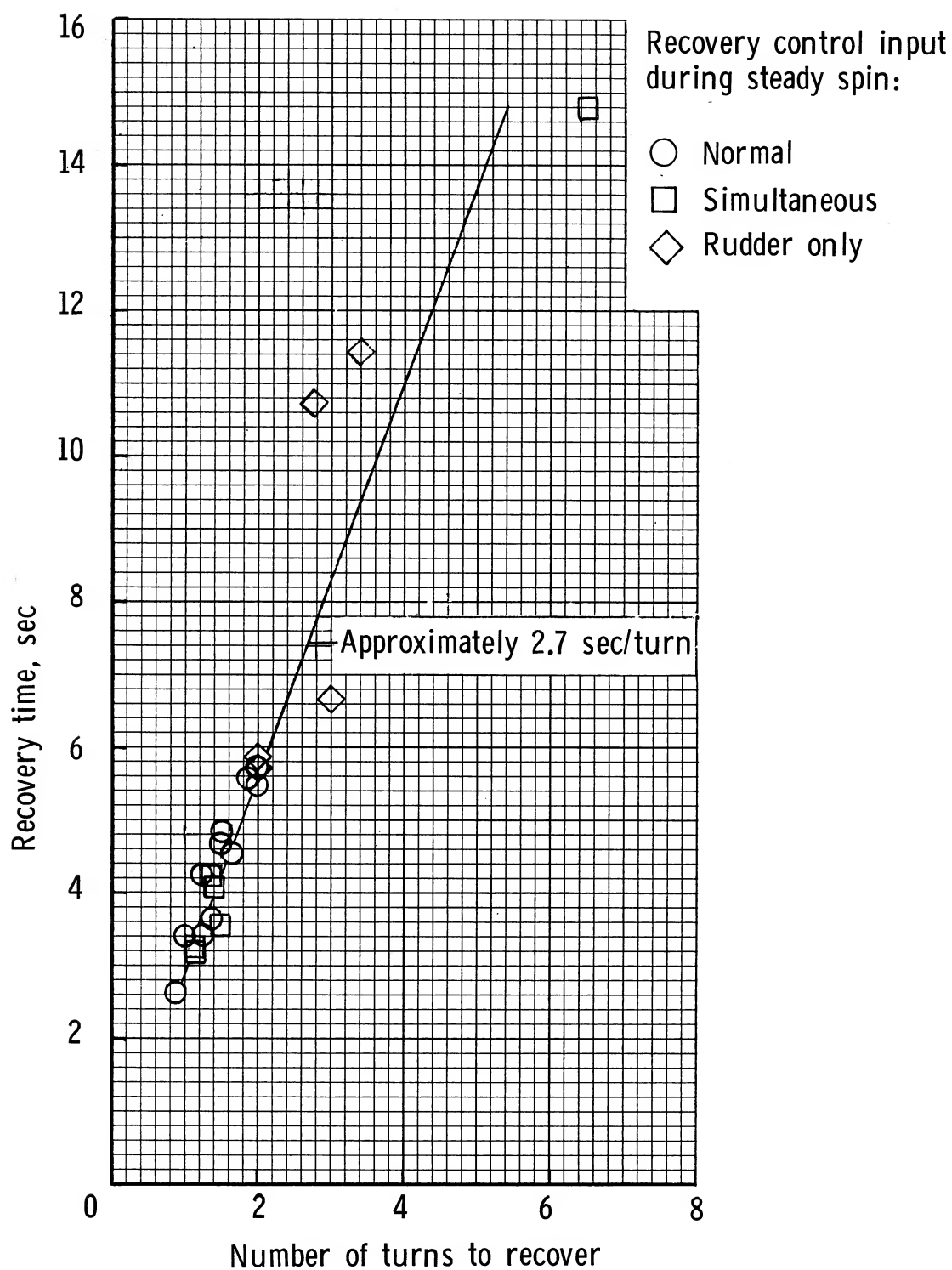


Figure 22. Recovery time as a function of number of turns required to recover from steady spins at idle power, flaps and gear retracted. Twenty-seven spins that did not stop when initial recovery controls were applied are not included.

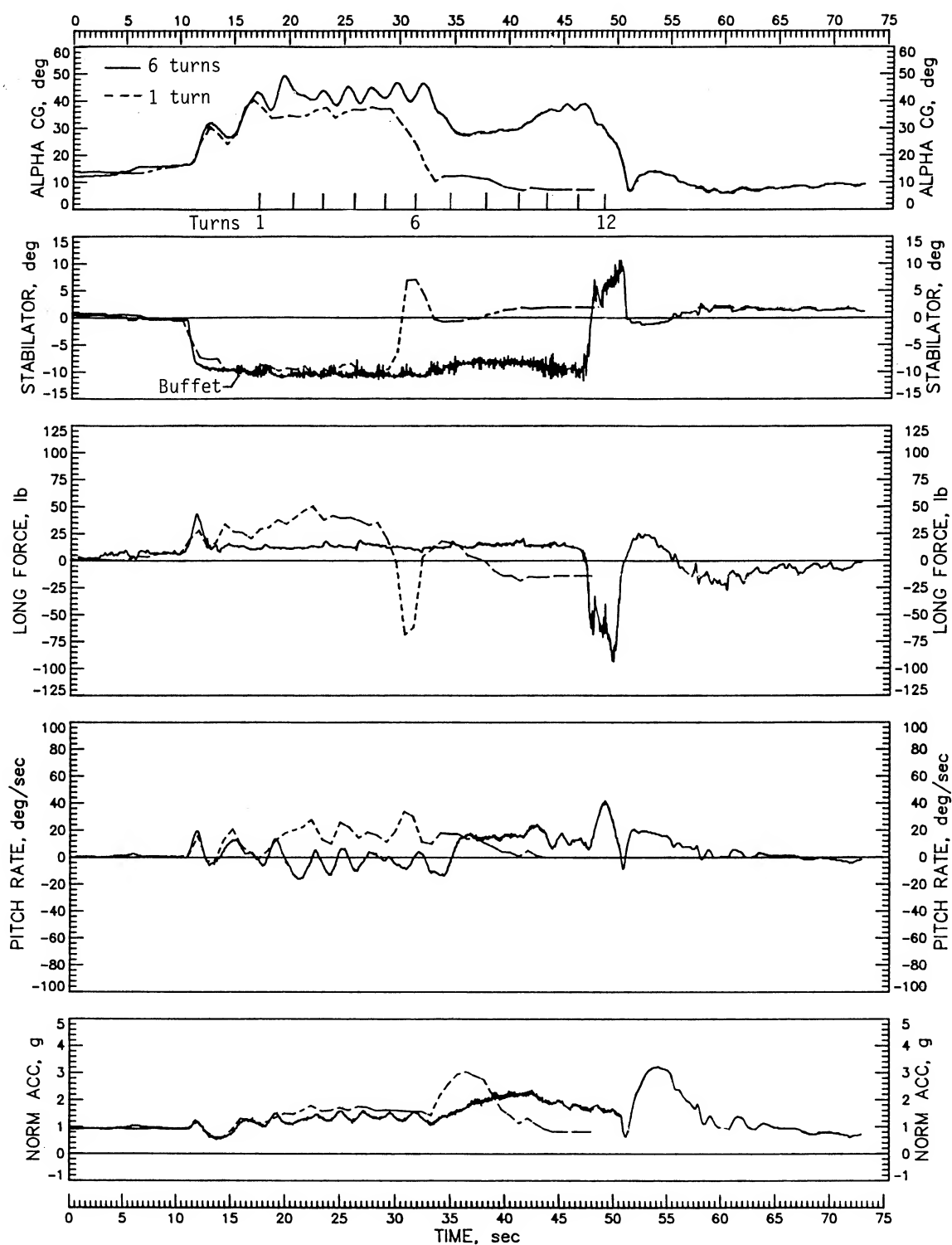


Figure 23. Examples of failure of rudder reversal alone to stop one- and six-turn spins at idle power, aileron against the spin, flaps and gear retracted.

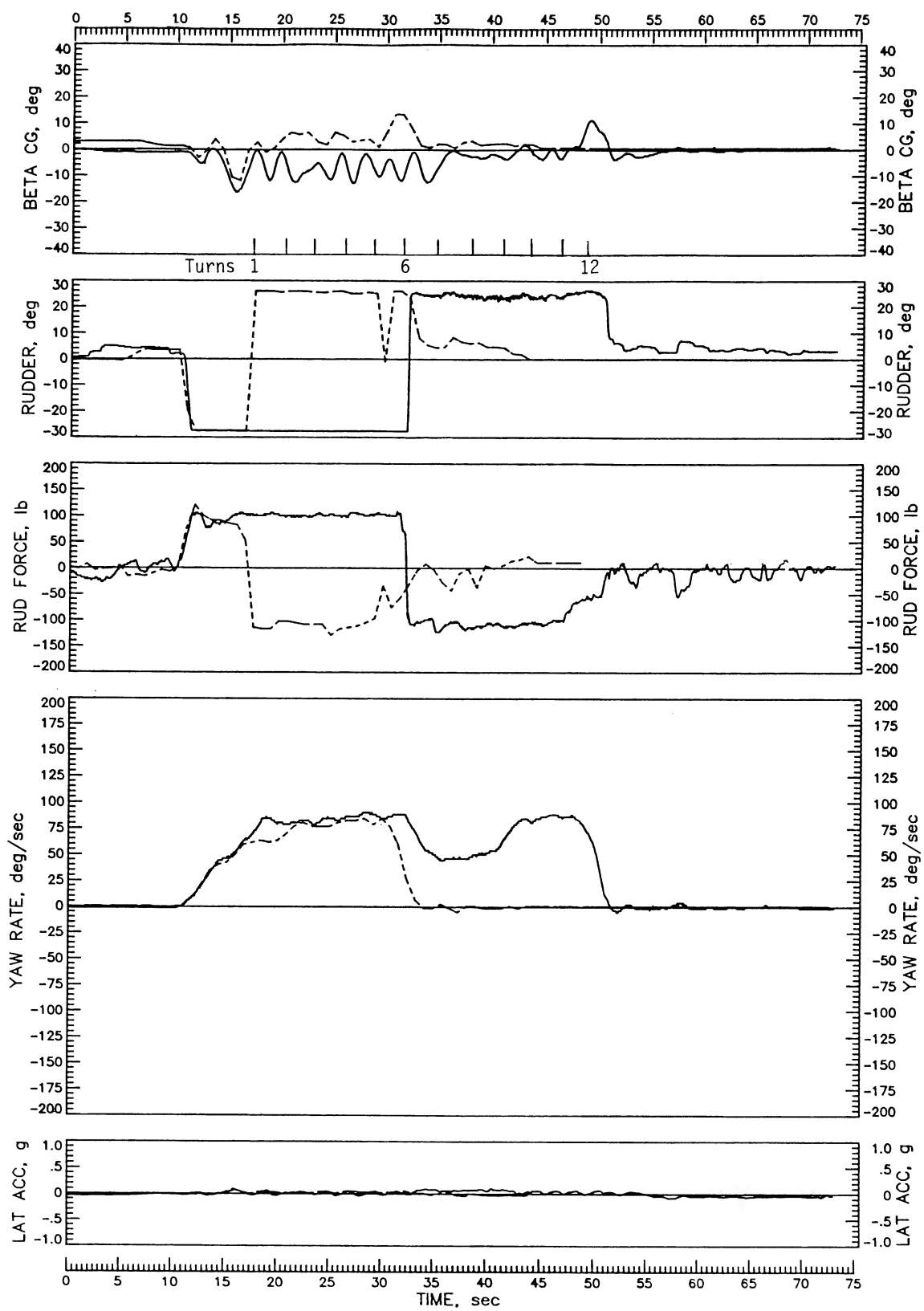


Figure 23. Continued.

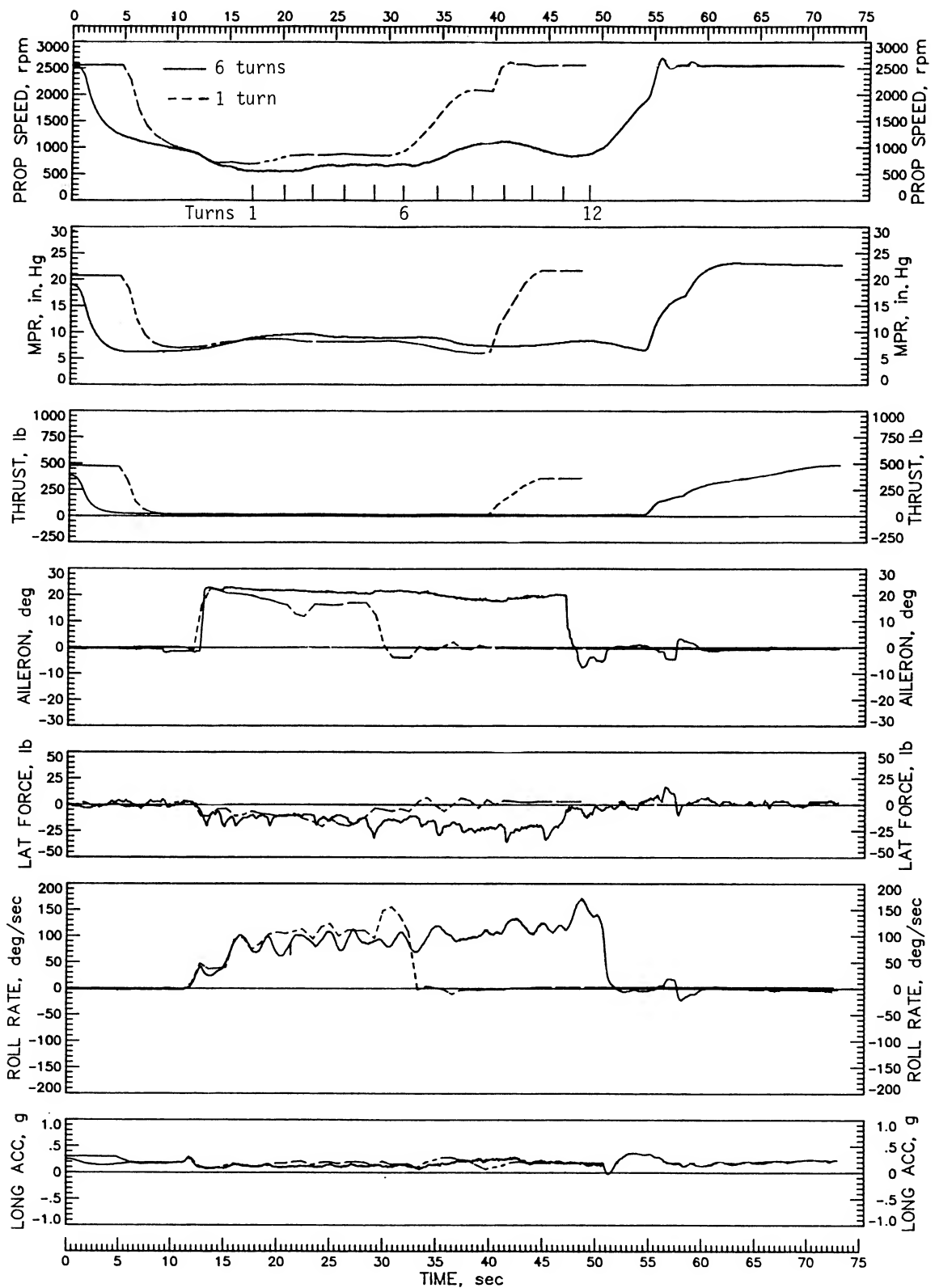


Figure 23. Continued.

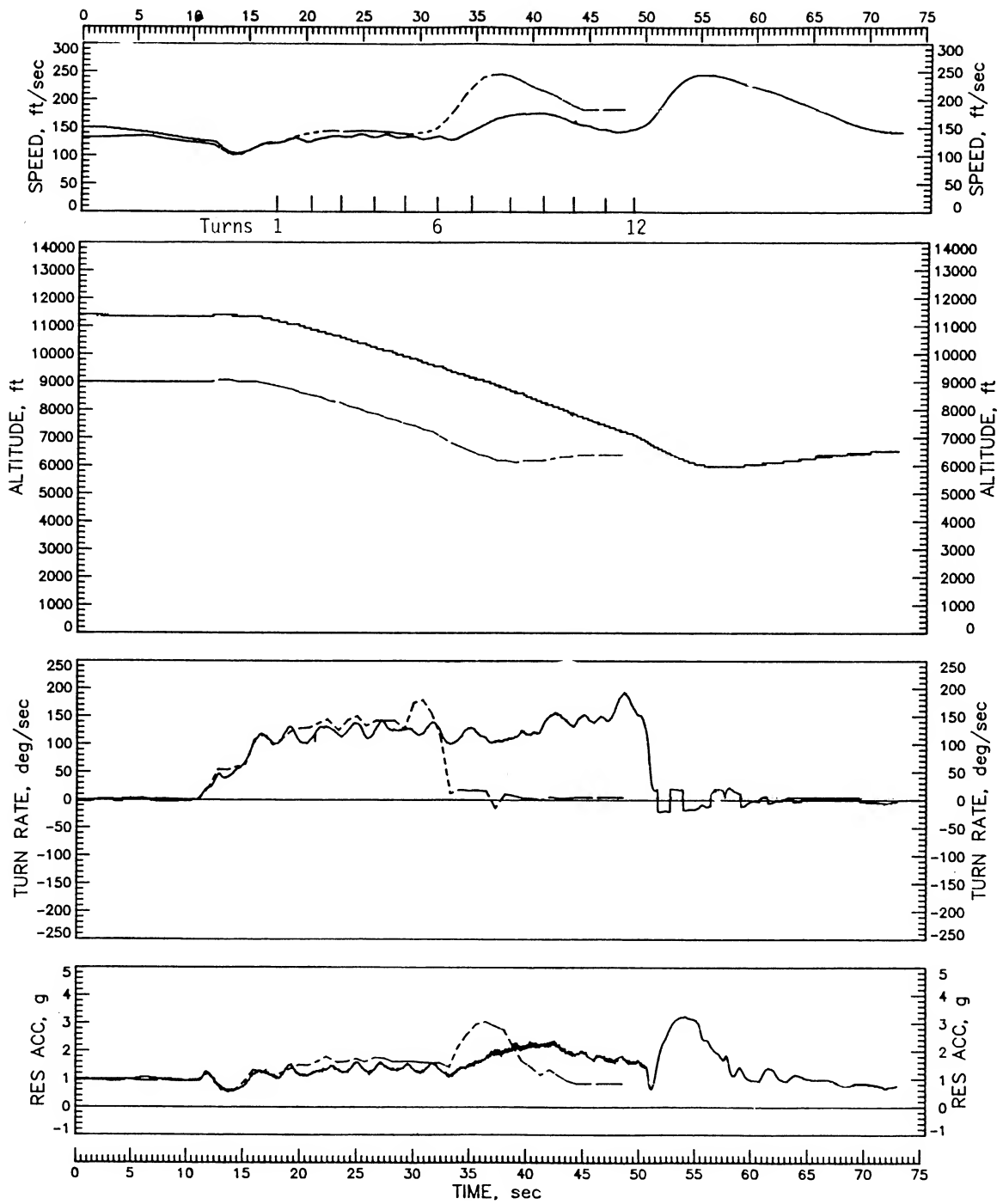


Figure 23. Concluded.

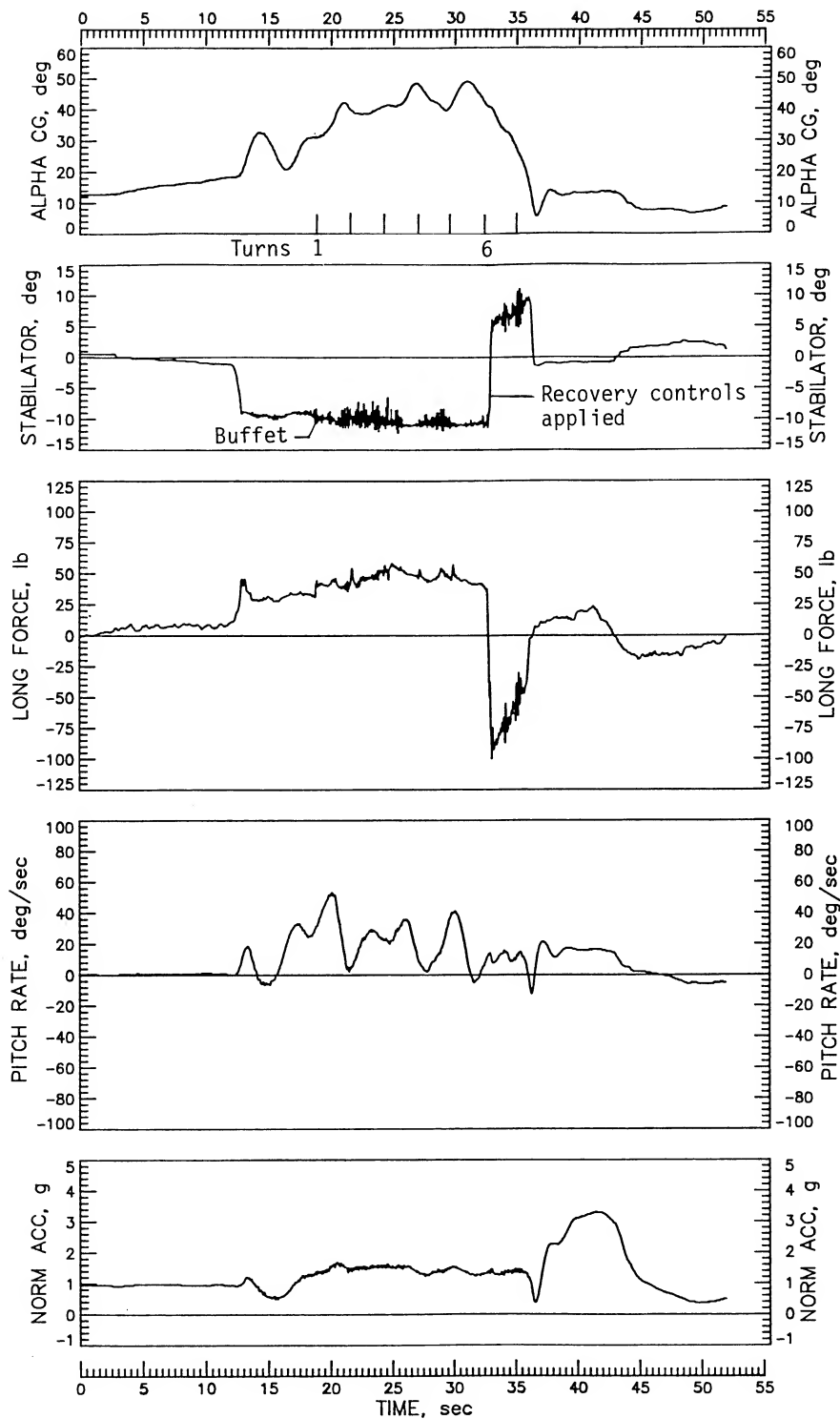


Figure 24. Left spin at idle power, ailerons neutral, flaps and gear retracted. Longitudinal wheel force changes during spin recovery are shown.

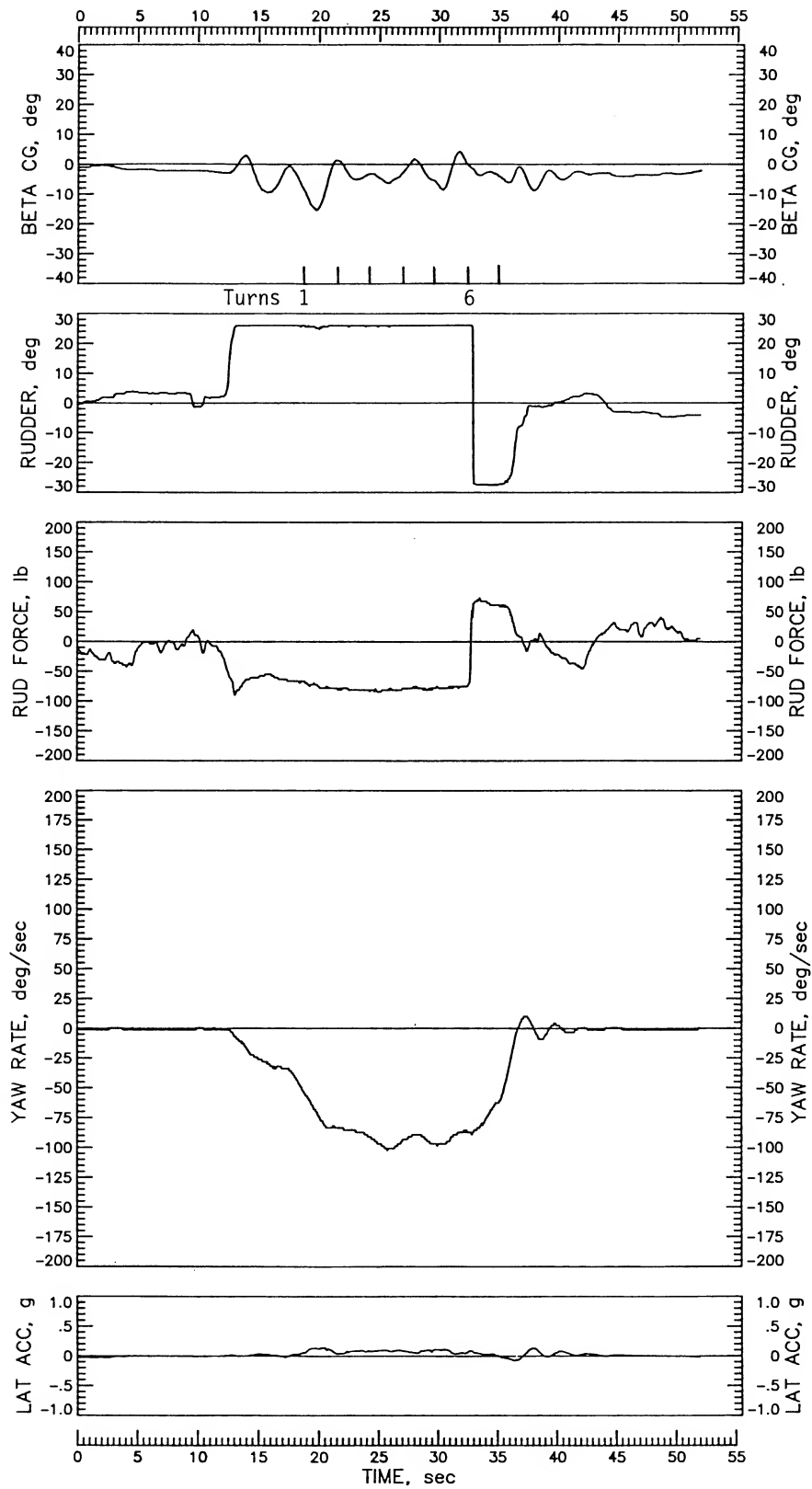


Figure 24. Continued.

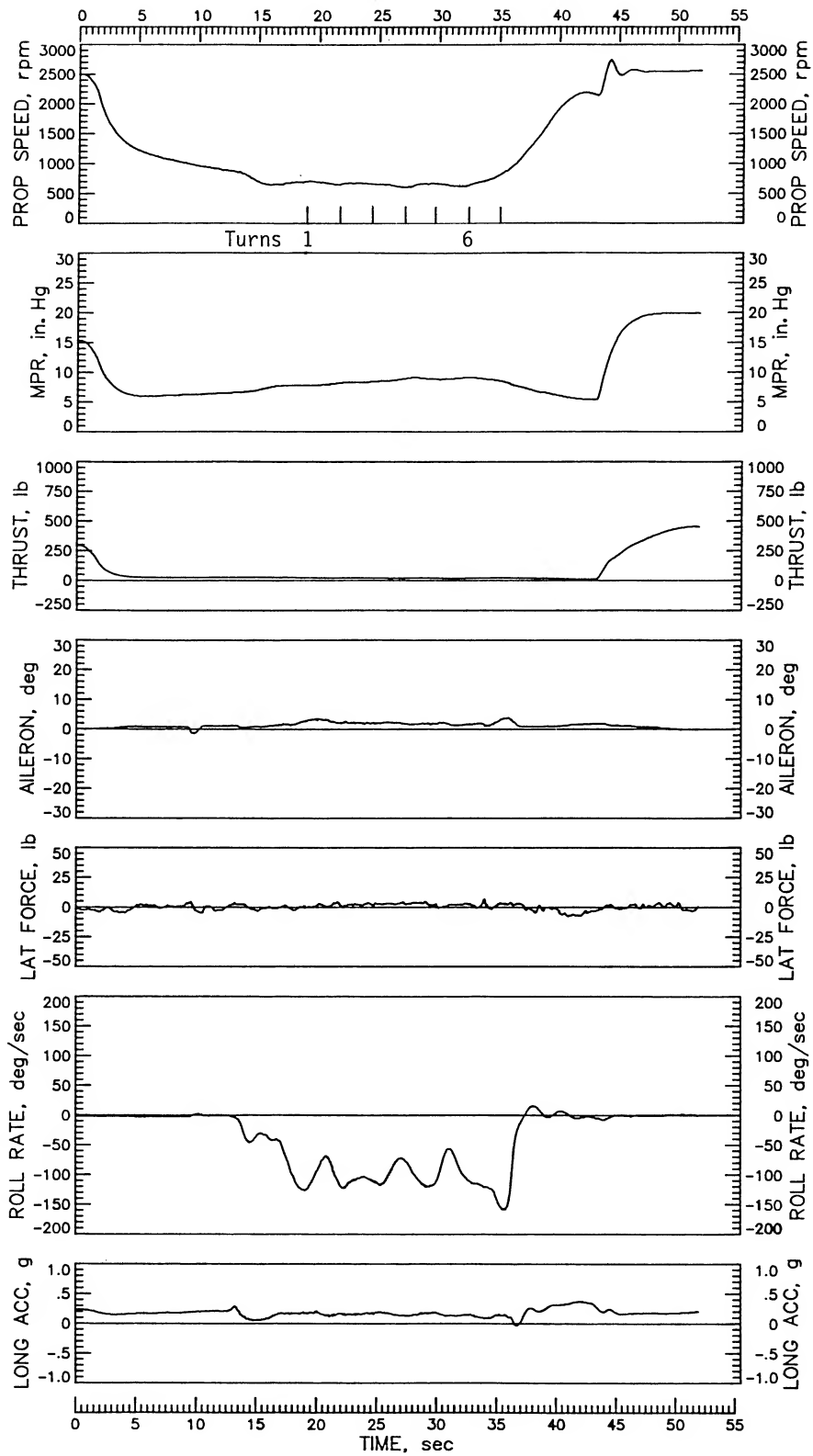


Figure 24. Continued.

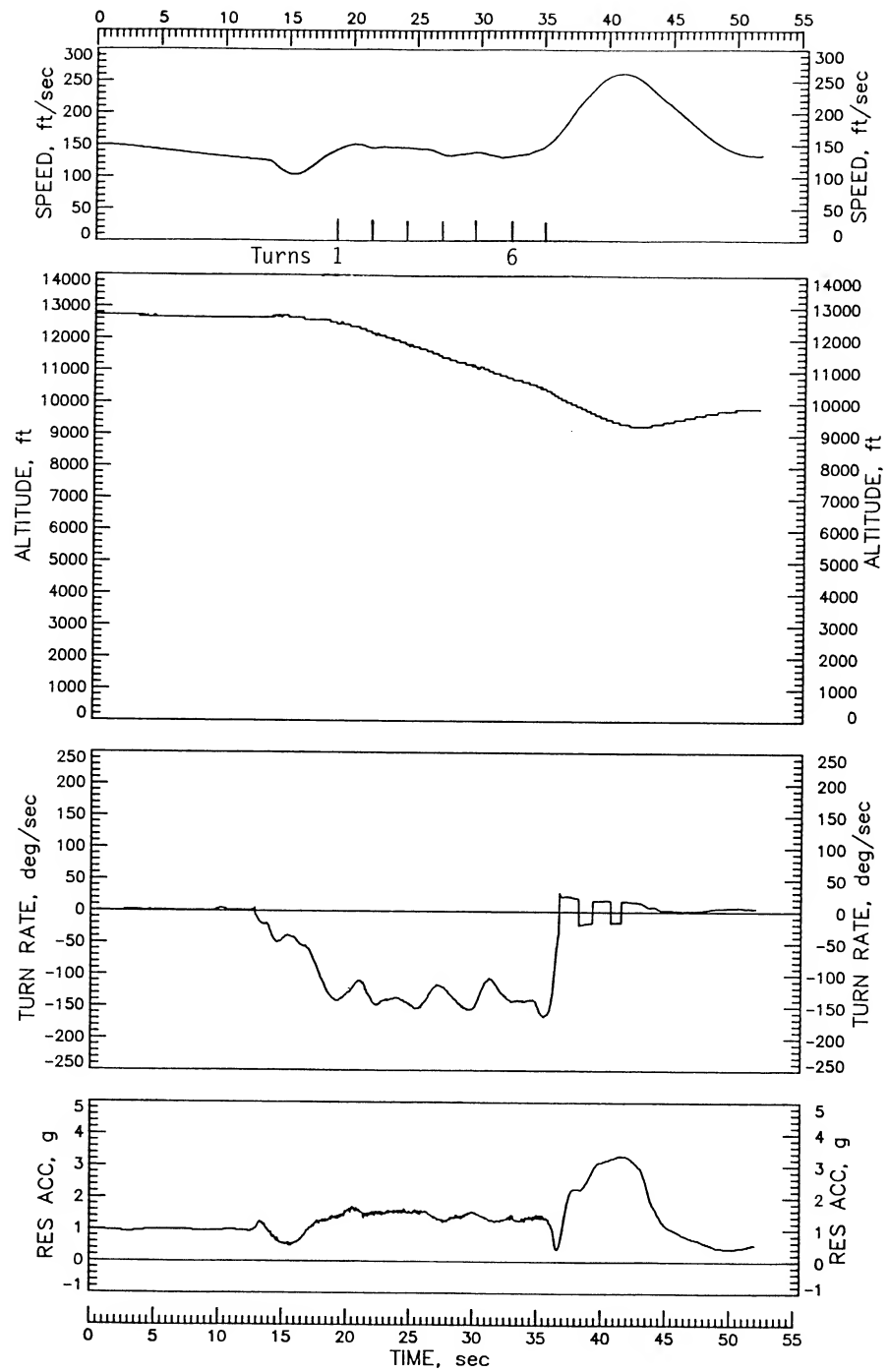


Figure 24. Concluded.

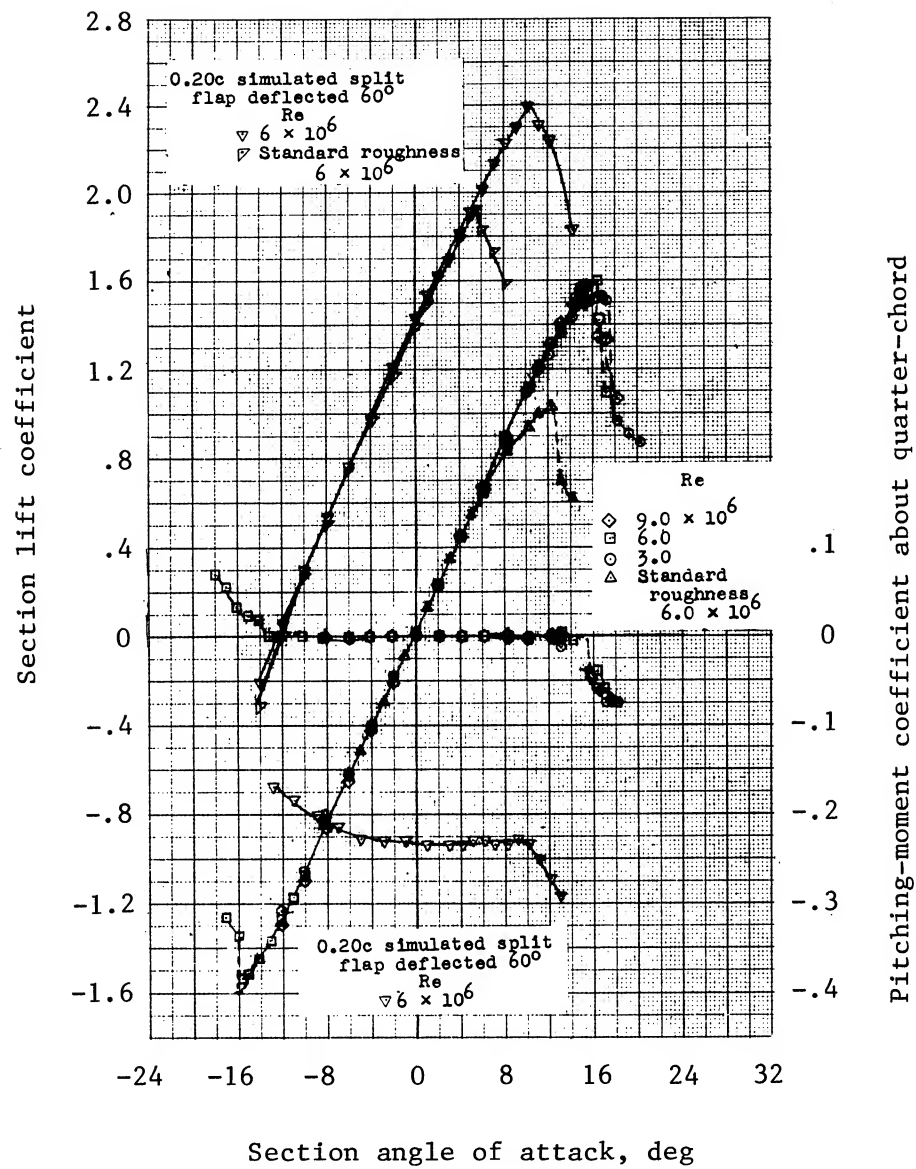


Figure 25. NACA 0012 wing section characteristics. (From ref. 18.)

